Kamil Hamati
Kamil.Hamati@etu.unige.ch

Certificat complémentaire de géomatique
19-337-864

Remote sensing for the assessment of the impacts of a refugee crisis: A case study from the Middle East region.

A research “mémoire” by Kamil Hamati, for the fulfillment of the requirements of the “Certificat Complémentaire de Géomatique - 2021”.

Geneva, June 16, 2022

Table of Contents

Table of figures

Table of tables

1. Introduction

In September 2015, 193 countries agreed to join hands to create a better future for humanity by adopting the United Nation's 2030 Agenda for Sustainable Development that advocates for eradicating poverty through economic and social development, all while tackling climate change and environmental protection, and strengthening peace (United Nations General Assembly, 2015). In its preamble, the Agenda boldly states that "there can be no sustainable development without peace and no peace without sustainable development". This statement comes in homage to the development-reversing effects of conflict explored by Collier et al., (2003) which inspired Raworth, (2012), to suggest that peaceful societies exist in a "Safe and Just Space for humanity" where people live within the limits of their natural environment's carrying capacity, while having access to at least basic social and economic services that guarantee their wellbeing[1]. The Safe and Just Space (SJS) framework, which builds upon earlier scholarly work that identified 9 thresholds known as the Planetary Boundaries (PB) within which humanity can operate "safely[2]" (Rockström et al., 2009b, 2009a), thus informed the UN's 2030 Agenda.

Paradoxically, several years into the global adoption of the Agenda, nearly one person is being forcibly displaced every two seconds as a result of either conflict or persecution, leading to a staggering 82.4 million forcefully displaced people globally (estimated in 2020) (Grande & United Nations High Commissioner for Refugees, 2019; United Nations High Commissioner for Refugees, 2020). Among these populations, 24.6 million people crossed international borders to flee conflict or persecution and are thus labeled refugees (United Nations High Commissioner for Refugees, 2019b, 2020). This unprecedented number of refugees, currently dubbed a crisis, is consequently taking up a greater focus on international agendas, as host countries struggle to learn how to balance between their developmental priorities in light of their commitment to achieving the 2030 Agenda, their moral obligations and their ratification of the 1951 Refugee Convention and the 1967 Protocol (and/or the Global Compact on Refugees), and their response to the increasingly intensifying effects of climate change.

Consequently, anti-refugee sentiments and xenophobia have been gaining popularity across the world and the subject of refugees has recently become a polarizing topic (Nasser Yassin, 2019) that is being increasingly portrayed through a neo-Malthusian[3] lens especially with the increasingly felt impacts of climate change (Nasser Yassin, 2019; Pierigh, 2017).

[1] Such as food security, education, and decent employment, among others.

[2] The notion of safety here was in reference to Earth systems' tipping points beyond which, abrupt and irreversible environmental changes were not excluded, consequently jeopardizing the geological state of equilibrium within which human societies thrive (Steffen, 2005).

[3] In the late 18th century, Thomas Malthus presented a theory (Malthusian theory) suggesting that as demographic growth is exponential and food supply growth is linear, humanity if left *unchecked* (without illnesses, famine, wars, contraceptive policies, etc… limiting population growth) will get to a tipping point triggering a high rate of death among the population, which will thus restore the equilibrium between available food and population. Neo-Malthusianism adds an environmental dimension to this theory and argues that in light of a continuous population growth, the planet's environmental resources will reach a tipping point of scarcity and irreversible damage (Chris Park, 2012; Mellos, 1988).

1.1. Problem statement and research design

Refugees are being blamed – with little to no scientific evidence – for all problems in host societies, whether social, economic, or environmental, and are therefore being deprived of foundational social rights (Black, 1994, 1998; Jacobsen, 1997; Kibreab, 1997; Nasser Yassin, 2019; Oucho, 2007; Pierigh, 2017). This is also driving, in certain cases, hate-motivated crimes against refugees (Amnesty International, 2019; Habib, 2019; Kheireddine et al., 2020; K. Müller & Schwarz, 2020; Obeid et al., 2019; Saada Allaw, 2020; The Economist, 2019).

To understand how to break this cycle of animosity, the world needs more scientific evidence of the actual impact of refugees on their host countries, which could lead the way to more comprehensive and science-based policies that truly "*leave **no one** behind*"[4]. This research suggests an adaptation of the SJS framework to a refugee-hosting situation in a context that is vulnerable to climate change to assess the validity of the claims that accuse refugees of being "exceptional resource degraders".

Using spatial imaging and remote sensing technology, I aim to assess selected indicators from the SJS framework, particularly those that are:

a- Mostly adapted to a refugee setting (by basing this selection on the foundational social rights of refugees, guaranteed in the 1951 Convention and its 1967 Protocol as well as the Global Compact on Refugees);
b- Most recurrent in political discourse in the selected geographical area of interest; and
c- Most recurrent in academic literature on the environmental impact of refugees (based on indicators chosen by prominent scholars in this field, such as the works of (Black, 1994, 1998; Jacobsen, 1997; Kibreab, 1997; Maystadt et al., 2020; Susan F. Martin et al., 2016)).

The expected result is an assessment of the state of several environmental and socio-economic parameters before and after the influx of refugees. Parameters and their spatial proxies are determined based on pre-existing studies such as (M. F. Müller et al., 2016; Susan F. Martin et al., 2016) and through expert consultations that I conducted with the committee that was supervising the process of this work. An overview of these suggested indicators is provided in the following table:

[4] "Leaving no one behind" is the slogan of the UN's 2030 Agenda for Sustainable Development.

Table 1: Indicators and spatial proxies for the spatial analysis of environmental and socio-economic parameters

Boundary type	Parameter	Indicator	Spatial proxy
Environmental	Land cover change	• Area of forested land as % of potential forest	• Differencing of NDVI • Classification of land cover
	Freshwater use	• Blue water withdrawal as % of mean monthly river flow	• Variation of mNDWI
	Biogeochemical flows (Nitrogen and Phosphorus cycles)	• P flow from fertilizers to erodible soils • Industrial and intentional biological fixation of N	• Spatial assessment of eutrophication using chl-*a* concentrations
Socio-economic	Energy	• Population lacking access to electricity	• Nightlight intensity imaging
	Water & Sanitation	• Population without access to at least basic drinking water • Population without access to at least basic sanitation facilities	• Spatial proximity to drinking water sources • Spatial proximity to sanitation facilities
	Health	• Population estimated to be without regular access to essential medicines	• Spatial proximity to healthcare facilities

1.2. Case study

Following the ravaging war in Syria that started in 2011, millions of people fled their homes to neighboring countries that were not prepared to receive them, the following map illustrates the spatial distribution of Syrian refugees' population densities across neighboring countries as of March 2015. The triangles on the map – as shown in the legend – illustrate formal refugee camps, managed by one of the many international and intergovernmental agencies on the ground in surrounding countries.

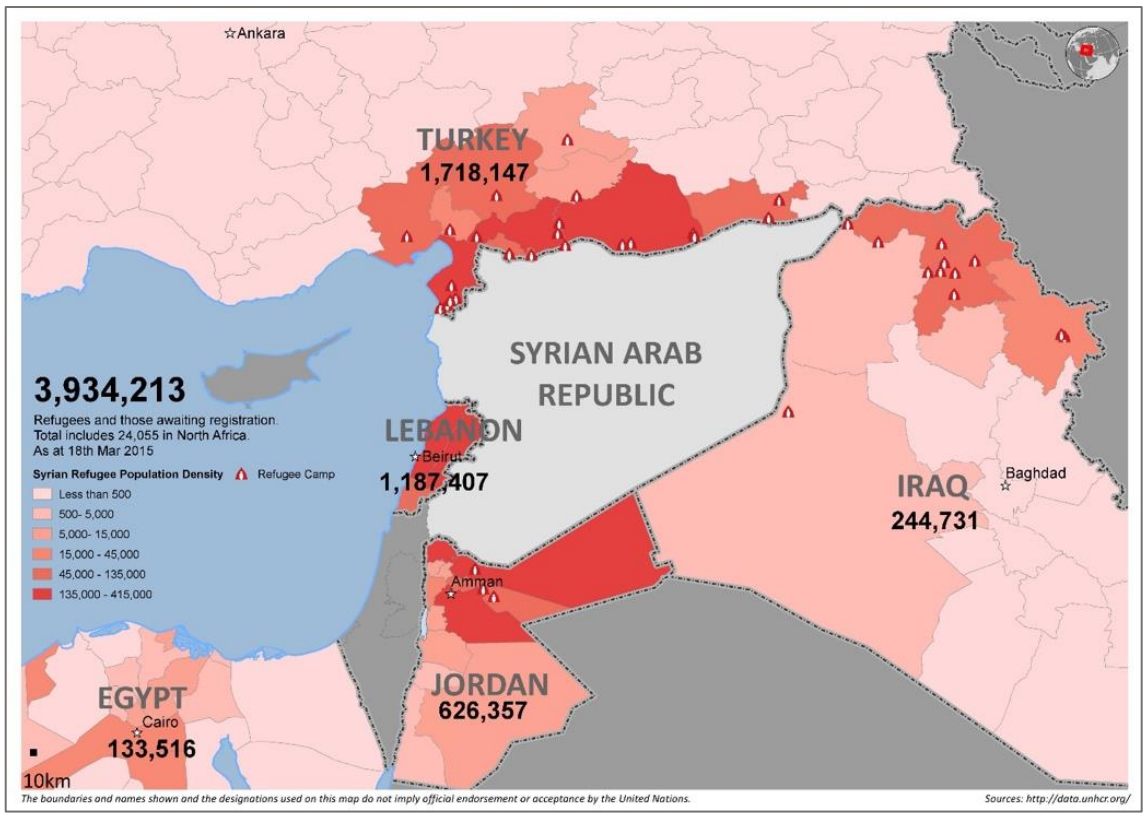

Figure 1: Distribution of Syrian refugee population density in the Middle East and North Africa Region (Source : https://data.unhcr.org/)

As can be clearly seen in Figure 1, Lebanon, Turkey, Jordan, and Iraq were under varying extents of pressures due to the influx of Syrian refugees, and therefore represent different interesting cases to study the impacts of the influx of Syrian refugees. In this respect, the latest statistics by the United Nations High Commissioner for Refugees (UNHCR, 2021) indicate that the Syrian refugee population as of 2021 counts over 5.6 million people, compared to 3.9 million in 2015 (Figure 1). Although Turkey received the largest number of Syrian refugees in absolute terms (around 3.7 million Syrian refugees), Lebanon takes the first place in terms of refugee to national population ratio, with almost 20% of its population comprising of refugees (compared to 5% for Turkey) (Eirik Christophersen, 2021). This data makes of Lebanon an interesting case to study the changes in the environmental and socio-economic landscape between the pre- and post-refugee influx periods.

1.2.1. Lebanon between pre- and post- Syrian refugee influx

The large exodus of refugees arriving to Lebanon, settled either in informal camps along the Lebanese-Syrian borders, or in urban or sub-urban areas due to the government's no-camp-policy (Majed, 2018; Yahya & Muasher, 2018). Consequently, according to the United Nations High Commissioner for Refugees, (2019a), refugees' shelter solutions were distributed between renting units in residential buildings with dire conditions[5] (the case for 73% of refugees), living in makeshift tents in spontaneously set-up settlements (18% of refugees), or living in non-residential structures[6] (9%). These populations were geographically distributed in a heterogenous manner, with 27% settling in North Lebanon, 23% in the capital – Beirut, 11% in the South, and the remaining 39% residing in the Beqaa[7] plain – the agricultural hinterland (United Nations High Commissioner for Refugees, 2021b). Based on these numbers, the Beqaa plain would present an interesting focus to study the multi-dimensional impact of the Syrian refugee influx on the host region. The spatial distribution of registered refugees across the Beqaa plain is better illustrated in the following map (Figure 2).

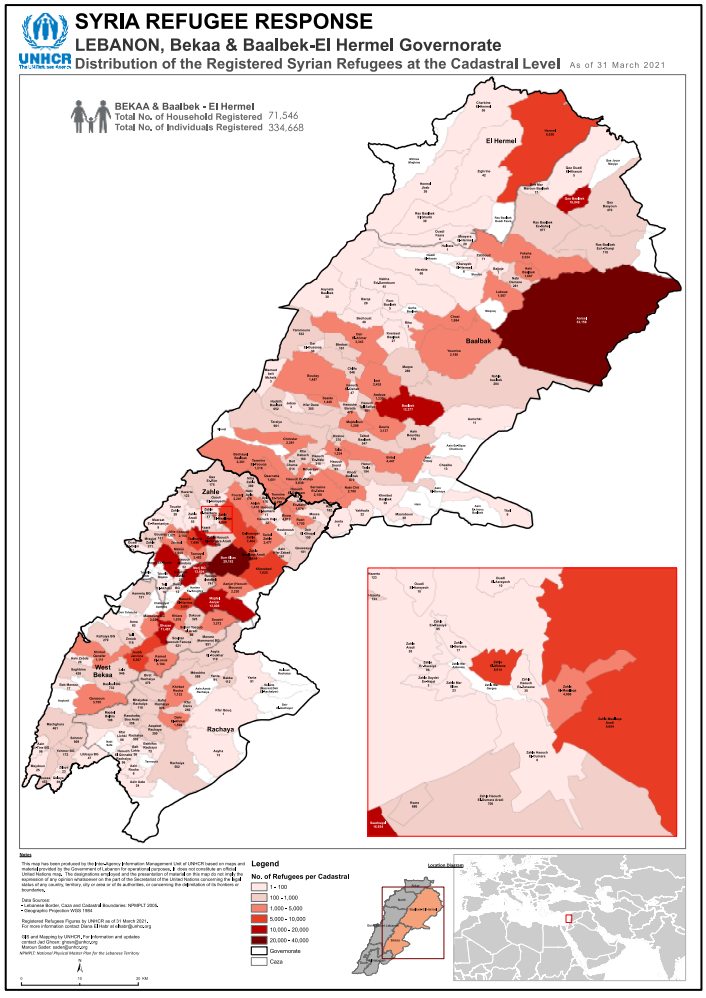

Figure 2: Distribution of registered Syrian refugees across the Beqaa plain (as of 31 March 2021). Source: (United Nations High Commissioner for Refugees, 2021a)

[5] Rented units in residential buildings were reported to be lacking kitchen, toilet, doors, windows, electricity, and/or running water. Out of these refugee households, 33% were reportedly sharing their residential unit with other families.

[6] Non-residential structures in this case refer to garages, shops, worksites, and farm buildings.

[7] The plain administratively stretches over two governorates: Beqaa, and Baalbek El-Hermel.

The Beqaa plain situated at 34.0089° N, 36.1453° E, approximately 39 km east[8] of Beirut, is a fertile land stretching on a 120 Km long corridor with a width of 8-12 Km. It is drained by the Assi river from the North and the Litani river from the South (Figure 3**Error! Reference source not found.**), and is home to a large agricultural activity (R. Khoury et al., 2015) accounting for almost 42% of Lebanon's total cultivated area (Food and Agriculture Organization of the United Nations, 2008) and consisting mainly of cereals, legumes, vegetables, and fruit trees (Lebanese Republic, Ministry of Environment & United Nations Development Programme, 2011) (Figure 4). The plain is irrigated either by surface water (48%) or by groundwater (52%) originating from the Litani river (Food and Agriculture Organization of the United Nations, 2008, 2019; Lebanese Republic, Ministry of Environment & United Nations Development Programme, 2011). As irrigation water is considered as the main vehicle for transmission of contaminants to fresh vegetables (Mcheik et al., 2018), the water quality and quantity of the Litani river are of critical importance to the entire country. The river's basin is divided into two sub-basins through the Qaraoun dam[9] and its reservoir that serves to store the river's annual flows. The largest sub-basin – the upper one, stretches from the Beqaa plain to the dam and hosts the largest anthropological activity which includes industrial, agricultural, and residential activities (International Resources Group, 2011; Jurdi et al., 2002).

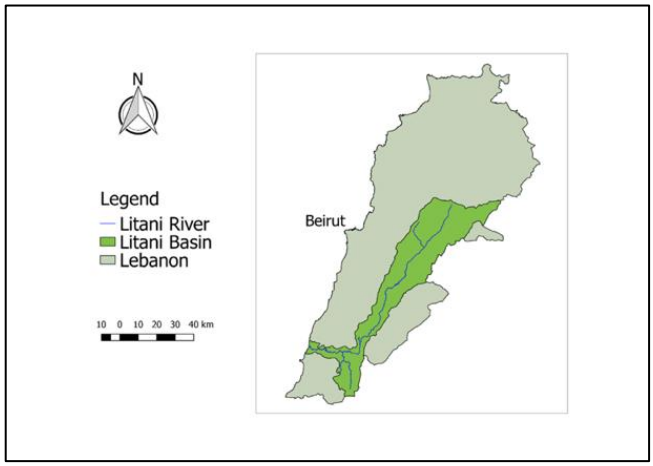

Figure 3: Map of Lebanon showing the Litani river and its basin. Source: (The CHAAMS Project, 2019)

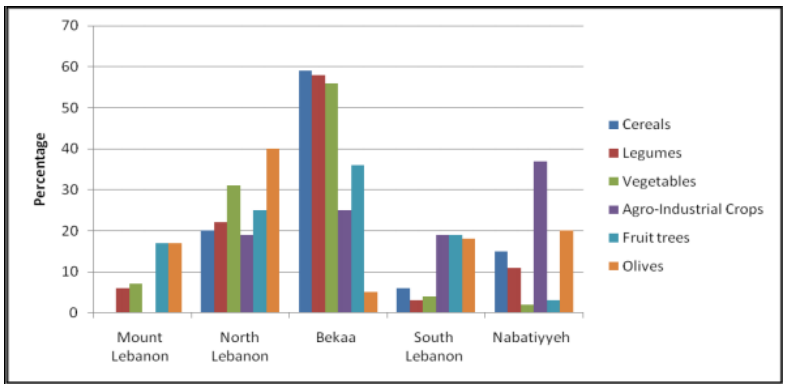

Figure 4: Percentage distribution of crops grown by governorate in Lebanon. Source: (Lebanese Republic, Ministry of Environment and United Nations Development Programme, 2011)

[8] This distance is the distance line between the Beqaa plain and Beirut, equivalent to an 88 km drive by road (Stephan Georg, 2021).

[9] The Qaraoun dam was built in the 1960s at the following coordinates: 33.5716° N, 35.6943° E.

Following the 2011 Syrian refugee influx, the Lebanese Ministry of Environment (MoE) published two assessments of the environmental impact of the Syrian refugee crisis on Lebanon, in 2014 and 2015, in an aim to highlight priority areas for intervention and fundraising (Lebanese Republic, Ministry of Environment et al., 2014, 2015). Divided into four thematic sections, both reports conclude with identical findings, summarized hereafter:

a- **Solid waste**: the existing infrastructure reportedly manages 48% of the incremental quantities of municipal solid waste generated by refugees, whereas the remaining 52% is being disposed of in already-existing open dumps, promoting additional contamination of land and soil.
b- **Water and wastewater**: the report indicates an increase in demand on public water networks leading to 1-20-meter decreases in the depth of groundwater levels in different wells distributed in different regions across the country. Also, fecal coliforms have been reportedly found in municipal water networks in different municipalities across Lebanon. There was also an estimated increase of 34-56 million m^3 of wastewater generation, equivalent to an increase of 8-14% in the national rate of wastewater generation.
c- **Air quality**: the report forecasted a 20% increase in air pollution compared to 2010 values (18% in CO, 20% in NO_x, 4% in SO_2, 11% in PM10, and 13% in PM2.5). These projections were attributed to different sources, namely: on-road transport, residential heating, open burning of solid waste, and electricity production.
d- **Land use and ecosystems**: the report tries to establish a causal relation between the high rate of population density in the country and higher demand on the housing market, to haphazard urban sprawl and development by the local population. The report also indicates that a large part of Syrian refugees lives in informal tented settlements and estimates that this shelter solution might eventually encroach on agricultural lands and put them out of production.

However, the methodology of the 2014 report, which was replicated in 2015, contains inconsistencies and recurrence of "anecdotal evidence" used for benchmarking of several environmental indicators. Therefore, it remains important to visualize the changes from *before* to *after* the influx of refugees, to either support or refute the claims of the MoE's reports in corroboration with other studies that present scientific evidence that could be helpful to better clarify the picture.

The methodology used across the four themes and briefly described in the MoE's 2014 report, mainly consisted of a review of national legislation and reports, along with a consultative process with several stakeholders (including the concerned governmental bodies, and humanitarian and international organizations) and interviews (with seven representatives of municipalities – out of 1030 municipalities – in the North, the Beqaa, and the South, 5 of which are unions of municipalities). Field visits were also reportedly conducted within the scope of this study in two regions, the Beqaa, and the North. Data used for benchmarking and for the analysis was collected mainly from secondary sources including government documentation and data repositories of international organizations. The assessment aimed at drawing a causal relationship between the influx of refugees and worsening environmental conditions; as such, it used baseline data from 2010 or 2011 before the influx of refugees from Syria (choice of the year depended on data availability for each indicator), and calculated the estimated impact based on the number of registered refugees with UNHCR until the start date of the first assessment (31 May 2014) as well as the projected number for December 2014. The methodological description ends with a disclaimer noting that "data availability in the field of environment is limited in Lebanon" and that consequently, quantification of impacts in the four studied areas "was faced with limitations". On top of that, the report includes an annex that reiterates the challenges that jeopardized the quality of collected data, including the constrained timeline that was perceived for this report, which resulted in "a lack of accuracy and of verification for certain

information"; and the lack of reliable and consolidated sources of information for the studied sectors, stating that "information [was] scattered and difficult to trace". The annex also highlights that some data was acquired through interviews with certain stakeholders who provided "non-technical estimations and anecdotal evidence", thus jeopardizing the reliability of both the used benchmarks and the estimated impacts. Finally, accuracy in the isolation of the impact of the Syrian refugees from the initial state of the environment before the influx could not be guaranteed due to the reliance on anecdotal data from a restricted number of municipalities.

This further highlights the importance of this present study in providing scientific evidence to assess the impact of the Syrian refugee influx to Lebanon.

2. Methods and data

In different developing regions around the world, environmental monitoring networks and infrastructure are either insufficient or inexistent and they therefore hinder real-time decision-making in contexts that need it most. Consequently, remote sensing using satellite imagery is increasingly becoming an essential source of information to replace or complement in-situ environmental monitoring, especially in settings of water resources management (M. F. Müller et al., 2016; Sheffield et al., 2018). Relating this to the Lebanese context, environmental monitoring data is extremely scarce, and the Qaraoun reservoir and the Litani river basin are no exception to this (Baydoun & Amacha, 2016; Fadel et al., 2016; Lebanese Republic, Ministry of Environment et al., 2014; Saadeh et al., 2012).

Therefore, data for this study is taken from secondary sources that provide in-situ information and is complemented with spatial images that carry the same – or a similar – timestamp in order to validate and ensure the accuracy of the remotely sensed data. This information is then used to extrapolate values for other time periods where in-situ data is not available, based on remotely sensed information. This methodology is inspired from Fadel et al., (2016) and M. F. Müller et al., (2016).

2.1. Area Of Interest

Our area of interest (AOI) is chosen in conjunction with the spatial distribution of refugees across the Beqaa plain and the Litani River Basin, outlined in Figure 2. Figure 5 shows the AOI covering part of the Beqaa plain, from Baalbek (the town) to the Qaraoun reservoir (in Qaraoun, the town). This is roughly situated between the coordinates[10]: 33.5447° N, 35.6579° E and 34.0723° N, 36.0564° E.

[10] More detailed coordinates are available in Annex 1: Spatial images additional information, under Table 6 and Figure 21

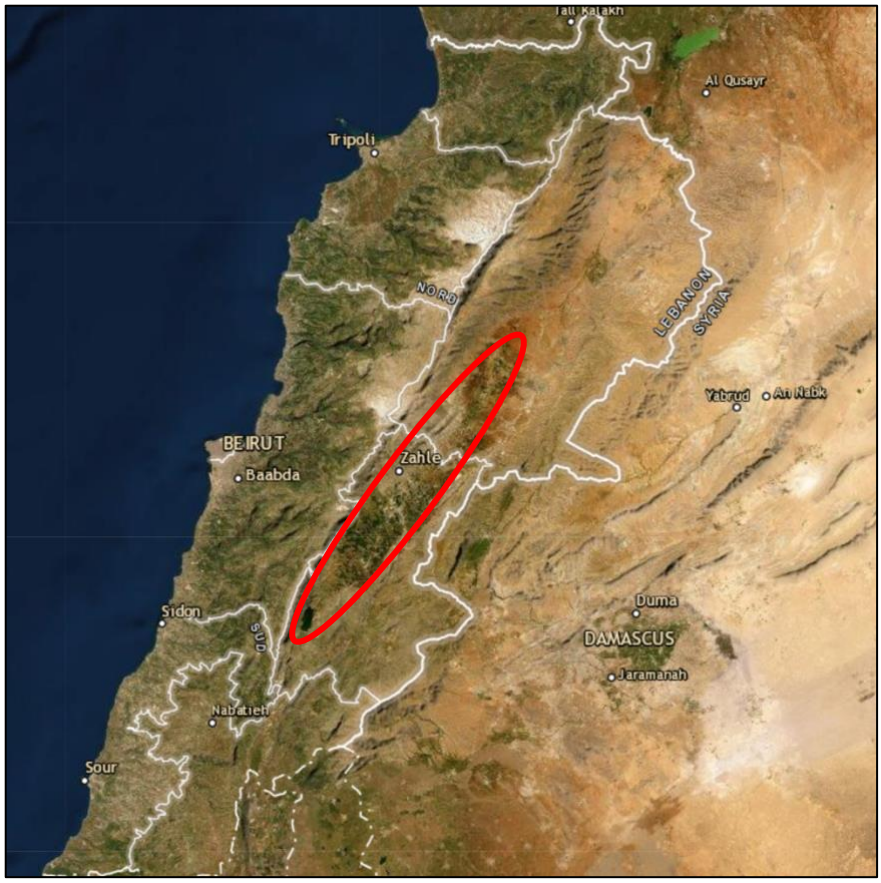

*Figure 5: Lebanon map, highlighting area of interest in red contour. Source: (*EarthExplorer*, n.d.)*

2.2. Spatial data and metadata

To establish a temporal comparison, we first need to define a moment in time that precedes the onset of the studied event (i.e. *before* the influx of Syrian refugees to Lebanon, 2010), the moment of onset of the event (shortly after the beginning of the influx, in parallel with the official environmental impact assessment in 2014, referred to hereafter), and a moment after (since this has become a protracted situation, refugees are still living in the AOI, therefore this moment is in 2021). To account for the vegetation cycles in the region and the variations in water levels in the Qaraoun (Fadel et al., 2016), we're opting for spatial images between August and September for each of the selected years.

Spatial images are downloaded through the EarthExplorer online portal, using the following criteria:

- Geocoder: World Features
- Polygon: Use map
- Date range: from 01/08/2010 to 30/09/2010; (the same range is replicated for 2014 and 2021)
- Cloud cover: 0-30%
- Data Set:
    - Landsat:
      Landsat collection 2 Level-2:
        - Landsat 8 OLI/TIRS C2 L2
        - Landsat 7 ETM+ C2 L2

      Landsat collection 2 Level-1:
        - Landsat 8 OLI/TIRS C2 L1
        - Landsat 7 ETM+ C2 L1

After verifying that the footprint covers our AOI among the different search results, images were chosen and downloaded. Their properties may be consulted under the following Table 2, alternatively, detailed properties may be viewed in Table 7 under Annex 1: Spatial images additional information. The images for 2010, 2014, and 2020 are compiled, untreated, in Figure 6 (a, b, c) along with an indicator of the AOI in all three images. An important note to raise here is that even though our spatial images are provided by different satellites, their projections are identical which has facilitated the treatment of the images as well as the accurate choice of the computational region.

Table 2: Summary of the proprieties of the used Landsat spatial images

Date of acquisition	27/08/2021	24/08/2014	06/09/2010
WRS	Path = 174 / Row = 37	Path = 174 / Row = 37	Path = 174 / Row = 037
Projection	WGS84 / UTM ZONE = 36	WGS84 / UTM ZONE = 36	WGS84 / UTM ZONE = 36
Source	USGS EarthExplorer (https://earthexplorer.usgs.gov/)		
Satellite	LANDSAT 8 OLI TIRS	LANDSAT 8 OLI TIRS	Landsat 7 ETM+
Cloud Cover	0.01%	0.93%	2.00%
Quality	9	9	9
Type	GeoTIFF	GeoTIFF	GeoTIFF
Resolution	30 m	30 m	30 m

As nighttime imagery was not directly available through the same portal, night light images were downloaded from a homogenized dataset that was made available by Li et al., (2020) for 2010 and 2014, and from NASA's EOSDIS WorldView for 2021 (https://earthdata.nasa.gov/learn/backgrounders/nighttime-lights#data). The choice of images was rather limited, considering the relatively recent democratization and use of such data, and considering the change in satellites that capture this data and the decentralization of access to this information. The details of the nighttime images are summarized in the following Table:

Date of acquisition	Available metadata
n.a./n.a./2010	**Name** Harmonized_DN_NTL_2010_calDMSP **Path** /Users/kamilhamati/Downloads/Harmonized_DN_NTL_2010_calDMSP.tif **CRS** EPSG:4326 - WGS 84 - Geographic **Extent** -180.0000000000000000,-65.0083327732999976 : 180.0083318933000101,75.0000000000000000 **Unit** degrees **Width** 43201 **Height** 16801 **Data type** Byte - Eight bit unsigned integer **GDAL Driver Description** GTiff **GDAL Driver Metadata** GeoTIFF **Dataset Description** /Users/kamilhamati/Downloads/Harmonized_DN_NTL_2010_calDMSP.tif **Compression** PACKBITS **Band 1** • STATISTICS_APPROXIMATE=YES • STATISTICS_MAXIMUM=59 • STATISTICS_MEAN=0.87188818065396 • STATISTICS_MINIMUM=0 • STATISTICS_STDDEV=4.9639135806861 • STATISTICS_VALID_PERCENT=100 **More information** • AREA_OR_POINT=Area • TIFFTAG_SOFTWARE=MATLAB 8.6, Mapping Toolbox 4.2 **Dimensions** X: 43201 Y: 16801 Bands: 1 **Origin** -180,75 **Pixel Size** 0.008333333300000000596,-0.008333333300000000596

n.a./n.a./2014	**Name** Harmonized_DN_NTL_2014_simVIIRS **Path** /Users/kamilhamati/Downloads/Harmonized_DN_NTL_2014_simVIIRS.tif **CRS** EPSG:4326 - WGS 84 - Geographic **Extent** -180.0041666666500078,-65.0041661066500041 : 180.0041652266500023,75.0041666666499935 **Unit** degrees **Width** 43201 **Height** 16801 **Data type** Byte - Eight bit unsigned integer **GDAL Driver Description** GTiff **GDAL Driver Metadata** GeoTIFF **Dataset Description** /Users/kamilhamati/Downloads/Harmonized_DN_NTL_2014_simVIIRS.tif **Compression** PACKBITS **Band 1** • STATISTICS_COVARIANCES=20.41488345288872 • STATISTICS_MAXIMUM=63 • STATISTICS_MEAN=1.0349675235803 • STATISTICS_MINIMUM=0 • STATISTICS_SKIPFACTORX=1 • STATISTICS_SKIPFACTORY=1 • STATISTICS_STDDEV=4.5182832417732 **More information** • AREA_OR_POINT=Area • TIFFTAG_SOFTWARE=MATLAB 9.6, Mapping Toolbox 4.8 **Dimensions** X: 43201 Y: 16801 Bands: 1 **Origin** -180.004,75.0042 **Pixel Size** 0.008333333300000000596,-0.008333333300000000596
27/08/2021	**Name** snapshot-2021-08-27T00_00_00Z **Path** /Users/kamilhamati/Downloads/snapshot-2021-08-27T00_00_00Z (1)/snapshot-2021-08-27T00_00_00Z.tif **CRS** OGC:CRS84 - WGS 84 (CRS84) - Geographic **Extent** 35.3079225374302368,32.8271766279066739 : 36.3713697228674917,34.2281694204984674 **Unit** degrees **Width** 3872 **Height** 5101 **Data type** Byte - Eight bit unsigned integer **GDAL Driver Description** GTiff **GDAL Driver Metadata** GeoTIFF **Dataset Description** /Users/kamilhamati/Downloads/snapshot-2021-08-27T00_00_00Z (1)/snapshot-2021-08-27T00_00_00Z.tif **Compression** DEFLATE **Band 1** • STATISTICS_APPROXIMATE=YES • STATISTICS_MAXIMUM=255 • STATISTICS_MEAN=75.780303030303 • STATISTICS_MINIMUM=16 • STATISTICS_STDDEV=46.138298586085 • STATISTICS_VALID_PERCENT=100 **Band 2** • STATISTICS_APPROXIMATE=YES • STATISTICS_MAXIMUM=255 • STATISTICS_MEAN=75.780303030303 • STATISTICS_MINIMUM=16 • STATISTICS_STDDEV=46.138298586085 • STATISTICS_VALID_PERCENT=100 **Band 3** • STATISTICS_APPROXIMATE=YES • STATISTICS_MAXIMUM=255 • STATISTICS_MEAN=75.780303030303 • STATISTICS_MINIMUM=16 • STATISTICS_STDDEV=46.138298586085 • STATISTICS_VALID_PERCENT=100 **More information** • TIFFTAG_DOCUMENTNAME= • TIFFTAG_RESOLUTIONUNIT=2 (pixels/inch) • TIFFTAG_XRESOLUTION=72 • TIFFTAG_YRESOLUTION=72 **Dimensions** X: 3872 Y: 5101 Bands: 3 **Origin** 35.3079,34.2282 **Pixel Size** 0.00027465061607367203 87,-0.00027465061607367117 14

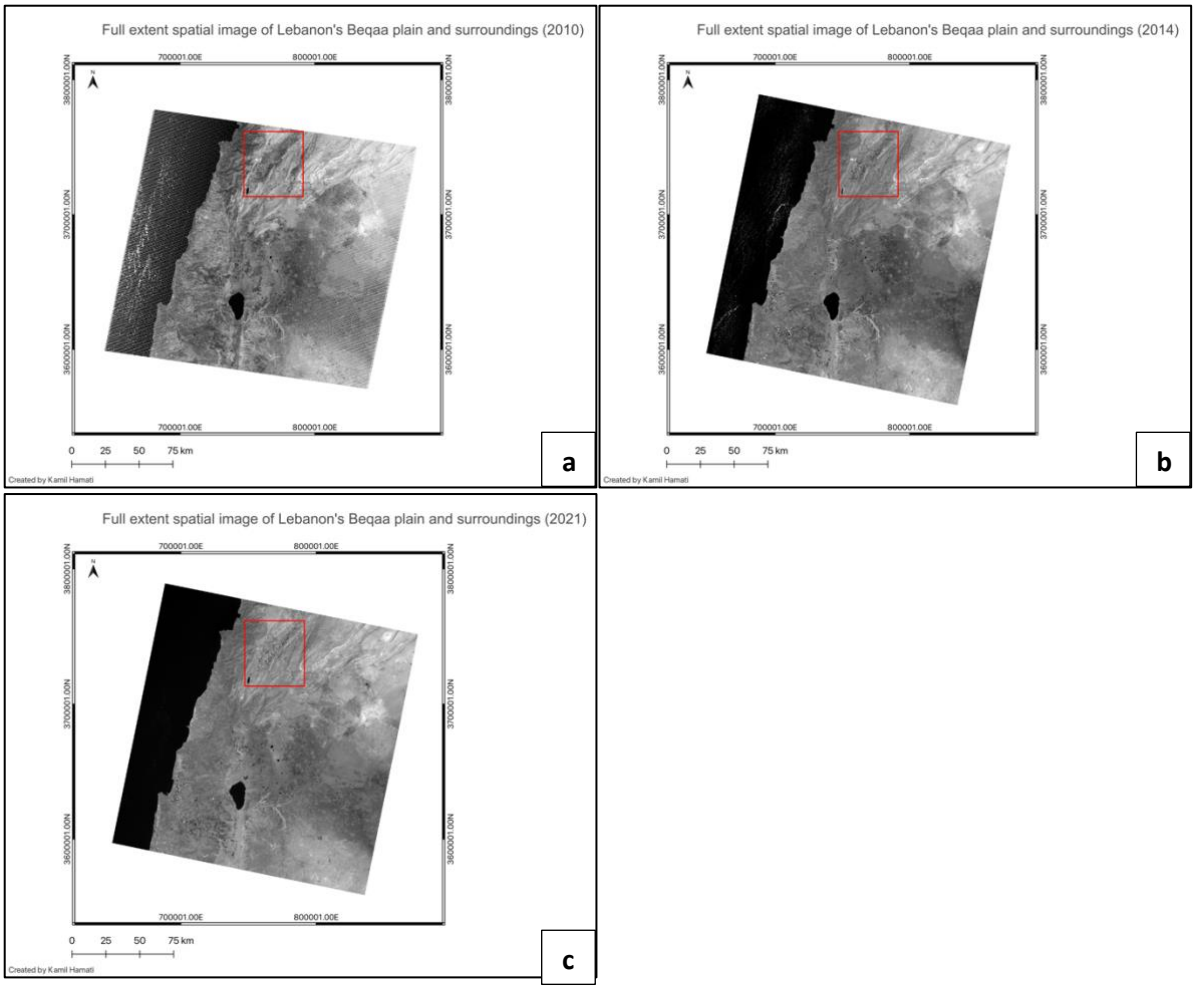

*Figure 6: Full extent spatial images downloaded for treatment and showing the AOI inside the red quadrant (**a**: Landsat 7, 2010; **b**: Landsat 8, 2014; **c**: Landsat 8, 2021))*

An untreated and zoomed-in computational region can be seen in Figure 7 (a, b, c) for 2010, 2014, and 2020 respectively. Unless indicated otherwise, this constituted the basis of the spatial analysis throughout the study.

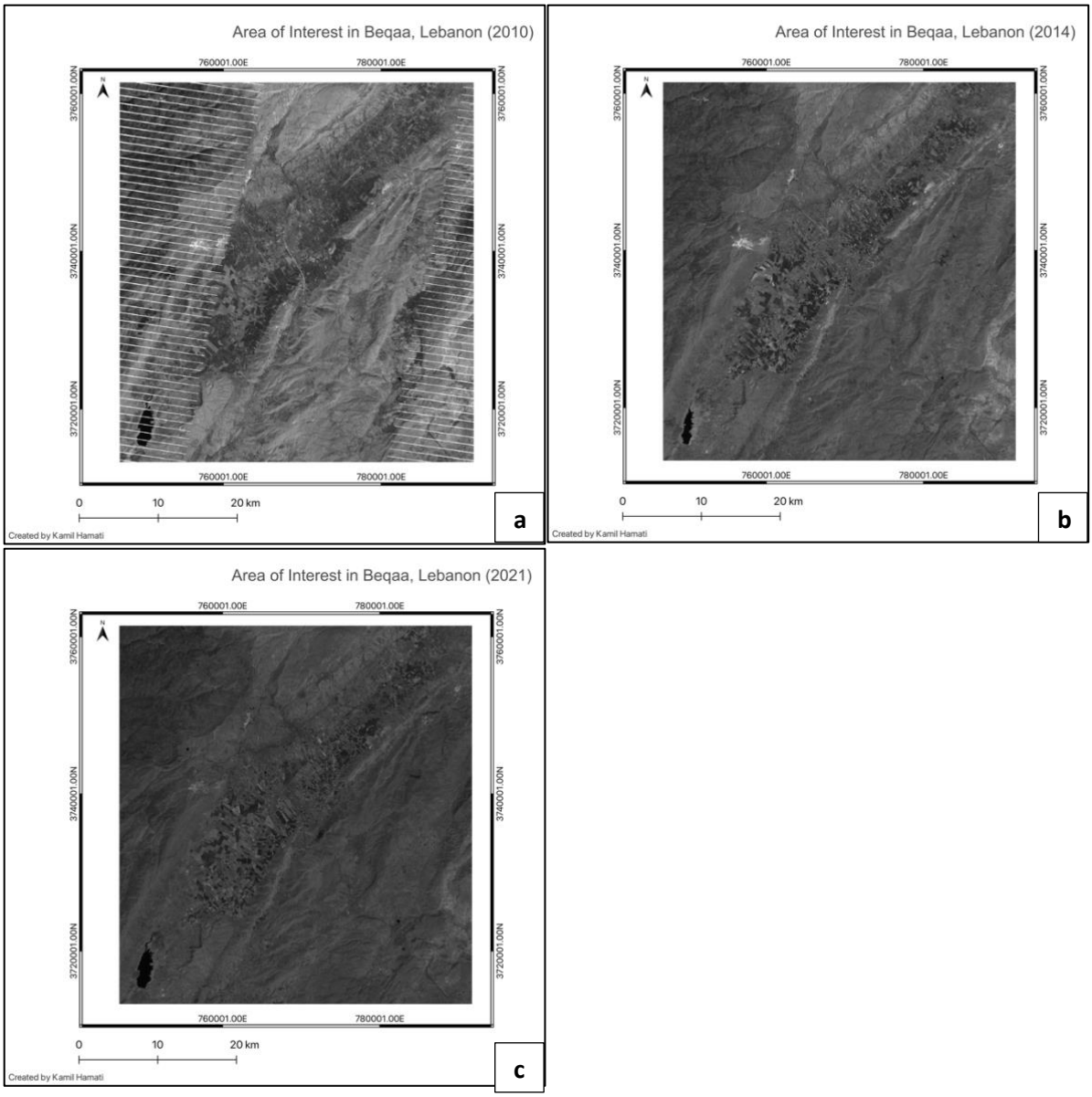

*Figure 7: Evolution of the AOI across time through untreated spatial images (**a**: 2010; **b**: 2014; **c**: 2021)*

All images were treated in Grass GIS 7.8.5. and were produced in map form using QGIS 3.16.16-Hannover.

2.3. Treatment of spatial images

As spatial images are acquired through different satellites, adequate and tailored pre-treatment had to be performed to facilitate the inter-comparability of the images, and therefore the analysis. Additionally, different band combinations were used in order to highlight a certain feature that serves the analysis. The entirety of this information is detailed in the following sections.

2.3.1. Band combinations

Each spatial image consists of several spectral bands, each of which is useful to emphasize ground features that are reflected within the band's spectrum of wavelengths. Different satellites capture images within different bands of wavelengths, as is the case in this study; for instance, Landsat 7 captures the red spectrum of wavelengths on Band 3 whereas Landsat 8 captures it on Band 4. In other terms, in each spatial image, each band is a distinct spatial image carrying a specific spectrum

of wavelengths captured at the exact same moment and the exact same position. Therefore, building upon the concept of additive synthesis of primary colors[11], allocating a different band to each primary color category (known as band combinations), thus producing a composite image, is an ideal way of visualizing ground features in colors. For instance, a true color image, visible to the human eye, allocates the red band to a red lens, the green band to a green lens, and the blue band to a blue lens. The result is useful in simulating an image seen through the human eye or a standard camera, and therefore in providing a quick overview of changes in a certain geographical area ahead of diving deeper in remote sensing analysis.

The band combinations that are used through this report are detailed in Table 3 below:

Table 3: RGB composite images used in the study

Composite image	Landsat 8			Landsat 7		
	Red	Green	Blue	Red	Green	Blue
True colors	4	3	2	3	2	1
False colors (Urban)	7	6	4	7	5	3
Agriculture	6	5	2	5	4	1
Land/Water	5	6	4	4	5	3

2.3.2. Multispectral transformations

To ensure accuracy in the treatment and analysis of our spatial imagery, we proceed with a transformation of all zero (NULL) values to "No Data" for all the images that are to be processed. Second, and as Landsat image pixels are stored as Digital Numbers (DN), they will need to be transformed to reflectance using GRASS' *i.landsat.toar* function, in order to facilitate the analysis of vegetation and water indexes.

2.3.3. Modified Normalized Difference Water Index (mNDWI)

The Modified Normalized Difference Water Index, summarized as mNDWI, was developed as an enhanced version of its predecessor the Normalized Difference Water Index (NDWI) as it is more accurate in the sense of removing noise created by urban areas (Ana Fernández Torralbo & Pablo Mazuelas Benito, 2012; Xu, 2006) and has shown more accuracy than its predecessor when used in temporal studies (Huang et al., 2018) such as the case here. It is calculated using the following formula:

$$mNDWI = \frac{GREEN - SWIR1}{GREEN + SWIR1}$$

2.3.4. Assessment of the trophic state of water

Researchers have been able to model band calculations that allow for the exact estimation of chl-*a* in water bodies using satellite imagery. Of particular pertinence to the context of this study, Fadel et al., (2016) not only assessed *chl-a* in the Qaraoun reservoir using Landsat 8 OLI images and validated their spatial analysis with in-situ samples, but they also made available their formula to replicate their measures and assessments with high accuracy.

$$chl_a = \frac{\left(\frac{B2}{B4}\right) * B5 - 98}{0.75}$$

[11] This principle consists in producing all colors through a combination of only three primary colors, Red, Green, and Blue, hence the name "the RGB system".

Where B2, B4 and B5 represent Bands 2, 4, and 5 respectively (Blue, Red, NIR). As the range of wavelengths identified by Fadel et al., (2016) in their calculations was applicable to Landsat 7 bands' wavelengths, we substituted Landsat 8 bands in the formula with their corresponding Landsat 7 bands and performed the calculation that allowed us to estimate chl-*a* concentration using Landsat 7 images, and consequently to estimate the trophic state of water across time.

2.3.5. Normalized Difference Vegetation Index (NDVI)

This index is usually calculated to assess changes in vegetation health and density using values that range between -1 and 1. A NDVI closest to 1 indicates a densely vegetated area, whereas near 0 or negative values represent water or built-up areas (Viana et al., 2019). More accurately, NASA suggests the following intervals to interpret NDVI values: 0.1 and below correspond to barren rock, sand, or snow; 0.2 to 0.3 indicate shrub and grassland; whereas 0.6 to 0.8 usually indicate temperate and tropical rainforests (John Weier & David Herring, 2000). NDVI is calculated using NIR and Red bands with the following formula:

$$NDVI = \frac{NIR - RED}{NIR + RED}$$

Within the scope of this study, NDVI does not cover the desired indicators, but is nevertheless essential for the classification step, and is therefore produced, but not visualized in the study.

2.3.6. Land-cover classification using Object Based Image Analysis (OBIA)

Classification is normally used to show distinctive categories in a spatial image to identify and quantify land cover features. OBIA classification techniques replicate what the human eye does, and bring the best classification technology to spatial imagery by using segmentation, which groups small, similar pixels together and makes it possible for the user to classify segmented objects using their spectral, geometrical, and spatial properties (Allenbach et al., 2021; GISGeography, 2021). Once the image is segmented using the adequate parameters (number of iterations, difference threshold, minimum number of cells), transformed into a vector, and is attributed the statistical values of the NDVI raster, classes were created using ranges of NDVI values based on the work of Akbar et al., (2019), which attributes land cover classes to NDVI average values as per the following:

Class	**NDVI Range**
Water	-0.28 - 0.015
Built-up	0.015 - 0.14
Barren land	0.14 - 0.18
Shrub and Grassland	0.18 - 0.27
Sparse vegetation	0.27 - 0.36
Dense vegetation	0.36 - 0.74

2.3.7. Night-time imagery

Night-light data was collected between 1992 and 2013 by the United States Air Force Defense Meteorological Satellite Program (DMSP) Operational Linescan System (OLS). More recently, the Visible and Infrared Imaging Suite (VIIRS) Day Night Band (DNB) on board of the Joint Polar-orbiting Satellite System (JPSS) has been collecting night-light data of better quality compared to the DMSP-

OLS. Although identical in purpose, data from these two systems needs to be homogenized in order to be usable for temporal comparisons. Li et al., (2020) provide an open-source dataset of harmonized images that are ready to use by GIS professionals; this provided the source of our 2010 and 2014 images. However, the limitation with this dataset was the choice of days and months as the images represent spans of entire years.

Additionally, NASA provides an interactive online tool for visualizing and downloading night-light spatial imagery, which was used to download the image for 2021. The online platform provides the option to download an image as a snapshot, with the user being able to choose the resolution and format of the downloaded image. As the 2021 image did not go through the same harmonization process as the first two, it was rescaled using Grass software (r.rescale) to fit the DN scale of the harmonized dataset (0-64), and it was reprojected and realigned with the remaining rasters to match their projection and geographical positioning, thereby allowing a correct comparability, using QGIS software (Warp(Reproject), and Align Rasters, respectively).

Intensity of light in nighttime spatial images can be read through the DN number, i.e., from 0 to 64, with 64 being the brightest light or the highest light intensity. This makes it easier to interpret the images that were produced for this report in the following sections.

3. Results and discussion

A first “true color” look at the AOI provides us with an overview of the situation on the ground and its evolution between 2010, 2014, and 2021. As illustrated in Figure 8 below (a, b, c), and although not yet processed, the images clearly show an oscillation in the size of the Qaraoun reservoir (circled in red) between the three years which may be attributed not only to anthropogenic activity and uncontrolled water withdrawals, but also to weather conditions as this reservoir collects annual rainfall in the region for later use (International Resources Group, 2011; Jurdi et al., 2002). Additionally, a reduction in the density of the green area that represents the Beqaa plain is visible across the years along with an increase in a red tint that might insinuate desertification (upper right quadrant of the 3 images). However, these remain dubious allegations without a deeper analysis and processing of these images to extract the necessary information to validate or refute these claims. The said processing and analysis were guided by the choice of indicators laid out in Table 1, above, and eventually led to the production of the spatial images that are analyzed in the following sub-sections.

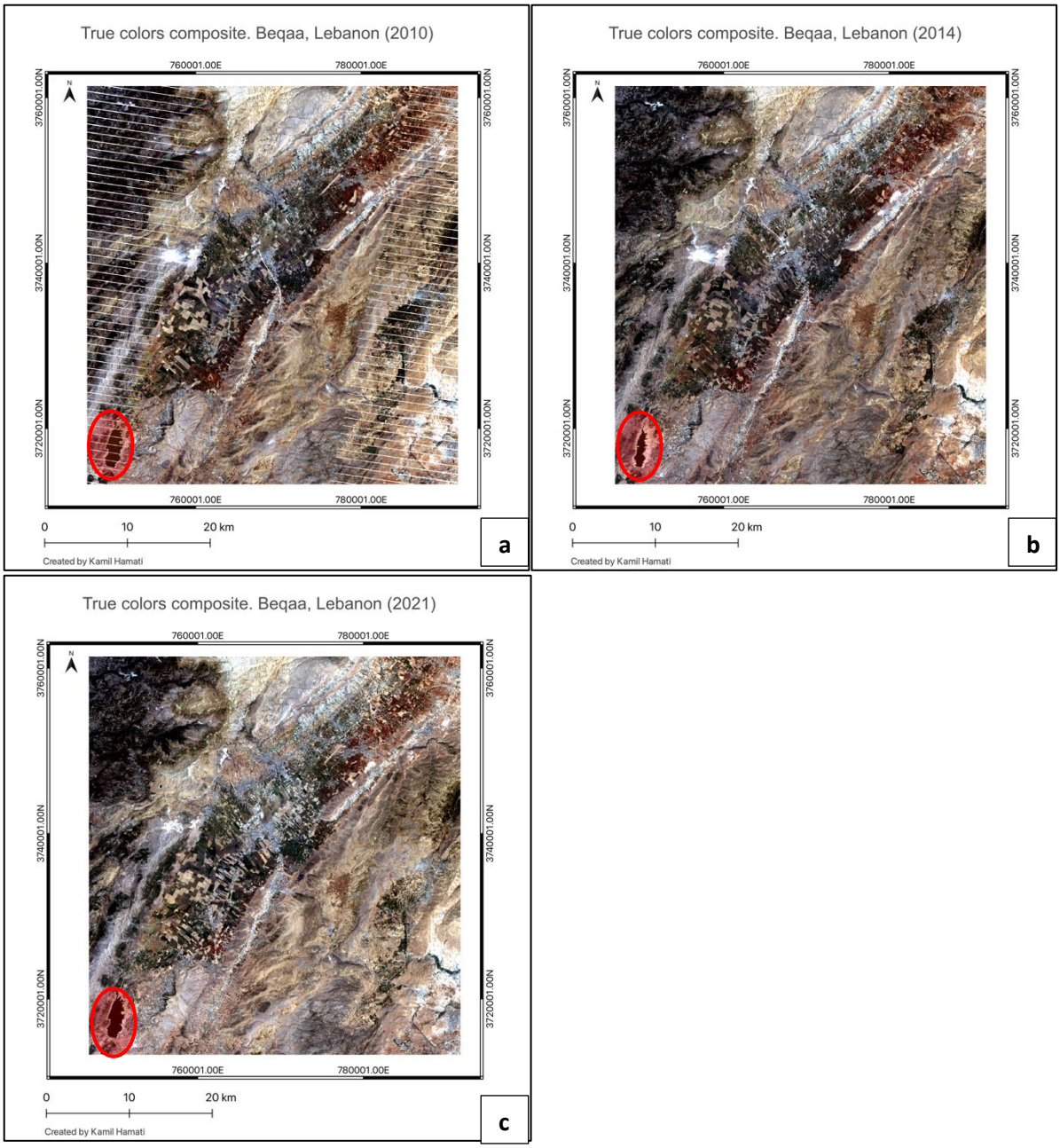

*Figure 8: "True Color" composite images of the AOI in 2010 (**a**), 2014 (**b**), and 2021 (**c**). The RGB composite for (**a**) is 321 whereas for (**b**) and (**c**) it is 432*

3.1. Environmental boundaries

A quick overview of the situation in the AOI may be acquired using false color band composites, which serve to highlight certain features, depending on the order of the bands. Figures 9, 10, and 11, below, highlight respectively, agriculture in the AOI and its evolution across time, urbanization, and land and water features to give an overall idea of the analysis to be expected out of the following sub-sections[12].

[12] These same figures may be found in a larger format under Annex 2 of this document for ease of analysis and reference.

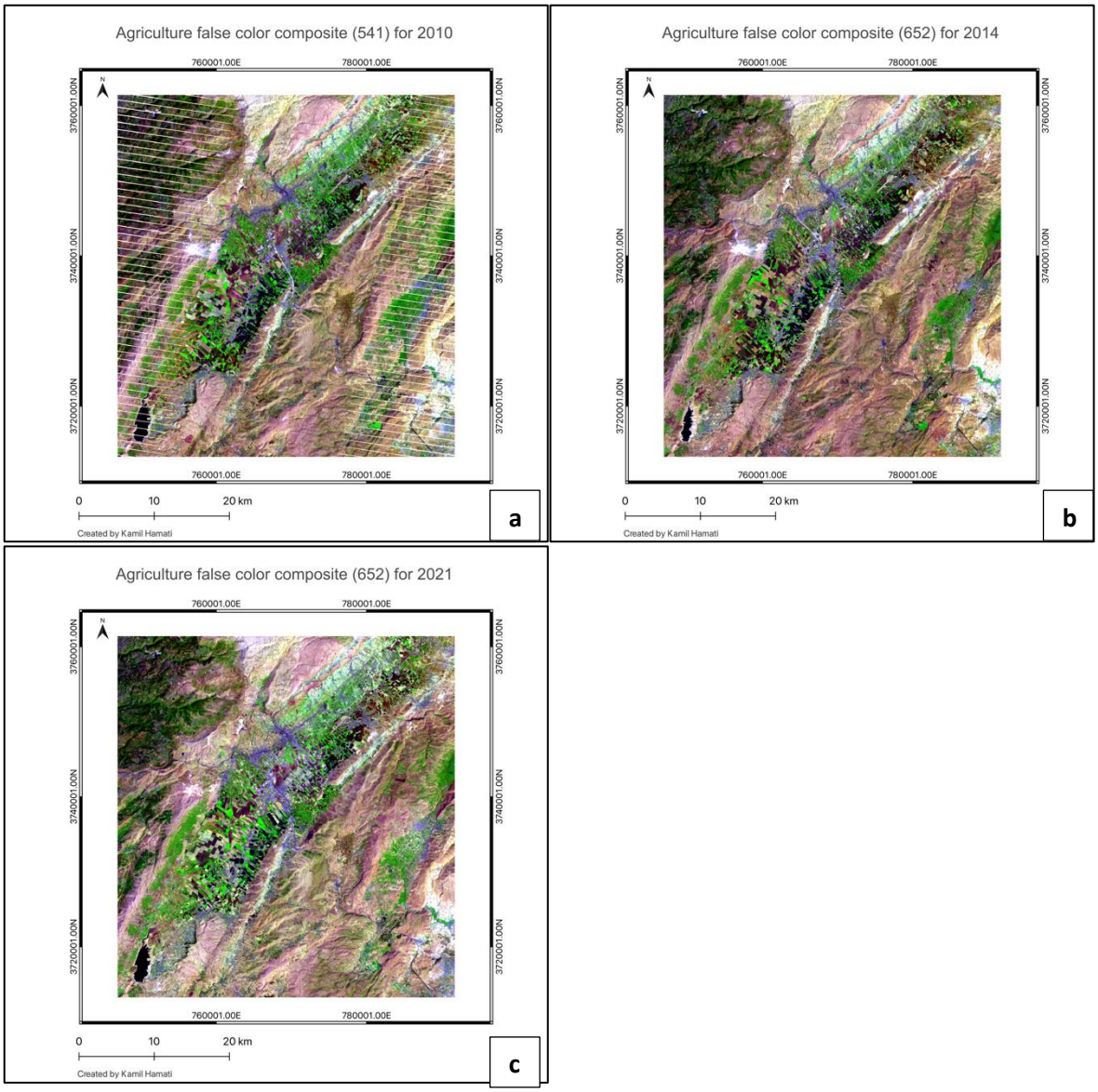

*Figure 9: False color composites showing agricultural changes between 2010 (**a**), 2014 (**b**), and 2021 (**c**)*

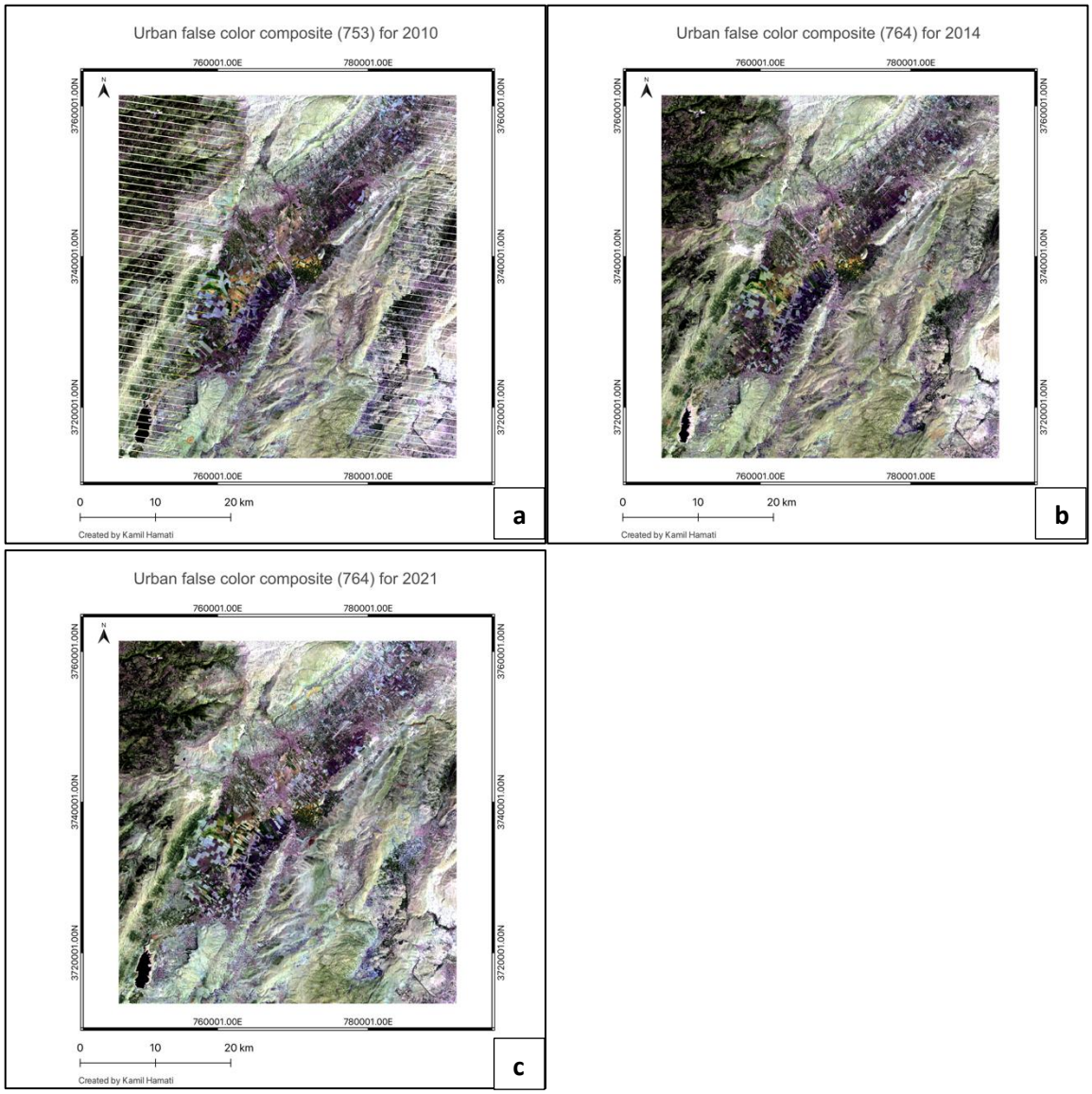

*Figure 10: False color composite images showing changes in urbanization in the AOI in 2010 (**a**), 2014 (**b**), and 2021 (**c**)*

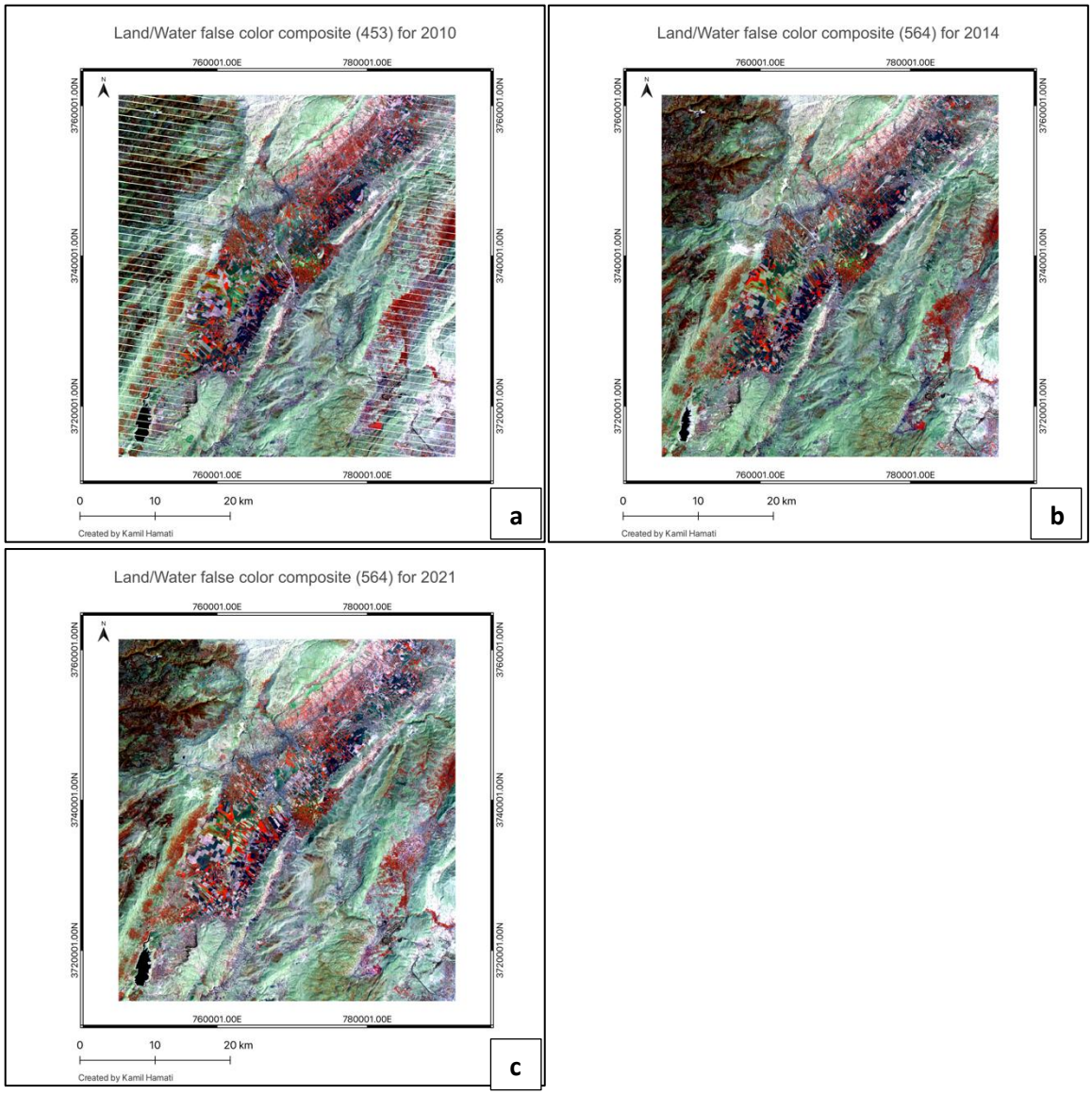

*Figure 11: False color composite images highlighting land and water features and their changes between 2010 (**a**), 2014 (**b**), and 2021 (**c**)*

Through these images, environmental changes (both natural and built) can be discerned, although neither with high precision nor with measurable scale. Nevertheless, this provides a vague idea of the direction in which this study is heading.

3.1.1. Biogeochemical flows (Nitrogen and Phosphorus cycles)

This boundary represents the Nitrogen and Phosphorus cycles, which are both indicators of the quality of water bodies. High concentrations of nutrients, such as – notably – Nitrogen and Phosphorus, lead to eutrophication of water bodies, which may be detected and calculated using remote sensing and spatial imaging techniques such as NIR reflectance.

Water quality analysis in different points of the Litani river basin, and most notably in the Qaraoun reservoir reveals high levels of Chemical Oxygen Demand (COD ≥ 250 mg/L) (World Bank, 2003), low phytoplankton biodiversity, and regular blooms of toxic cyanobacteria (*Aphanizomenon ovalisporum* and of *Microcystis aeruginosa*) (Fadel et al., 2014). Analysis of water samples from the river across several years show concentrations of Phosphates and Ammonia frequently surpassing 10-fold their recommended thresholds (0.1 mg/L and 0.35 mg/L to 7 mg/L respectively (Canadian Council of

Ministers of the Environment, 2010; Environmental Protection Agency, Ireland, 2001; Yasmina El Amine, 2019)) (Figure 12). Additionally, the Qaraaoun water reservoir, located on the Litani river, was found to be hypereutrophic[13] since 2004 – almost 40 years after its construction (Fadel et al., 2014). This information is sufficient to conclude that the Litani river does indeed suffer from a serious eutrophication problem, and that this indicator is valid to be used as a spatial proxy to assess water quality.

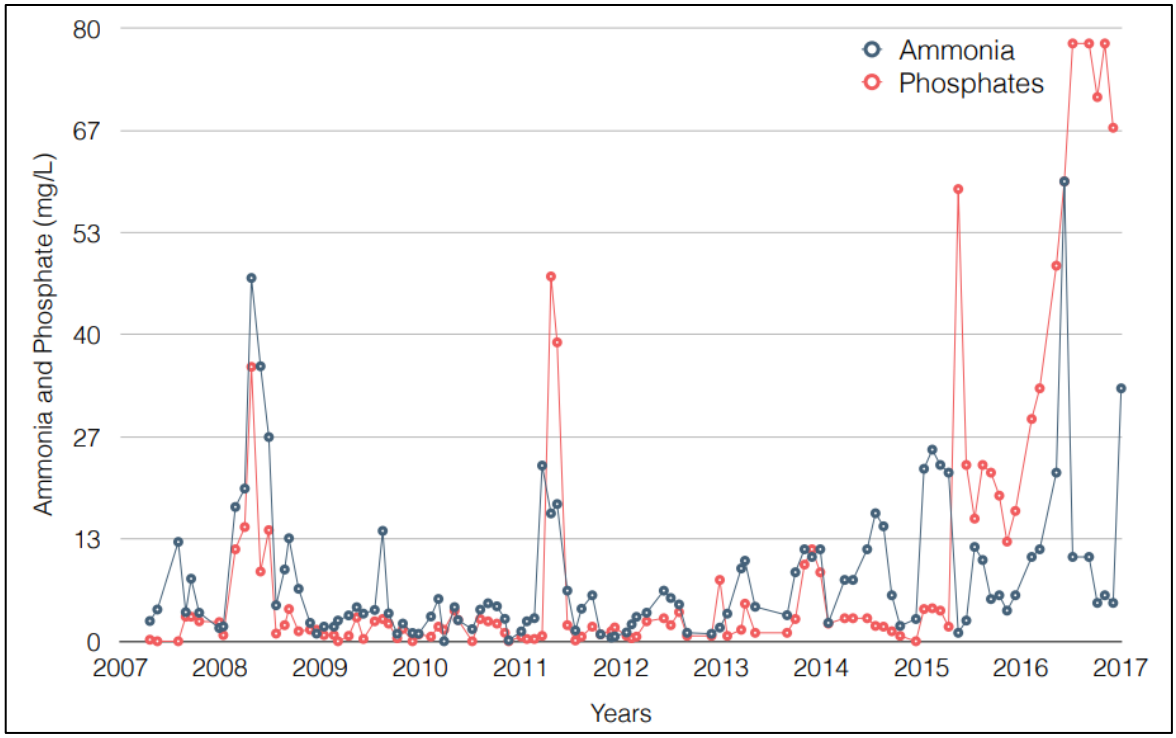

Figure 12: Ammonia and Phosphate levels in the Litani river (2007-2017). Source: (Yasmina El Amine, 2019).

Chlorophyll-a (chl-*a*) concentration has long been used as an indicator of the trophic state and productivity of waterbodies (Baydoun & Amacha, 2016) but as regular monitoring of environmental parameters is not always available in developing countries, researchers resorted to using remote sensing to estimate chl-*a* in water bodies, and thereby to estimate their trophic state (Baydoun & Amacha, 2016; Hussein & Assaf, 2020; Watanabe et al., 2015). Particularly, in 2016, Fadel et al., (2016) not only suggested using remote sensing to assess *chl-a* in the Qaraoun reservoir and validated their spatial analysis with in-situ samples, but they also suggested a particular formula to replicate their measures and assessments with high accuracy for Landsat 8 OLI images. Assessment of the trophic state of the water may be done using the guiding values of Table 4, below. But simply put, the higher the concentration of chl-*a* in water, the lower is the quality of water and denser is eutrophication.

Table 4: Trophic state classification and equivalence in chl-a concentration (mg.m-3). Source:(Watanabe et al., 2015)

Trophic State	Ultraoligotrophic	Oligotrophic	Mesotrophic	Eutrophic	Supertrophic	Hypertrophic
Chl-a (mg.m^{-3})	≤ 1.17	1.17–3.24	3.24–11.03	11.03–30.55	30.55–69.05	> 69.05

[13] The trophic state of water, usually used to describe lake waters, refers to the levels of nutrients and algae in water. Hypertrophic waters, as the name indicates, contain excessive amounts of nutrients (phosphorus and nitrogen in particular) and algal growth (phytoplankton), which induces poor water clarity and restricts the anthropological usability of the lake and the habitat for fish (New Zealand Government, 2019).

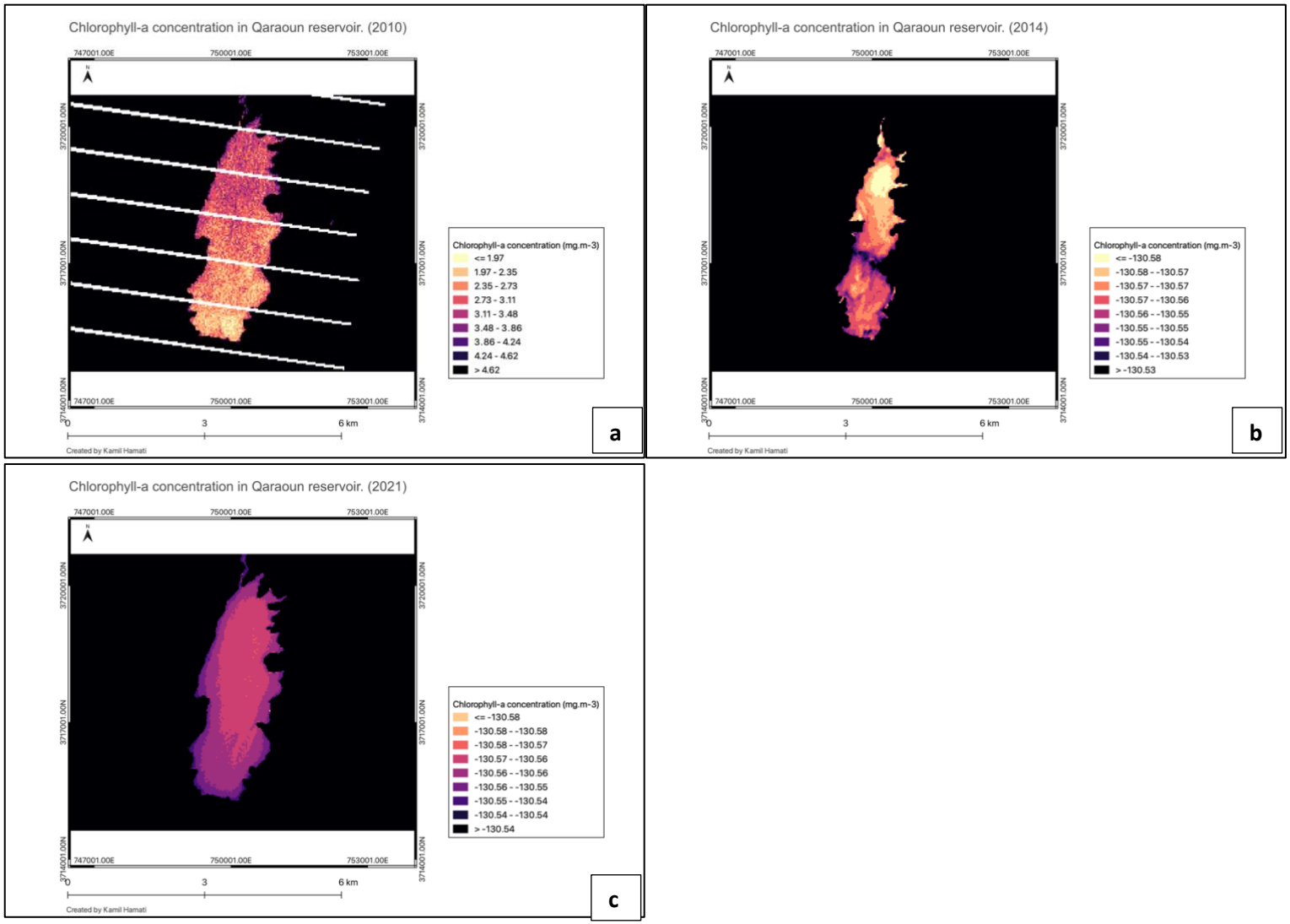

*Figure 13: Variation of chl-a concentration in the Qaraoun reservoir between 2010 (**a**), 2014 (**b**), and 2021 (**c**)*

On one hand, the choice of Landsat images for 2010 was limited within the restrained timeframe, which, eventually led to the jeopardizing of the quality of the image, as can be clearly seen with the white stripes in Figure 13 (a). This has significantly inhibited our ability to use and interpret this image in the context of trophic state analysis. On another hand, it is interesting to note that, contrary to the findings of the MoE's reports, poor water conditions of the Litani river have been attributed to high agricultural runoff and discharge of wastewater in the river on top of quasi absent monitoring of water quality and poor governance since the early 1990s (Baydoun & Amacha, 2016; Darwish et al., 2021; Shaban, 2014; Yasmina El Amine, 2019). Therefore, it would be interesting for future research ventures to explore a longer temporal comparability starting from the 1990s and until 2021 (including another period in 2010, 2014, and 2021, all while noting the fluctuations of the Qaraoun reservoir throughout the seasons, as noted by Fadel et al., (2016)).

Lebanon treats only 8% of its generated wastewater, while the rest is discharged into open lands or waterways, a practice that is particularly pertinent to the Beqaa region and specifically to the Litani river basin and that dates to the early 1990s, which is well before the influx of the Syrian refugees (Deutsch & Alameddine, 2018; Food and Agriculture Organization of the United Nations, 2008; Haydar et al., 2014; Lebanese Republic, Ministry of Environment & United Nations Development Programme, 2011; Mcheik et al., 2018; Saadeh et al., 2012; Shaban, 2014, p. 20). Additionally, Deutsch and Alameddine, (2018) recorded an increase in eutrophication during summer months over the period 2005-2015 as compared to the 20 preceding years, accompanied by an increase in the variability of chlorophyll-a concentrations, and a domination of algae in the Qaraaoun reservoir. These results, as well as those of Fadel et al., (2014), attribute the persistent problem of eutrophication to increased anthropogenic pressures within the area of the basin, which is consistent with Wetzel, (1992)'s observations where the increased nutrient load from anthropogenic sources led to eutrophication of many aquatic systems across the world. In this context, Jurdi et al., (2002) attribute the increased anthropogenic pressures in the Litani river basin area to rapid and unregulated growth in local agriculture and industry, observed as of the end of the Lebanese civil war in 1990. On this, agricultural practices in Lebanon reportedly involve heavy use of fertilizers and pesticides; for instance, in 1999, Lebanon reportedly imported 1530 tons of pesticides and around 32000 tons of fertilizers (World Bank, 2003), which, when applied in agriculture in Lebanon would be consistent with the registered high prevalence of water pollution. These findings, on top of remarks made by the MoE on the accuracy of the methodology, data, and results presented in their report, raise legitimate doubts about the claims that point the finger to refugees being solely to blame for the Litani's pollution.

3.1.2. Freshwater use (Blue water withdrawal as % of mean monthly river flow)

Increased population counts insinuate larger demand for water, whether it is for drinking, cooking, hygienic or domestic use, or other non-domestic purposes.

The Litani river is the longest in Lebanon and it is one of three rivers whose basins cover around 45% of Lebanon[14], yet it is the only one to run entirely in Lebanon. Along with a high per capita share of renewable water resources and a high yearly precipitation rate, this gave Lebanon the reputation of the "water tower of the middle east" (Shaban, 2011). However, this is no longer the case as the per capita share of renewable water resources in Lebanon has entered the "water stress" zone estimated at 740 m^3/capita/year (Food and Agriculture Organization of the United Nations, 2019), and the Litani river's stream flow is decreasing over time (Shaban et al., 2014). The latter can be attributed to three main factors:

[14] The Assi (Orontes) river in the north, the Hasbani in the southeast, and the Litani in the east and south.

I) Anthropogenic interference manifested through unsustainable water use across different areas of the country and through unregulated and illegal well-drilling, which was also reported by Khoury et al., (2015) and El-Kareh et al., (2018);

II) Lebanon's predominant geological structure of karstic limestone which affects the capacity for groundwater recharge, consistently with what was noted by the Food and Agriculture Organization of the United Nations, (2008); and

III) Climate change, particularly temperature rise which would affect the water balance as precipitation rates were not expected to change, as was already estimated by Shaban, (2011) and Bou-Zeid and El-Fadel, (2002) who concluded that Lebanon is expected to suffer from water shortages as an eventual impact of climate change.

Mismanagement of wastewater and waste disposal into rivers and streams which has negatively affected water quality in the Beqaa region, as clearly seen through the deteriorating quality of the Litani river, was only one of the major factors that predisposed the Beqaa region to conflict over water resources. Other contributing factors included the unorganized institutional management of water resources that created uncertainty over the role of each stakeholder in the water sector and the extents of their responsibility. Additionally, the sudden influx of Syrian refugees to the Beqaa region – particularly those residing in informal tented settlements – is believed to have increased demand on water resources through illegal practices of network tapping, or due to their dependency on trucked water, which commonly comes from illegal and unregulated pumping from surface and subsurface sources (El-Kareh et al., 2018). This increase in demand was also identified as one of the major factors that contributed to increased tension over water resources in the Beqaa region (El-Kareh et al., 2018). Figure 14 and Figure 15 below, map both the predisposition to water conflict as well as the increased demand on water resources in the Beqaa region.

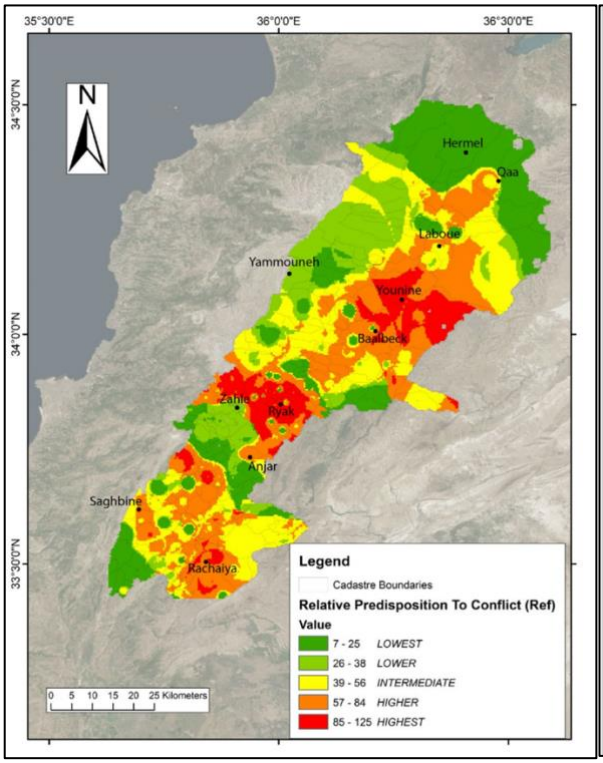

Figure 14: Predisposition to water conflict in the Beqaa region. Source: (El-Kareh et al., 2018)

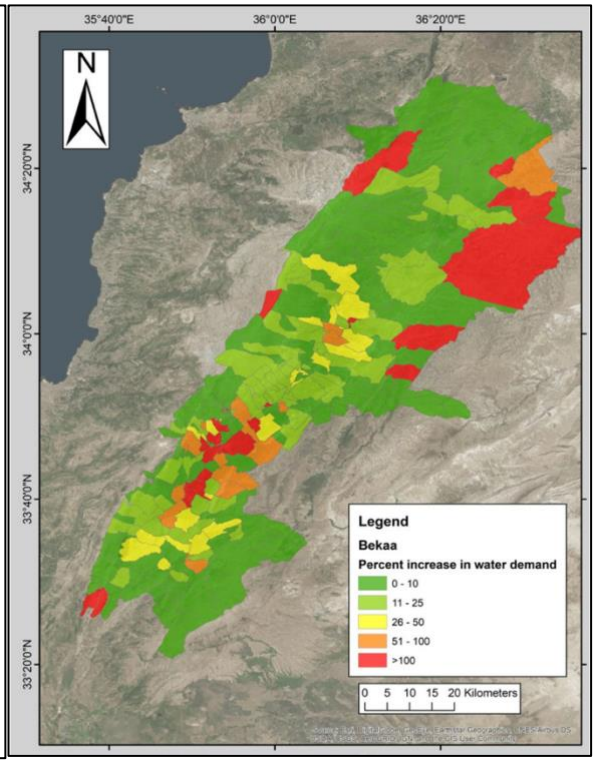

Figure 15: Water demand increase caused by the influx of refugees. Source: (El-Kareh et al., 2018)

Water changes spanning a certain timeframe are easily estimated through remote sensing using specially dedicated indexes. The Normalized Difference Water Index (NDWI) as well as its more recent version, the Modified Normalized Difference Water Index (mNDWI) are the most popular among their peers, especially that the mNDWI performs better than its original version at removing noise created by urban areas (Ana Fernández Torralbo & Pablo Mazuelas Benito, 2012; Xu, 2006). Additionally, the mNDWI has shown to be more accurate when used in temporal studies, such as this one (Huang et al., 2018).

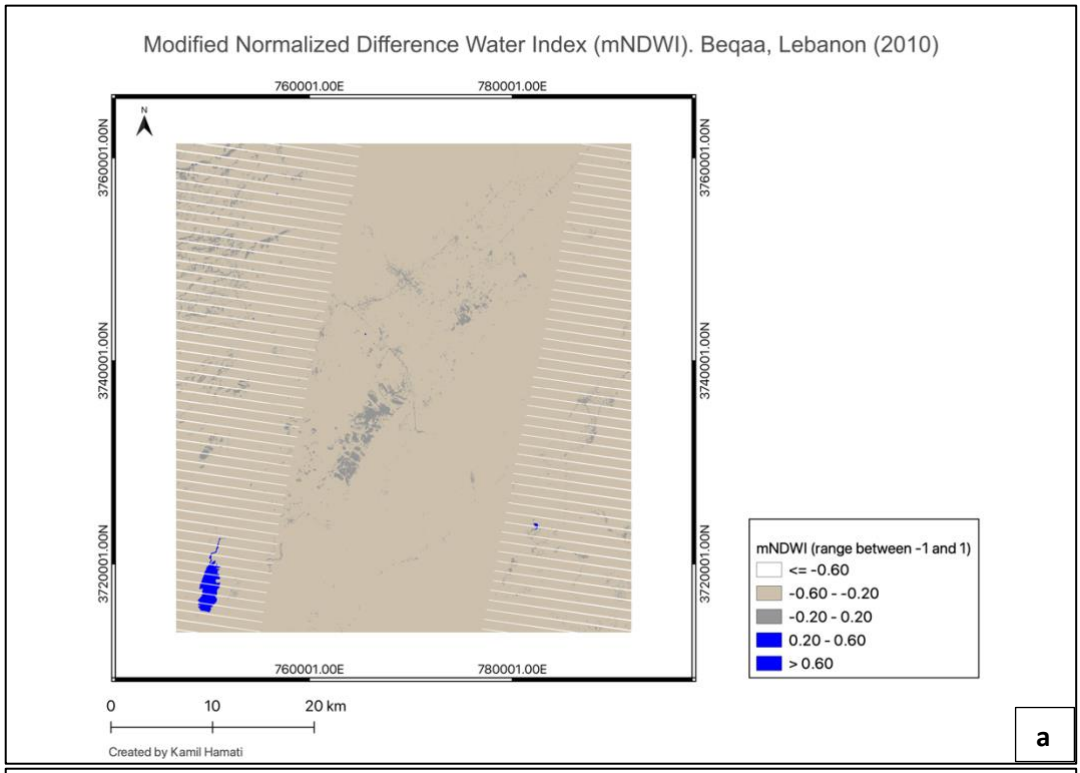

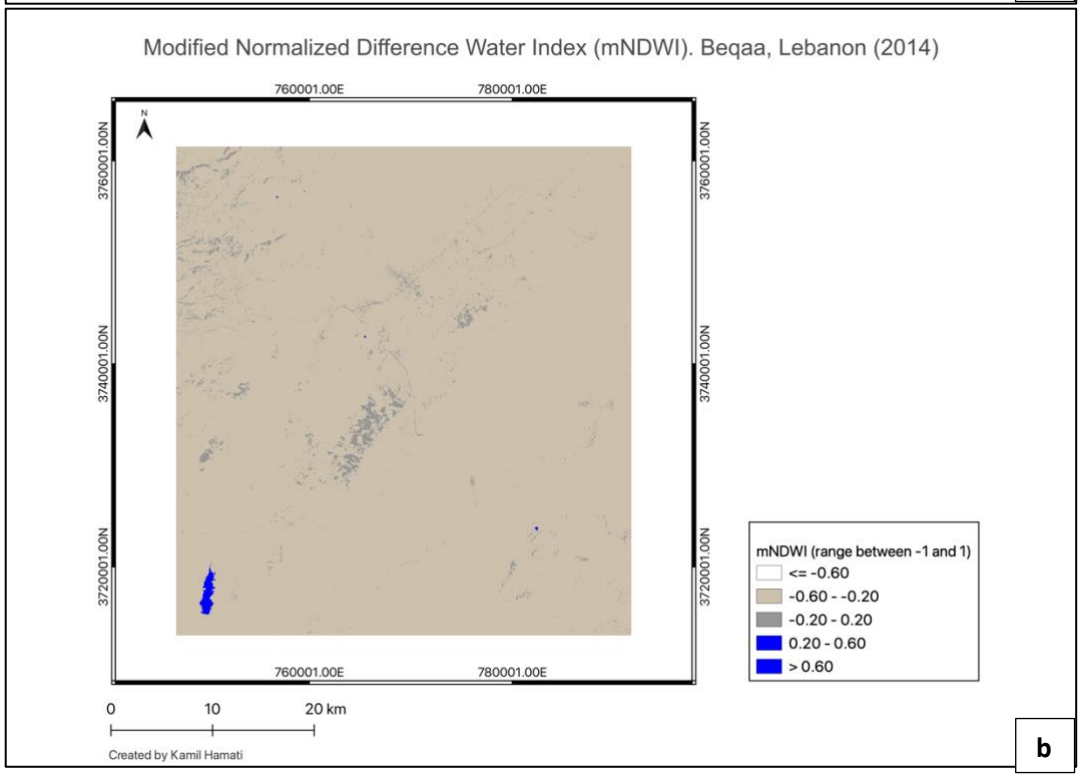

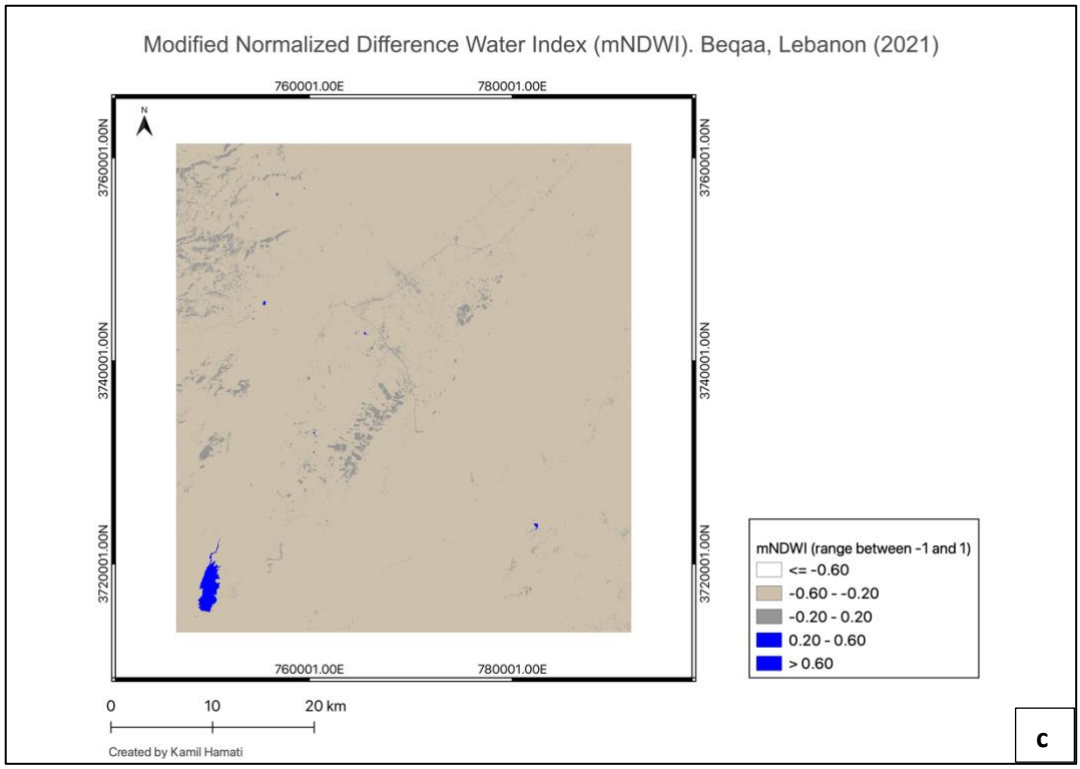

*Figure 16: mNDWI for 2010 (**a**), 2014 (**b**), and 2021 (**c**) in the AOI in Beqaa, Lebanon. mNDWI values normally range between -1 and 1.*

The issue of the size of the Qaraoun reservoir is also recurrent in this phase of the analysis where Figure 16(b) shows a clear contrast with both (a) and (c) insinuating a lower stock of water in 2014. Additionally, small patches of water can be identified across all three pictures, but with a more pronounced prevalence in 2021. Given the general practice of illegal drilling of wells and canalization of water to individual farms (El-Kareh et al., 2018; R. Khoury et al., 2015), this could provide one explanation of the identified scattered patches of water reservoirs.

3.1.3. Land cover change (Area of forested land as % of potential forest)

The Beqaa plain that is already subject to rapid and frequent land-cover change due to a lack of land management plans and inadequate urban regulations, which in turn are exposing the plain – among other areas – to over-exploitation and degradation of lands, is witnessing an increasing trend of urban sprawl at the expense of forest land and brushwood, as found by Hassan et al., (2019). On top of that, the Lebanese Republic, Ministry of Agriculture, (2018), estimates that around 67% of the Lebanese territory is at high- or very high- risk of land degradation, and they attributed the loss of cropland in the Beqaa during the period 2000 – 2010, to unregulated and ill-planned urban sprawl. Additionally, Pollock et al., (2019) found that the risk of landslide in Lebanon was accentuated on one hand by manifestations of climatic changes – such as severe weather events – and on another hand by the lack of consistent and organized urban planning policies in the country. Additionally, the authors identified increased risk of landslide due to the chaotic urbanization that followed the sudden influx of Syrian refugees and attributed the cause to the government's no-camp policy that drove refugees to live either in already densely populated urban areas, or in makeshift informal tented settlements where their risk factor increased 9-11 times compared to urban populations, due to the sub-standard, risk-prone, and vulnerable nature of tented settlements.

However, to which extent has land cover changed in the Beqaa region? And does this change stem from the influx and settlement of refugees?

A primary analysis of the bidimensional diagram (or scatterplot) of the red and panchromatic bands for each of our spatial images allows us to have a preliminary idea of the composition of the different land cover classes in the image (soil, water, vegetation, etc.…), as illustrated in the example in Figure 17 below. Generally, land cover classes having no vegetation are adjacent to a "soil line" which is a line crossing the origin of the plot. Different vegetation classes are above this line due to their higher reflectance in the NIR band as compared to other visible bands, whereas water classes are normally close to the origin (Allenbach et al., 2021).

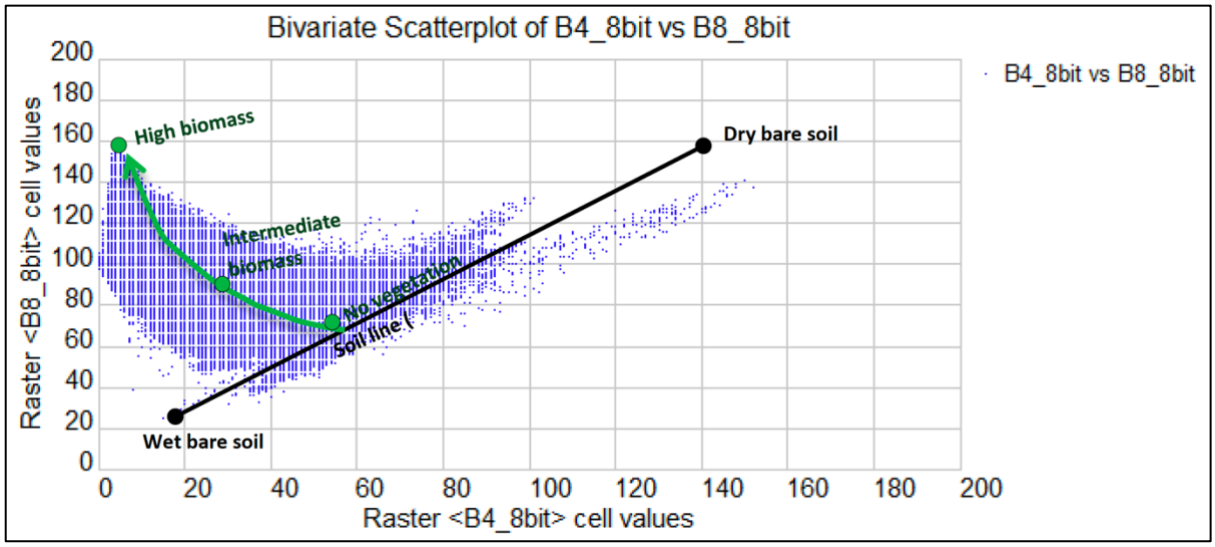

Figure 17: Example of a Bivariate scatterplot for analysis of land cover classes. Source:(Allenbach et al., 2021)

Our AOI's bivariate scatterplots for 2010, 2014, and 2021, shown in Figure 18 (a, b, c, respectively) shows a clear decrease in the density of vegetation biomass across years (decreasing range of Y axis) as well as in the density of dry bare soil, along with an increase of wet bare soil reflectance, which might be an indicator of an increase in informal tented settlements.

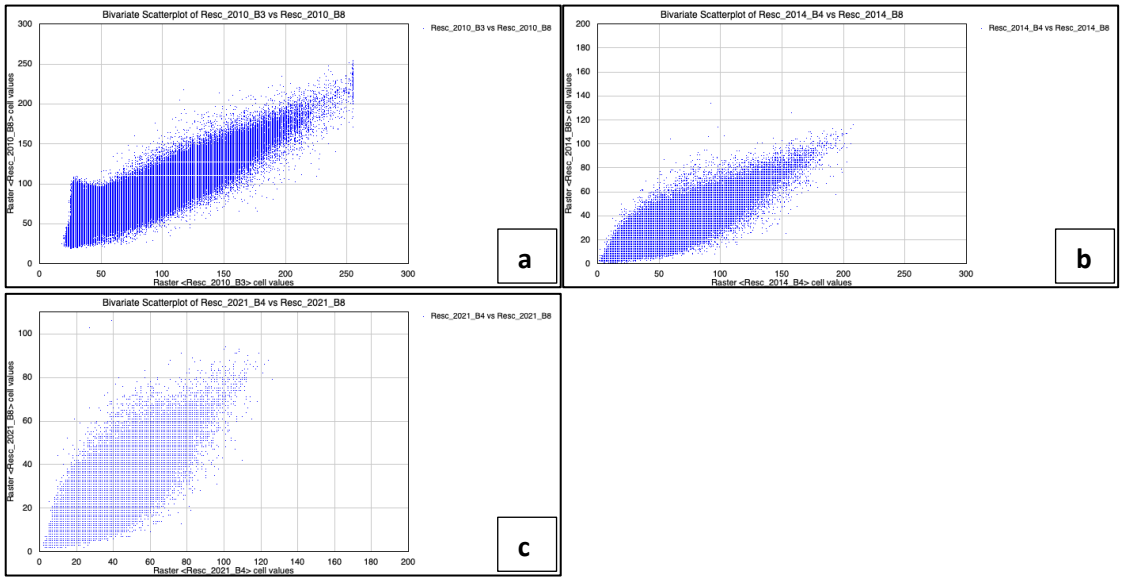

*Figure 18: Bivariate scatterplots of Landsat images used for our AOI for 2010 (**a**), 2014 (**b**), and 2021 (**c**).*

Further analysis through image classification reveals how and to which extents land cover has changed in the AOI across our studied period.

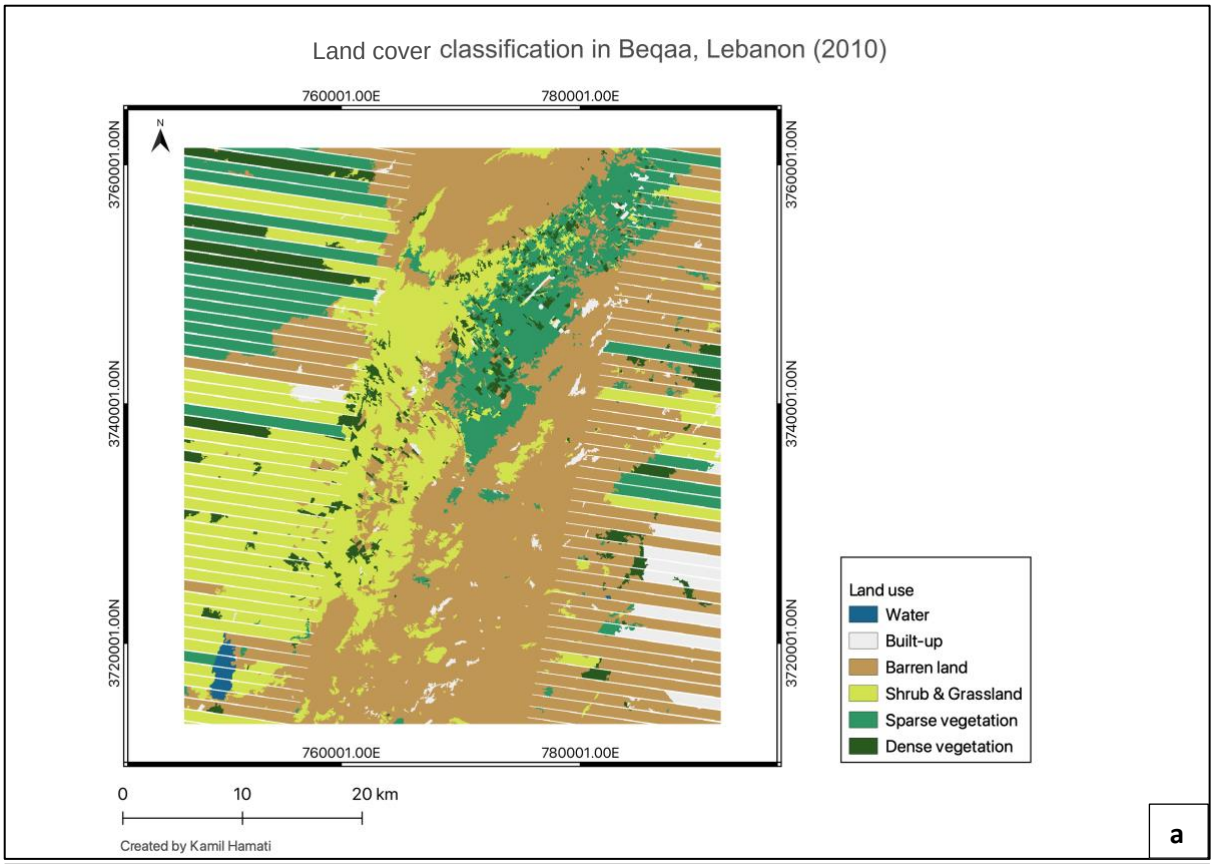
Land cover classification in Beqaa, Lebanon (2010)
760001.00E
780001.00E
3760001.00N
3740001.00N
3720001.00N
N
Land use
Water
Built-up
Barren land
Shrub & Grassland
Sparse vegetation
Dense vegetation
0
10
20 km
Created by Kamil Hamati
a

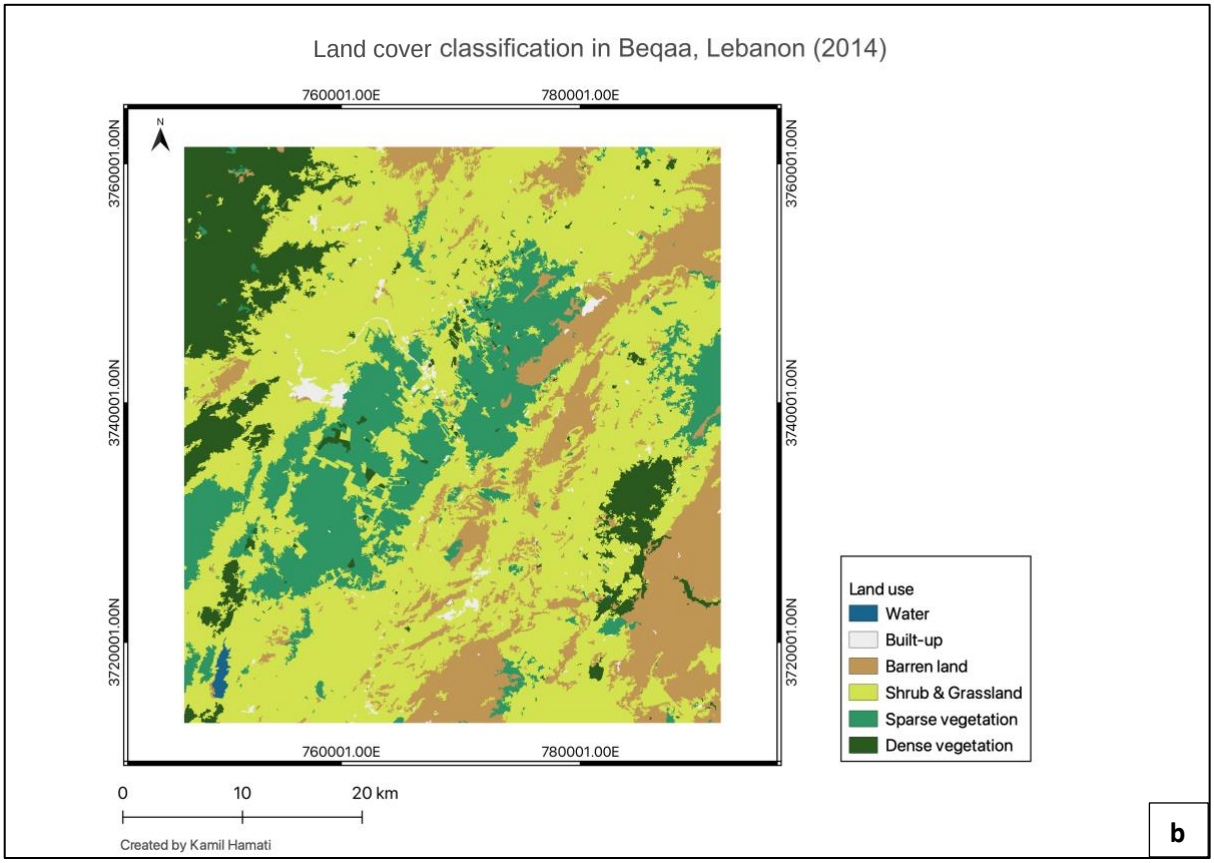
Land cover classification in Beqaa, Lebanon (2014)
760001.00E
780001.00E
3760001.00N
3740001.00N
3720001.00N
N
Land use
Water
Built-up
Barren land
Shrub & Grassland
Sparse vegetation
Dense vegetation
0
10
20 km
Created by Kamil Hamati
b

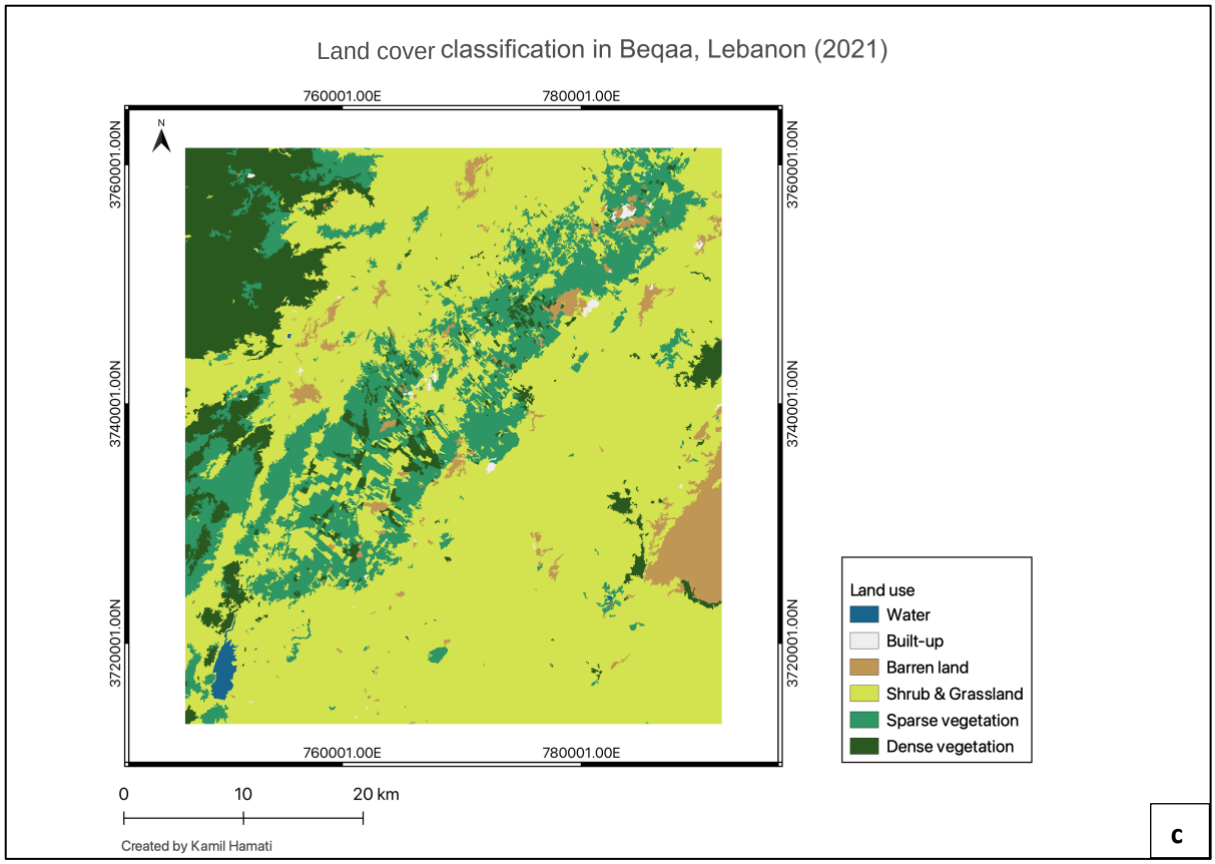

*Figure 19: Land cover classification for the AOI in 2010 (**a**), 2014 (**b**), and 2021 (**c**). Classification ranges based on NDVI values were adapted according to the recommendations of (Akbar et al., 2019).*

Apart from the distortion displayed in the image from 2010 due to the quality of the original Landsat image, land cover changes, visualized in Figure 19 above, are consistent with the primary analysis that we were able to extract from the scatterplots of Figure 18[15]. Indeed, there seems to be a decrease in barren land across years, and an increase in shrubs & grassland, and in sparse vegetation, which could as well be attributed to the informal tented settlements that are spread across the Beqaa plain where refugees might have used some land to grow consumable vegetables for their own needs. Statistical analysis of these changes in land cover, summarized in Table 5 below, highlights, in numbers, the extents of these changes. It should be noted here that, specifically for the 2010 Landsat image, a new classification category has appeared with the label "No data". This could be due to the visible distortions in the 2010 image which might have jeopardized the quality and the amount of data that can be extracted from the image. What is also interesting is the large decrease of built-up in the AOI across years. This gives way to several hypothesis, including an urban sprawl to the capital, Beirut, in search of better livelihoods.

[15] These same plots in Figure 18 may be found in a larger format under Annex 2 of this document for ease of analysis and reference.

Table 5: Raster statistics for classified rasters (2010, 2014, 2021)

	2010			2014			2021		
	Hectares	**Cell count**	**% Cover**	**Hectares**	**Cell count**	**% Cover**	**Hectares**	**Cell count**	**% Cover**
Water	648.27	7'203	0.3	398.07	4'423	0.18	742.59	8'251	0.34
Built-up	6'451.74	71'686	2.99	2'184.93	24'277	1.01	539.46	5'994	0.25
Barren land	98'353.53	1'092'817	45.54	36,409.68	404'552	16.86	8'616.78	95'742	3.99
Shrub & Grassland	54'249.21	602'769	25.12	118,749.06	1'319'434	54.99	143'825.31	1'598'059	66.6
Sparse vegetation	32'871.51	365'239	15.22	34,850.88	387'232	16.14	37'445.49	416'061	17.34
Dense vegetation	10'646.37	118'293	4.93	23,360.13	259'557	10.82	24'783.12	275'368	11.48
Total	203'220.63	2'258'007.00	94.10	2'583.00	2'399'475	100	215'952.75	2'399'475	100
No data	12'732.12	141'468	5.9						

Note: The "No data" category in the above table may be attributed to the quality of the 2010 Landsat image and its visible distortions, especially that this category does not show for the remaining treated images.

3.2. Socio-Economic boundaries

Three solutions are usually promoted by UNHCR to "enable refugees to live their lives in dignity and peace" (United Nations High Commissioner for Refugees, 2019c); these include voluntary repatriation, local integration, and resettlement. However, resettlement highly depends on receiving states and is usually offered to a very small proportion of refugees (Garnier et al., 2018) which is neither a rapid solution nor a sufficiently encompassing one. And in cases of continued violence at the home country, such as the case for Syrian and Palestinian refugees, repatriation is not an option.

This practically leaves receiving countries with local integration as their only response to accommodate their unexpected guests. However, albeit the situation on the ground showing no durable peace in sight, and amid fears of a protracted refugee crisis, Lebanon adopted a non-integration policy that seeks to return refugees to their home countries and that deprives them of access to certain services, resources, and internationally-accorded rights (Yahya & Muasher, 2018). This situation has left refugees in vulnerable situations, economically, legally, and physically (Aranki & Kalis, 2014; Dahi, 2014; Thorleifsson, 2014). In fact, 87% of Syrian refugees along with 67% of the poorest Lebanese are living together in areas most affected by poverty, high youth unemployment, and high demand for basic services. Consequently, this led to intensified social friction between refugees and hosts and to a prevailing anti-refugee sentiment as well as to a manifestation of xenophobia against refugees (Habib, 2019; Kheireddine et al., 2020; Nasser Yassin, 2019; Obeid et al., 2019).

In this context, the Safe and Just Space (SJS) framework suggests that sustainably peaceful societies are built through provision of a number of basic social and economic services within the boundaries of the carrying capacity of the hosting natural environment (Raworth, 2012). Having examined these environmental boundaries in the previous section, the following section serves to shed the light on the socio-economic boundaries (or basics) within which the Litani's basin's population has lived since before the refugee influx in 2011, and their evolution across time, in order to provide a clearer picture about the underlying reasons behind the tension in this area between locals and refugees.

A proxy and multidimensional indicator that is used to assess development of rural areas is night-time spatial imagery. Researchers believe that higher electrification rates lead to, and result from, more economic development (Burlig & Preonas, 2021). Other basic services that contribute to development include clean water and adequate sanitation and health facilities.

3.2.1. Energy (Population lacking access to electricity)

Since the civil war (1975-1990), power cuts in Lebanon have become an integral part of residents' daily life. This is rooted in a state-adopted strategy of rationing, which reflects the public sector's inability to meet the constantly increasing demand of the incessantly growing population. This strategy has consequently paved the way for an alternative energy market controlled by private generator owners, which deepened inequalities in access to electricity (Verdeil, 2019). Albeit official numbers showing that 100% of residents have access to electricity in Lebanon (World Bank, 2019), this only means that they are connected to the official grid, but gives no indication as to the availability of electrical current. The recent economic crisis that also had its toll on the energy sector exacerbated both the access and the availability gaps in this field, and left people with 1-2 hours of electricity per day in some regions (Anna Foster, 2021; France 24, 2021, p. 24; Ioanes, 2021). On average, 96% of refugee populations reported having access to electricity either from the public electricity grid or from diesel generators (through private distributors), and they reported having relied on private distributors for up to 13 hours/day in 2020, which engendered a bigger electrical bill (sometimes up to 6-fold the usual bill for the public grid). This, however, did not spare them electricity outages, as

they also reported more than 5 hours of complete electricity outage per day (United Nations Children's Fund et al., 2020).

With the disparity between official numbers, those that are reported by relief organizations, and the experience of the people on-site, spatial imaging and remote sensing provide the best technology to verify – to the best possible extents – the reality of the ground (Li et al., 2017, p.).

In closer relevance to the scope of this study, and in line with the spread of informal tented settlements as a shelter solution for some refugee groups and families, particularly along the Litani river basin and the Beqaa plain at large, remote sensing provides a practical solution to estimate informal population growth on one hand, and access to electricity on the other, similarly to what M. F. Müller et al., (2016) resorted to. When looking at informal tented settlements in Jordan, as a result of the war in Syria, and using nightlight intensity analysis, M. F. Müller et al., (2016) were able to estimate population growth in informal tented settlements. Another project used similar remote sensing technology to estimate and link the electrification rate to economic development in a rural area in India (Burlig & Preonas, 2021).

Although remote sensing of night-time light is not a new avenue, its developments have only gained popularity since 2011 (Li et al., 2017), which poses several challenges in access to and availability of data, its geographical coverage, and its temporal scope. Within the context of this study, it was not possible to retrieve nightlight images with timestamps identical to the chosen Landsat images. Therefore, when applicable, the closest dates were chosen. After pre-treatment, the images are shown in Figure 20 (a, b, c, d) below, noting that (a) is used to provide an overview of the entire situation over Lebanon in 2021. As night imagery makes it difficult for the reader to discern topographical features that are easily identifiable in day-time images, image (a) below is produced against a backdrop of an openstreet map of Lebanon to facilitate the viewing for the inexpert reader:

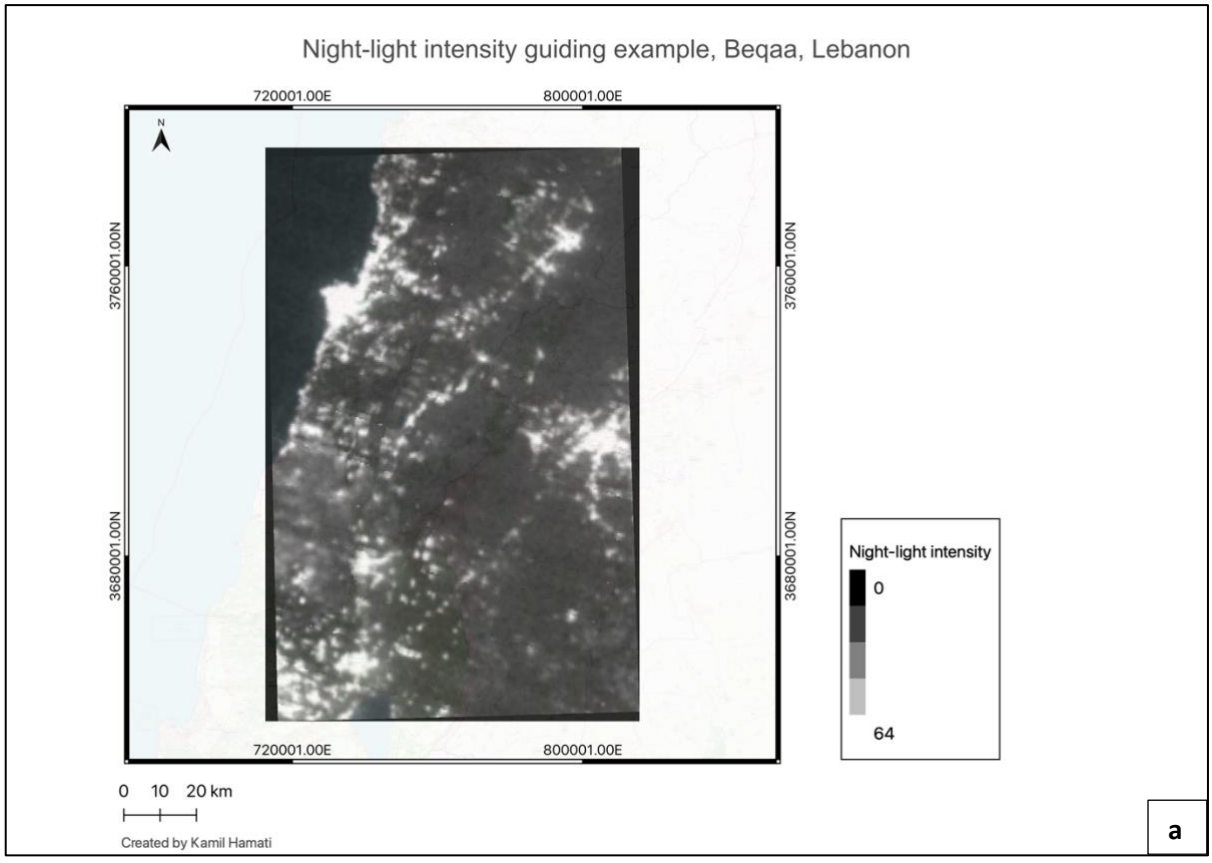

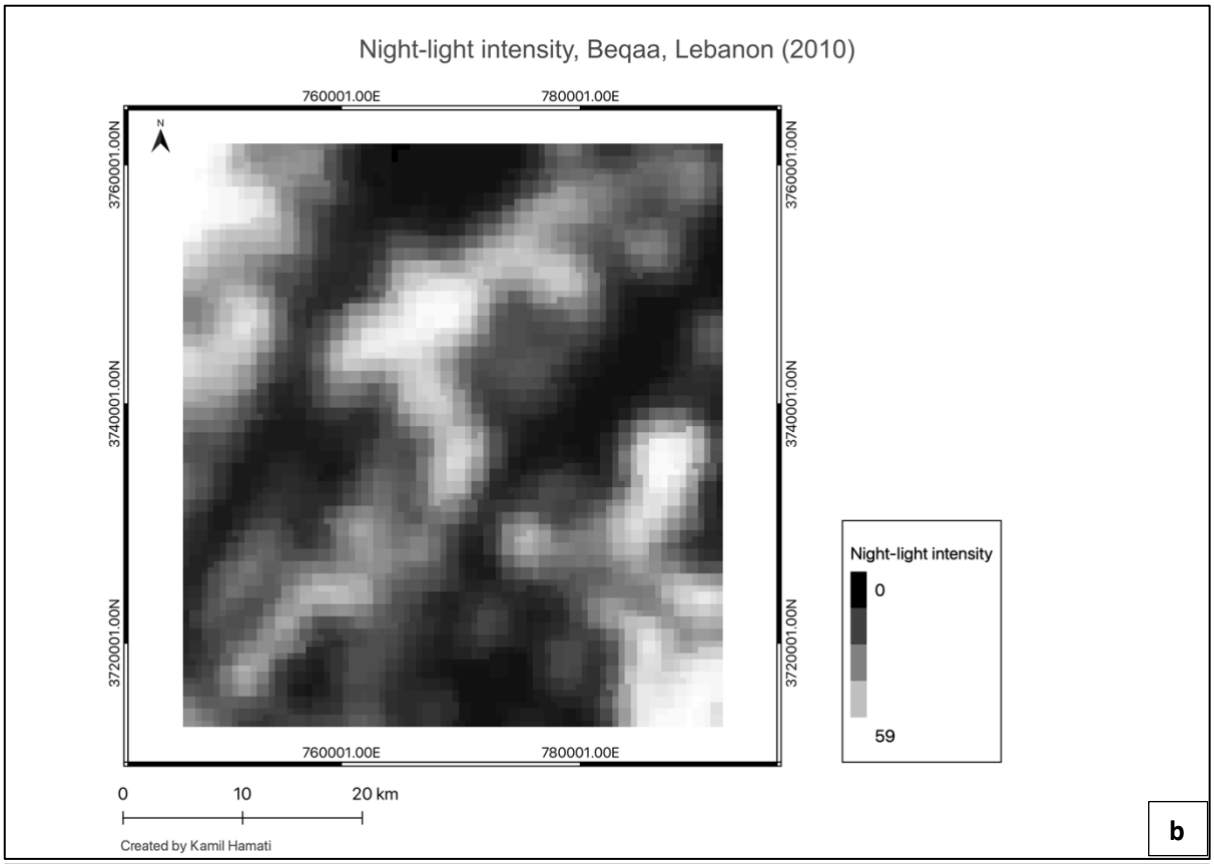
Night-light intensity, Beqaa, Lebanon (2010)
760001.00E
780001.00E
3760001.00N
3740001.00N
3720001.00N
N
Night-light intensity
0
59
0
10
20 km
Created by Kamil Hamati
b

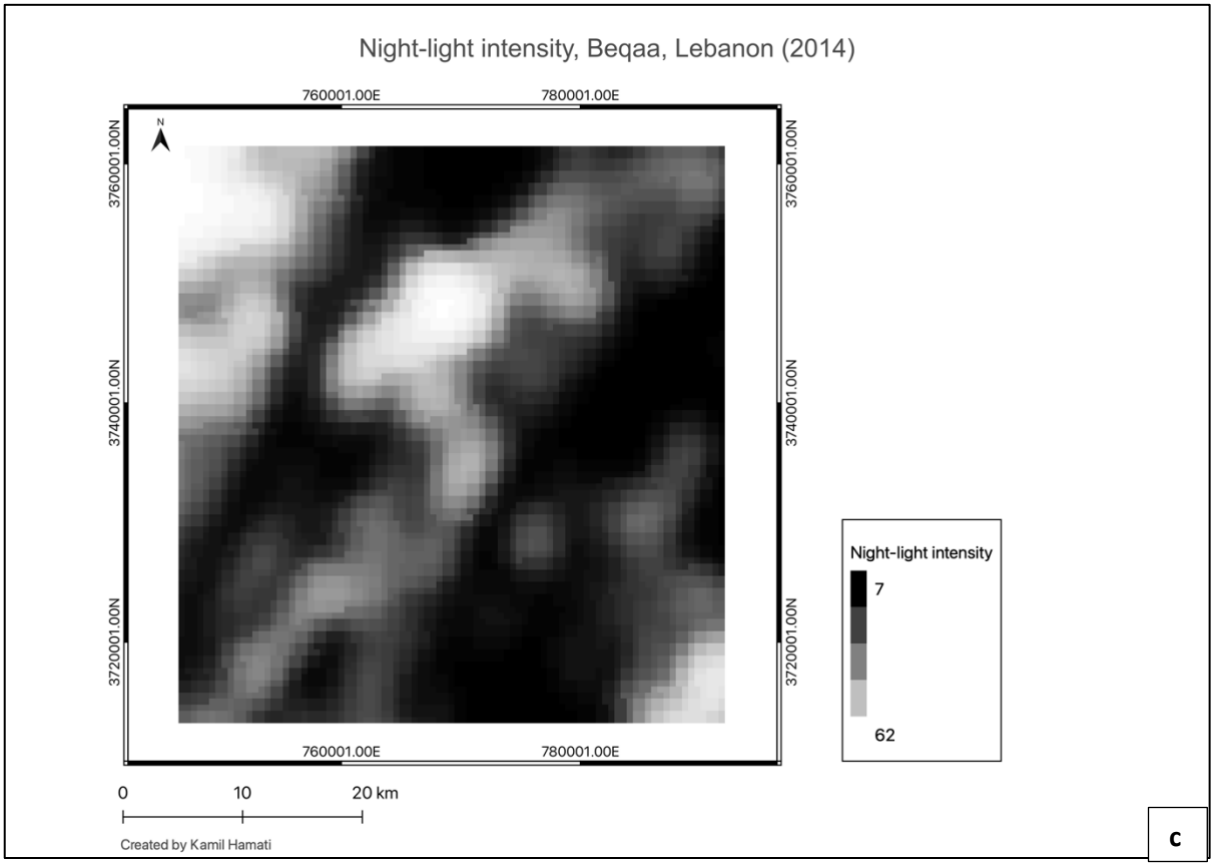
Night-light intensity, Beqaa, Lebanon (2014)
760001.00E
780001.00E
3760001.00N
3740001.00N
3720001.00N
N
Night-light intensity
7
62
0
10
20 km
Created by Kamil Hamati
c

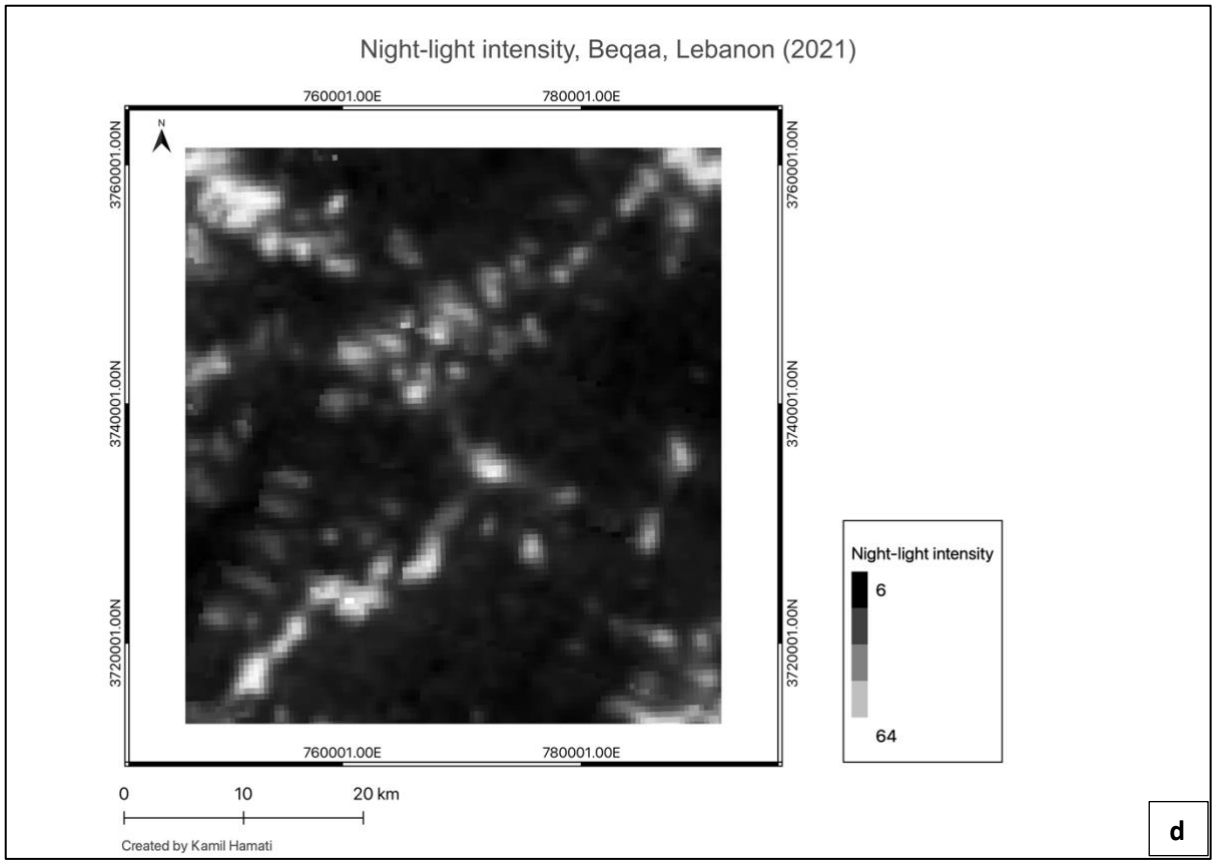

*Figure 20: Night-light intensity maps of the AOI in 2010 (**b**), 2014 (**c**), and 2021 (**d**). (**a**) provides a guiding example showing the Lebanese coast as well as the hinterlands including the Beqaa region.*

Across our AOI, a clear increase in night-light intensity may be seen from 2010 to 2014, especially along the upper part of the Litani River Basin (the upper central part of Figure 20 (b) and (c)) consistently with the existence and intensification of anthropological activity along this region. However, 2021 witnessed a drastic decrease in night-light intensity, consistently with the information cited earlier in this sub-section, following the economic crisis that hit Lebanon. Analysis of these images shows that the crisis did not only affect Lebanese households, but also refugees' as well as those residing in informal tented settlements as the lights that appeared in 2014, following the influx, cannot be discerned in 2021 during the crisis, insinuating that residents of these settlements either do not have electrical current anymore, or that they have migrated to other areas in search of better livelihoods.

3.2.2. Water & Sanitation (Population without access to at least basic drinking water & population without access to at least basic sanitation facilities)

Population density in Lebanon increased from around 471 people/km^2 to roughly 670 people/km^2, between 2009 (pre-influx of refugees) and 2018 (post-influx) (World Bank, 2019). The increase in population density eventually culminated in increased municipal solid waste (MSW) generation and a higher demand on the water infrastructure (The World Bank, 2018). It also reportedly resulted in overstretching the capacities of the few existing MSW management infrastructure and in a 40% increase in the MSW treatment bill between 2012 and 2013 (Boustany, 2017; Lebanese Republic, Ministry of Environment et al., 2014, 2015). On top of this, since before the refugee crisis, Lebanon had been suffering from an uncontrolled continuous dumping of around 2.5 million tons of unsorted solid waste per year, ending up in landfills created in residential and coastal areas. This has led to increased contamination of soil and pollution of water (both surface and groundwater) (Boustany,

2017; Lebanese Republic, Ministry of Environment et al., 2014, 2015); on many instances, "drinking water" or tap water in Lebanon was found to contain E. *coli* and a high total coliform count (Baalbaki et al., 2019; Bain et al., 2014; S. Khoury et al., 2016; Korfali & Jurdi, 2007). However, as the country had adopted a no-camp policy, shy efforts towards remediating the polluted water and catering for the increasing amounts of MSW were geographically scattered and ill-aimed (The World Bank, 2018) which drove people to increase their dependence on private suppliers who are not necessarily regulated or monitored, subsequently leading to increased risks on public health, and to increased water demand and stress on water resources (Boustany, 2017; Institute of Health Management and Social Protection (IGSPS) et al., 2012; Lebanese Republic, Ministry of Environment et al., 2015).

Unfortunately, geographic data that pinpoints water source points and geolocates sanitation facilities was not accessible neither through open data repositories nor through relief agencies operating on the ground. This kind of data would have been useful to map and visualize the distance that people have to commute in order to access adequate drinking water or adequate sanitation facilities. However, UNICEF's 2020 report on the living conditions of Syrian refugees in Lebanon highlights that bottled water (bought from small shops and supermarkets) represented to a large extent the main source of drinking water for refugees (more than 35%, whereas only 21% reported relying on tap water for drinking) (United Nations Children's Fund et al., 2020), rendering a mapping of tap water sources a rather useless exercise.

3.2.3. Health (Population without regular access to essential medicines)

Similarly to sub-section 3.2.2, access to healthcare facilities and spatial proximity to such facilities cannot be easily assessed due to lack of data, and to the difficulty in assigning clear coordinates to healthcare facilities as they are sometimes not allocated separate and clearly defined infrastructure (many healthcare facilities in the Beqaa region are dispensaries that exist either in residential buildings, in schools, or in other multi-purpose buildings such as city halls).

As was the case for water and sanitation, geographical data for healthcare facilities was not accessible neither through open data repositories nor through relief agencies operating on the ground. This indicator would have been used to assess the distance that refugees have to travel to access adequate health services.

3.3. General discussion

Although not entirely conclusive, the spatial imaging and remote sensing results that we were able to get, give an overall idea about the evolution of not only environmental, but also socio-economic parameters in the Beqaa region after the influx of refugees from Syria that started in 2011. Despite the lack of in-situ monitoring data for environmental parameters, we were able to get usable and comparable results using spatial imaging and remote sensing techniques, which was not entirely applicable to socio-economic indicators. Lack of field data and of specific spectral signatures (of water and sanitation points for instance, or of health facilities) posed a serious challenge in identifying and using these features in the geospatial analysis. Nevertheless, these tasks are not impossible to achieve; they hinge on either field visits or an active collaboration with field agents (humanitarian or other local actors), which could be an interesting venture for another research project in the future.

Spatial analysis and remote sensing are increasingly being used to monitor terrains that are difficult to reach, such as war-affected zones, remote areas, and other regions whose access is limited due to climatic, environmental, ethnic, cultural, or political conditions (among others). Also, these technologies are proving to be effective tools in establishing not only spatial but also temporal comparisons between selected areas. These features provide a layer of facility to understand, for example, the current state of the environment in a certain region, how long it took to get to this state,

when and what triggered the observed changes, an overall trend in which the changes are happening, as well as the implications that such changes are having on the surroundings.

Combining these technologies with the SJS framework, such as the case of this study, brings even further added value to monitoring the states and limits of environments in special humanitarian situations, and to understanding and anticipating the tipping points beyond which, a change of state is inevitable. This combination also expands the scope of use of spatial imaging to cover socio-economic parameters – which is less prevalent compared to other more physically tangible parameters. This eventually provides humanitarian as well as political actors with the necessary knowledge and tools to study, plan, implement, monitor, and anticipate situations in which populations at risk are in need of being seen from a different, broader, perspective.

4. Conclusion

Results of the geospatial analysis and remote sensing exercise conducted in this study have identified substantial discrepancies between the reality of the field, and political discourse. In fact, contrary to the official findings on the state of the environment after the influx of refugees from Syria to Lebanon, land cover allocation was already changing and urbanization was underway for a long time; freshwater use was already fluctuant with the absence of proper governance mechanisms and monitoring schemes and law enforcement; and pollution of the Litani River Basin (and the Qaraoun reservoir) due to anthropogenic activity was a topic of study and of discussion since the 1990s, well ahead of the arrival and settlement of the first Syrian refugee. As for the socio-economic boundaries, electrification rate clearly showed the evolution of the situation on the ground between the studied years, and the geospatial results were validated with UNICEF's 2020 report's findings. Although the need for in-situ data was successfully replaced – to a certain extent – with geospatial data for electrification rate, the same was not applicable to assess access to water and sanitation facilities. Identification of such facilities at the studied scale was not possible through remote sensing alone, and without sufficient in-situ data to corroborate the coordinates of these facilities with spectral signatures, it was almost impossible to solely rely on remote sensing for the assessment of these indicators.

These results, albeit the lack of in-situ data to satisfactorily assess all indicators and their temporal evolution, imply two conclusions:

a) With the current practices under Business-As-Usual, the Litani River Basin is pushing beyond its SJS limits, thus jeopardizing the livelihoods of both indigenous and refugee populations, as well as the carrying capacity of the surrounding environment. Therefore, countermeasures need to be employed by governing bodies to halt and reverse the damage that is happening in the region at both human and natural scales.
b) Refugee populations in the Litani River Basin are not particular resource degraders. Environmentally degrading practices have been in place in the region years before the arrival of refugees, which already put the region under substantial environmental strains before the influx of refugees. Additionally, water shortages and limited access to, and availability of, electricity, on top of a rapidly expanding urban sprawl, have pre-set the terrain with socio-economic conditions that fostered tensions amongst the local population, which later expanded to also include refugees.

It would be interesting to test the limits of this exercise in other geographical settings where in-situ monitoring data exists, making it easier to validate the geospatial findings. It would also be interesting to replicate this exercise in different climatic regions, or while additionally monitoring climatic parameters, allowing us to filter out the climatic factor that might have influenced certain environmental or socio-economic findings. Additionally, further research endeavors might be interesting for testing the combination between the SJS and remote sensing and geospatial analysis

on different scales, both sub-local (at the camp level, for instance, in the case of refugee situations), and global (such as the planetary boundaries, for instance).

5. Bibliography

Akbar, T. A., Hassan, Q. K., Ishaq, S., Batool, M., Butt, H. J., & Jabbar, H. (2019). Investigative Spatial Distribution and Modelling of Existing and Future Urban Land Changes and Its Impact on Urbanization and Economy. *Remote Sensing*, *11*(2), 105. https://doi.org/10.3390/rs11020105

Allenbach, K., Giuliani, G., Dao, H., & Planque, M. (2021, January 21). *Télédétection et traitement d'images (T406034)* [Course]. Certificat Complémentaire en Géomatique 2021, Université de Genève. https://moodle.unige.ch/course/view.php?id=9607

Amnesty International. (2019, June 12). Escalating hostility against Syrian refugees in Lebanon. *Amnesty International*. https://www.amnesty.org/en/latest/news/2019/06/lebanon-wave-of-hostility-exposes-hollowness-of-claims-that-syrian-refugee-returns-are-voluntary/

Ana Fernández Torralbo & Pablo Mazuelas Benito. (2012). *Landsat and MODIS Images for Burned Areas Mapping in Galicia, Spain* [Royal Institute of Technology (KTH)]. https://www.diva-portal.org/smash/get/diva2:553135/FULLTEXT01.pdf

Anna Foster. (2021, October 9). Lebanon left without power as grid shuts down—BBC News. *BBC News*. https://www.bbc.com/news/world-middle-east-58856914

Aranki, D., & Kalis, O. (2014). Limited legal status for refugees from Syria in Lebanon. *Forced Migration Review*, *47*. https://www.fmreview.org/syria/aranki-kalis

Baalbaki, R., Ahmad, S. H., Kays, W., Talhouk, S. N., Saliba, N. A., & Al-Hindi, M. (2019). Citizen science in Lebanon—A case study for groundwater quality monitoring. *Royal Society Open Science*, *6*(2). https://doi.org/10.1098/rsos.181871

Bain, R., Cronk, R., Wright, J., Yang, H., Slaymaker, T., & Bartram, J. (2014). Fecal Contamination of Drinking-Water in Low- and Middle-Income Countries: A Systematic Review and Meta-Analysis. *PLoS Medicine*, *11*(5). https://doi.org/10.1371/journal.pmed.1001644

Baydoun, S., & Amacha, N. (2016). Ecological status assessment of the Litani river, Lebanon using Chlorophyll-a. *International Journal of Current Research*, *08*, 36652–36656.

Black, R. (1994). Forced Migration and Environmental Change: The Impact of Refugees on Host Environments. *Journal of Environmental Management*, *42*(3), 261–277. https://doi.org/10.1006/jema.1994.1072

Black, R. (1998). *Refugees, Environment and Development*. Longman.

Boustany, I. (2017). *Darkening Horizons*. 43.

Bou-Zeid, E., & El-Fadel, M. (2002). Climate Change and Water Resources in Lebanon and the Middle East. *Journal of Water Resources Planning and Management*, *128*(5), 343–355. https://doi.org/10.1061/(ASCE)0733-9496(2002)128:5(343)

Burlig, F., & Preonas, L. (2021). *Out of the darkness and into the light? Development effects of rural electrification*. 46.

Canadian Council of Ministers of the Environment. (2010). *Canadian water quality guidelines for the protection of aquatic life: Ammonia* (Canadian Environmental Quality Guidelines, 1999). Canadian Council of Ministers of the Environment. http://ceqg-rcqe.ccme.ca/download/en/141

Chris Park. (2012). Neo-Malthusian. In *A Dictionary of Environment and Conservation* (1st edition). Oxford University Press. https://doi.org/10.1093/oi/authority.20110810105455393

Collier, P., Eliott, V. L., Hegre, H., Hoeffler, A., Reynal-Querol, M., & Sambanis, N. (2003). *Breaking the Conflict Trap: Civil War and Development Policy.* (p. 242) [World Bank policy research report]. World Bank and Oxford University Press. https://openknowledge.worldbank.org/bitstream/handle/10986/13938/567930PUB0brea10Box353739B01PUBLIC1.pdf?sequence=1&isAllowed=y

Dahi, O. S. (2014). The refugee crisis in Lebanon and Jordan: The need for economic development spending. *Forced Migration Review*, *47*. https://www.fmreview.org/syria/dahi#_edn1

Darwish, T., Shaban, A., Masih, I., Jaafar, H., Jomaa, I., & Simaika, J. P. (2021). Sustaining the ecological functions of the Litani River Basin, Lebanon. *International Journal of River Basin Management*, *0*(0), 1–15. https://doi.org/10.1080/15715124.2021.1885421

Deutsch, E. S., & Alameddine, I. (2018). Hindcasting eutrophication and changes in temperature and storage volume in a semi-arid reservoir: A multi-decadal Landsat-based assessment. *Environmental Monitoring and Assessment*, *191*(1), 41. https://doi.org/10.1007/s10661-018-7180-7

EarthExplorer. (n.d.). [Government website]. EarthExplorer. Retrieved February 16, 2022, from https://earthexplorer.usgs.gov/

Eirik Christophersen. (2021, June 23). These 10 countries receive the most refugees. *Norwegian Refugee Council, Perspectives*. https://www.nrc.no/perspectives/2020/the-10-countries-that-receive-the-most-refugees/

El-Kareh, J., Hajj, R. E., Farajalla, N., & Chehadeh, A. (2018). *Water Conflict in the Bekaa: Assessing Predisposition and Contributing Factors*. *3*, 4.

Environmental Protection Agency, Ireland. (2001). *Parameters of water quality: Interpretation and standards*. EPA. https://www.epa.ie/pubs/advice/water/quality/Water_Quality.pdf

Fadel, A., Faour, G., Slim, K., & Lebanese Atomic Energy Commission. (2016). Assessment of The trophic state and Chlorophyll-a concentrations using Landsat OLI in Karaoun reservoir, Lebanon. *Lebanese Science Journal*, *17*(2), 130–145. https://doi.org/10.22453/LSJ-017.2.130145

Fadel, A., Lemaire, B. J., Atoui, A., Vinçon-Leite, B., Amacha, N., Slim, K., & Tassin, B. (2014). First assessment of the ecological status of Karaoun reservoir, Lebanon. *Lakes & Reservoirs: Science, Policy and Management for Sustainable Use*, *19*(2), 142–157. https://doi.org/10.1111/lre.12058

Food and Agriculture Organization of the United Nations. (2008). *Irrigation in the Middle East region in figures – AQUASTAT Survey 2008* (AQUASTAT Survey, p. 16). FAO. http://www.fao.org/nr/water/aquastat/countries_regions/LBN/LBN-CP_eng.pdf

Food and Agriculture Organization of the United Nations. (2019). *AQUASTAT database*. http://www.fao.org/nr/water/aquastat/data/query/index.html?lang=en

France 24. (2021, October 9). Lebanon left without electricity as main power stations run out of fuel. *France 24*. https://www.france24.com/en/middle-east/20211009-lebanese-power-outage-will-last-several-days-govt-official-says

Garnier, A., Sandvik, K. B., & Jubilut, L. L. (2018, October 24). *What are the challenges facing refugee resettlement?* World Economic Forum. https://www.weforum.org/agenda/2018/10/the-needs-challenges-and-power-dynamics-of-refugee-resettlement/

GISGeography. (2021, October 29). *OBIA - Object-Based Image Analysis (GEOBIA)*. GIS Geography. https://gisgeography.com/obia-object-based-image-analysis-geobia/

Grande, F. & United Nations High Commissioner for Refugees. (2019). *UNHCR - Global Trends 2019: Forced Displacement in 2019* (p. 84). https://www.unhcr.org/globaltrends2019/

Habib, R. R. (2019). Ethical, methodological, and contextual challenges in research in conflict settings: The case of Syrian refugee children in Lebanon. *Conflict and Health*, *13*. https://doi.org/10.1186/s13031-019-0215-z

Hassan, H. E. H., Ardillier-Carras, F., & Charbel, L. (2019). Les changements d'occupation des sols dans la Béqaa Ouest (Liban): Le rôle des actions anthropiques. *Cahiers Agricultures*, *28*, 10. https://doi.org/10.1051/cagri/2019010

Haydar, C. M., Nehme, N., Awad, S., Koubaissy, B., Fakih, M., Yaacoub, A., Toufaily, J., Villeras, F., & Hamieh, T. (2014). Water Quality of the upper Litani River Basin, Lebanon. *Physics Procedia*, *55*, 279–284. https://doi.org/10.1016/j.phpro.2014.07.040

Huang, C., Chen, Y., Zhang, S., & Wu, J. (2018). Detecting, Extracting, and Monitoring Surface Water From Space Using Optical Sensors: A Review. *Reviews of Geophysics*, *56*(2), 333–360. https://doi.org/10.1029/2018RG000598

Hussein, N. M., & Assaf, M. N. (2020). Multispectral Remote Sensing Utilization for Monitoring Chlorophyll-a Levels in Inland Water Bodies in Jordan. *The Scientific World Journal*, *2020*, e5060969. https://doi.org/10.1155/2020/5060969

Institute of Health Management and Social Protection (IGSPS), Lebanese Ministry of Public Health, & World Health Organization. (2012). *National Health Statistics Report in Lebanon* (No. 2; p. 139). Saint Joseph University. https://www.usj.edu.lb/intranet/annonce/files/pdf/175_pdf_1.pdf

International Resources Group. (2011). *Litani River Basin Management Support Program. Litani River Walk-Through Survey Report* (p. 58). USAID Lebanon. http://www.litani.gov.lb/wp/wp-content/uploads/LRBMS/039-LRBMS-LITANI%20RIVER%20WALK%20-%20THROUGH%20SURVEY%20REPORT-%20ENGLISH.pdf

Ioanes, E. (2021, October 10). Lebanon's electricity was down for a day, but the crisis was years in the making. *Vox*. https://www.vox.com/2021/10/10/22719115/lebanon-power-grid-collapse-beirut-crisis

Jacobsen, K. (1997). Refugees' Environmental Impact: The Effect of Patterns of Settlement. *Journal of Refugee Studies*, *10*(1), 19–36. https://doi.org/10.1093/jrs/10.1.19

John Weier & David Herring. (2000, August 30). *Measuring Vegetation (NDVI & EVI)* [Text.Article]. NASA Earth Observatory. https://earthobservatory.nasa.gov/features/MeasuringVegetation

Jurdi, M., Ibrahim Korfali, S., Karahagopian, Y., & Davies, B. E. (2002). Evaluation of Water Quality of the Qaraaoun Reservoir, Lebanon: Suitability for Multipurpose Usage. *Environmental Monitoring and Assessment*, *77*(1), 11–30. https://doi.org/10.1023/A:1015781930601

Kheireddine, B. J., Soares, A. M., & Rodrigues, R. G. (2020). Understanding (in)tolerance between hosts and refugees in Lebanon. *Journal of Refugee Studies*, *feaa056*. https://doi.org/10.1093/jrs/feaa056

Khoury, R., Antoun, N., Khater, C., & Abou Habib, N. (2015). *Fifth national report of Lebanon to the convention on biological diversity* (No. 5; p. 146). ELARD, Lebanese Ministry of Environment, GEF, UNEP. https://www.cbd.int/doc/world/lb/lb-nr-05-en.pdf

Khoury, S., Graczyk, T., Burnham, G., Jurdi, M., & Goldman, L. (2016). Drinking water system treatment and contamination in Shatila Refugee Camp in Beirut, Lebanon | Volume 22, issue

8 | EMHJ volume 22, 2016. *Eastern Mediterranean Health Journal*, *22*(8). http://www.emro.who.int/emhj-volume-22-2016/volume-22-issue-8/drinking-water-system-treatment-and-contamination-in-shatila-refugee-camp-in-beirut-lebanon.html

Kibreab, G. (1997). Environmental Causes and Impact of Refugee Movements: A Critique of the Current Debate. *Disasters*, *21*(1), 20–38. https://doi.org/10.1111/1467-7717.00042

Korfali, S. I., & Jurdi, M. (2007). Assessment of domestic water quality: Case study, Beirut, Lebanon. *Environmental Monitoring and Assessment*, *135*(1), 241–251. https://doi.org/10.1007/s10661-007-9646-x

Lebanese Republic, Ministry of Agriculture. (2018). *Final National Report on Land Degradation Neutrality Target Setting Programme* (p. 108). Ministry of Agriculture. https://knowledge.unccd.int/sites/default/files/ldn_targets/Lebanon%20LDN%20TSP%20Country%20Report.pdf

Lebanese Republic, Ministry of Environment, European Union, & United Nations Development Programme. (2014). *Lebanon Environmental Assessment of the Syrian Conflict & Priority Interventions* (No. 1; p. 182). https://www.undp.org/content/dam/lebanon/docs/Energy%20and%20Environment/Publications/EASC-WEB.pdf

Lebanese Republic, Ministry of Environment, European Union, & United Nations Development Programme. (2015). *Lebanon Environmental Assessment of the Syrian Conflict & Priority Interventions. Updated Fact Sheet* (No. 2; p. 8). Ministry of Environment. https://reliefweb.int/sites/reliefweb.int/files/resources/64715.pdf

Lebanese Republic, Ministry of Environment & United Nations Development Programme. (2011). *Climate risks, vulnerability & adaptation assessment* (National Communication No. 2; CLIMATE CHANGE VULNERABILITY AND ADAPTATION, p. 72). Ministry of Environment. http://climatechange.moe.gov.lb/viewfile.aspx?id=33

Li, X., Elvidge, C., Zhou, Y., Cao, C., & Warner, T. (2017). Remote sensing of night-time light. *International Journal of Remote Sensing*, *38*(21), 5855–5859. https://doi.org/10.1080/01431161.2017.1351784

Li, X., Zhou, Y., Zhao, M., & Zhao, X. (2020). A harmonized global nighttime light dataset 1992–2018. *Scientific Data*, *7*(1), 168. https://doi.org/10.1038/s41597-020-0510-y

Majed, R. (2018). Les réfugiés syriens au Liban. *Esprit*, *Avril*(4), 102–103.

Maystadt, J.-F., Mueller, V., Hoek, J. V. D., & Weezel, S. van. (2020). Vegetation changes attributable to refugees in Africa coincide with agricultural deforestation. *Environmental Research Letters*, *15*(4), 044008. https://doi.org/10.1088/1748-9326/ab6d7c

Mcheik, A., Awad, A., Fadel, A., Mounzer, C., & Nasreddine, S. (2018). Effect of Irrigation Water Quality on the Microbial Contamination of Fresh Vegetables in the Bekaa Valley, Lebanon. *American Journal of Agriculture and Forestry*, *6*(6), 191. https://doi.org/10.11648/j.ajaf.20180606.16

Mellos, K. (1988). Neo-Malthusian Theory. In K. Mellos (Ed.), *Perspectives on Ecology: A Critical Essay* (pp. 15–42). Palgrave Macmillan UK. https://doi.org/10.1007/978-1-349-19598-5_2

Müller, K., & Schwarz, C. (2020). Fanning the Flames of Hate: Social Media and Hate Crime. *Journal of the European Economic Association*, *jvaa045*. https://doi.org/10.1093/jeea/jvaa045

Müller, M. F., Yoon, J., Gorelick, S. M., Avisse, N., & Tilmant, A. (2016). Impact of the Syrian refugee crisis on land use and transboundary freshwater resources. *Proceedings of the National Academy of Sciences*, *113*(52), 14932–14937. https://doi.org/10.1073/pnas.1614342113

Nasser Yassin. (2019). *101 Facts & Figures on the Syrian Refugee Crisis Volume II* (Vol. 2). The Issam Fares Institute for Public Policy and International Affairs. http://www.aub.edu.lb:80/ifi/news/Pages/20190702-101-facts-and-figures-on-syrian-refugee-crisis-volume-2.aspx

New Zealand Government. (2019). *Water quality glossary*. Waikato Regional Council. https://www.waikatoregion.govt.nz/environment/natural-resources/water/lakes/water-quality-glossary/

Obeid, S., Haddad, C., Salame, W., Kheir, N., & Hallit, S. (2019). Xenophobic attitudes, behaviors and coping strategies among Lebanese people toward immigrants and refugees. *Perspectives in Psychiatric Care*, *0*(0). https://doi.org/10.1111/ppc.12415

Oucho, J. (2007, November 15). *Environmental Impact Of Refugees And Internally Displaced Persons In Sub-Saharan Africa*. African Migration Alliance Biennial Workshop on Climate Change, Environment and Migration, East London, South Africa.

Pierigh, F. (2017). *Changing the Narrative – Media Representation of Refugees and Migrants in Europe*. World Association for Christian Communication – Europe Region & Churches' Commission for Migrants in Europe. https://www.refugeesreporting.eu/report/

Pollock, W., Wartman, J., Abou-Jaoude, G., & Grant, A. (2019). Risk at the margins: A natural hazards perspective on the Syrian refugee crisis in Lebanon. *International Journal of Disaster Risk Reduction*, *36*, 101037. https://doi.org/10.1016/j.ijdrr.2018.11.026

Raworth, K. (2012). *A safe and just space for humanity. Can we live within the doughnut?* [Data set]. Oxfam. https://doi.org/10.1163/2210-7975_HRD-9824-0069

Rockström, J., Steffen, W., Noone, K., Persson, Å., Chapin, F. S. I., Lambin, E., Lenton, T., Scheffer, M., Folke, C., Schellnhuber, H. J., Nykvist, B., de Wit, C., Hughes, T., van der Leeuw, S., Rodhe, H., Sörlin, S., Snyder, P., Costanza, R., Svedin, U., … Foley, J. (2009a). Planetary Boundaries: Exploring the Safe Operating Space for Humanity. *Ecology and Society*, *14*(2). https://doi.org/10.5751/ES-03180-140232

Rockström, J., Steffen, W., Noone, K., Persson, Å., Chapin, F. S., Lambin, E. F., Lenton, T. M., Scheffer, M., Folke, C., Schellnhuber, H. J., Nykvist, B., de Wit, C. A., Hughes, T., van der Leeuw, S., Rodhe, H., Sörlin, S., Snyder, P. K., Costanza, R., Svedin, U., … Foley, J. A. (2009b). A safe

operating space for humanity. *Nature*, *461*(7263), 472–475. https://doi.org/10.1038/461472a

Saada Allaw. (2020, April 30). Syrian Refugees in Lebanon Caught Between Corona and Destitution. *Legal Agenda*. https://english.legal-agenda.com/syrian-refugees-in-lebanon-caught-between-corona-and-destitution/

Saadeh, M., Semerjian, L., & Amacha, N. (2012). Physicochemical Evaluation of the Upper Litani River Watershed, Lebanon. *The Scientific World Journal*, *2012*. https://doi.org/10.1100/2012/462467

Shaban, A. (2011). Analyzing Climatic and Hydrologic Trends in Lebanon. *Journal of Environmental Science and Engineering*, *5*, 11.

Shaban, A. (2014). Physical and Anthropogenic Challenges of Water Resources in Lebanon. *Journal of Scientific Research and Reports*, 479–500. https://doi.org/10.9734/JSRR/2014/6990

Shaban, A., Telesca, L., Darwich, T., & Amacha, N. (2014). Analysis of long-term fluctuations in stream flow time series: An application to Litani River, Lebanon. *Acta Geophysica*, *62*(1), 164–179. https://doi.org/10.2478/s11600-013-0175-4

Sheffield, J., Wood, E. F., Pan, M., Beck, H., Coccia, G., Serrat-Capdevila, A., & Verbist, K. (2018). Satellite Remote Sensing for Water Resources Management: Potential for Supporting Sustainable Development in Data-Poor Regions. *Water Resources Research*, *54*(12), 9724–9758. https://doi.org/10.1029/2017WR022437

Steffen, W. L. (Ed.). (2005). *Global change and the Earth system: A planet under pressure*. Springer.

Stephan Georg. (2021). *Distance calculator*. fr.distance.to. https://fr.distance.to/Beyrouth,LBN/Beqaa,LBN

Susan F. Martin, Douglas A. Howard, Lahra Smith, Nili Sarit Yossinger, Lara Kinne, & Mark Giordano. (2016). *Environmental Resource Management in Refugee Camps and Surrounding Areas: Lessons Learned and Best Practices* (p. 94). Georgetown University, Walsh School of Foreign Service. https://georgetown.app.box.com/s/lh8poindaangbo49q73ekmxkaj4ne7cb

The CHAAMS Project. (2019). *Map of Lebanon, showing Litani river and basin* [Map]. http://chaams.eranetmed-chaams.org/chaams/index.php/studysites/consultation/lebanon-litani

The Economist. (2019, August 22). Politicians are stoking anti-refugee sentiment in Lebanon. *The Economist*. https://www.economist.com/middle-east-and-africa/2019/08/22/politicians-are-stoking-anti-refugee-sentiment-in-lebanon

The World Bank. (2018). *Implementation, completion, and results report on a Lebanon-Syria crisis trust fund grant* (p. 63). World Bank. http://documents.worldbank.org/curated/en/306681546027934957/pdf/icr00004600-12192018-636810265727354070.pdf

Thorleifsson, C. (2014, September). *Coping strategies among self-settled Syrians in Lebanon*. Forced Migration Review. https://www.fmreview.org/syria/thorleifsson

United Nations Children's Fund, United Nations High Commissioner for Refugees, & United Nations World Food Programme. (2020). *Vulnerability Assessment of Syrian Refugees in Lebanon* (No. 8; VASyR, p. 120). http://ialebanon.unhcr.org/vasyr/#/

United Nations General Assembly. (2015). *Transforming our world: The 2030 Agenda for Sustainable Development*. United Nations. https://www.un.org/sustainabledevelopment/development-agenda/

United Nations High Commissioner for Refugees. (2019a). *Figures at a Glance*. UNHCR. https://www.unhcr.org/figures-at-a-glance.html

United Nations High Commissioner for Refugees. (2019b). *Internally Displaced People*. UNHCR. https://www.unhcr.org/internally-displaced-people.html

United Nations High Commissioner for Refugees. (2019c). *Solutions*. UNHCR. https://www.unhcr.org/solutions.html

United Nations High Commissioner for Refugees. (2020). *UNHCR Global Trends—Forced displacement in 2020* [Global trends]. United Nations High Commissioner for Refugees. https://www.unhcr.org/flagship-reports/globaltrends/

United Nations High Commissioner for Refugees. (2021a). *Distribution of the Registered Syrian Refugees at the Cadastral Level* [Map]. United Nations High Commissioner for Refugees. https://data2.unhcr.org/en/documents/details/87183

United Nations High Commissioner for Refugees. (2021b, November 15). *Situation Syria Regional Refugee Response*. Operational Portal - Refugee Situations. https://data2.unhcr.org/en/situations/syria/location/71

Verdeil, É. (2019). The Eletricity Crisis. In G. Faour, E. Verdeil, & M. Hamzé (Eds.), *Atlas of Lebanon: New Challenges* (pp. 100–101). Presses de l'Ifpo. http://books.openedition.org/ifpo/13296

Viana, C. M., Oliveira, S., Oliveira, S. C., & Rocha, J. (2019). 29—Land Use/Land Cover Change Detection and Urban Sprawl Analysis. In H. R. Pourghasemi & C. Gokceoglu (Eds.), *Spatial Modeling in GIS and R for Earth and Environmental Sciences* (pp. 621–651). Elsevier. https://doi.org/10.1016/B978-0-12-815226-3.00029-6

Watanabe, F. S. Y., Alcântara, E., Rodrigues, T. W. P., Imai, N. N., Barbosa, C. C. F., & Rotta, L. H. da S. (2015). Estimation of Chlorophyll-a Concentration and the Trophic State of the Barra Bonita Hydroelectric Reservoir Using OLI/Landsat-8 Images. *International Journal of Environmental Research and Public Health*, *12*(9), 10391–10417. https://doi.org/10.3390/ijerph120910391

Wetzel, R. G. (1992). Clean water: A fading resource. In V. Ilmavirta & R. I. Jones (Eds.), *The Dynamics and Use of Lacustrine Ecosystems* (pp. 21–30). Springer Netherlands. https://doi.org/10.1007/978-94-011-2745-5_2

World Bank. (2003). *Lebanon: Policy Note on Irrigation Sector Sustainability* (Policy Notes, p. 89). World Bank. https://openknowledge.worldbank.org/handle/10986/14392

World Bank. (2019). *World Development Indicators*. World Bank Open Data. https://data.worldbank.org/

Xu, H. (2006). Modification of normalised difference water index (NDWI) to enhance open water features in remotely sensed imagery. *International Journal of Remote Sensing*, *27*(14), 3025–3033. https://doi.org/10.1080/01431160600589179

Yahya, M., & Muasher, M. (2018). Refugee Crises in the Arab World. *Carnegie Endowment for International Peace*. https://carnegieendowment.org/2018/10/18/refugee-crises-in-arab-world-pub-77522

Yasmina El Amine. (2019). *A Broader View of the Litani's Pollution Crisis: Mounting Conflicts and Hidden Pitfalls* (AUB Policy Briefs, p. 4). AUB Policy Institute. https://www.aub.edu.lb/ifi/Documents/publications/policy_briefs/2018-2019/20190405_litani_pollution_crisis.pdf

6. Annexes

Annex 1: Spatial images additional information

The AOI is shown in more details in the following highlight in Figure 21 below.

Figure 21: Highlighted AOI in Lebanon

This highlighted AOI is situated at the following coordinates:

Table 6: Exact coordinates of AOI, as shown in Annex 1

33.5444° N	35.6578° E
33.5275° N	35.6908° E
33.9986° N	36.2539° E
34.0723° N	36.0564° E
33.7586° N	35.8056° E

The properties of the chosen images are summarized in the following table:

Table 7: Properties of Landsat 7 ETM+ and Landsat 8 OLI/TIRS chosen images

Date of acquisition	27/08/2021			24/08/2014			06/09/2010		
WRS	Path = 174 / Row = 37			Path = 174 / Row = 37			Path = 174 / Row = 037		
Projection	WGS84 / UTM ZONE = 36			WGS84 / UTM ZONE = 36			WGS84 / UTM ZONE = 36		
Source	USGS EarthExplorer (https://earthexplorer.usgs.gov/)								
Satellite	LANDSAT 8 OLI TIRS			LANDSAT 8 OLI TIRS			Landsat 7 ETM+		
Cloud Cover	0.01%			0.93%			2.00%		
Quality	9			9			9		
Type	GeoTIFF			GeoTIFF			GeoTIFF		
Band		Wavelength (µm)	Resolution (m)		Wavelength (µm)	Resolution (m)		Wavelength (µm)	Resolution (m)
Band 1	Coastal aerosol	0.43-0.45	30	Coastal aerosol	0.43-0.45	30	Blue	0.45-0.52	30
Band 2	Blue	0.45-0.51	30	Blue	0.45-0.51	30	Green	0.52-0.60	30
Band 3	Green	0.53-0.59	30	Green	0.53-0.59	30	Red	0.63-0.69	30
Band 4	Red	0.64-0.67	30	Red	0.64-0.67	30	Near Infrared (NIR)	0.77-0.90	30
Band 5	Near Infrared (NIR)	0.85-0.88	30	Near Infrared (NIR)	0.85-0.88	30	SWIR 1	1.55-1.75	30
Band 6	SWIR 1	1.57-1.65	30	SWIR 1	1.57-1.65	30	Thermal Infrared	10.40-12.50	60

Band 7	SWIR 2	2.11-2.29	30	SWIR 2	2.11-2.29	30	SWIR 2	2.09-2.35	30
Band 8	Panchromatic	0.50-0.68	15	Panchromatic	0.50-0.68	15	Panchromatic	.52-.90	15
Band 9	Cirrus	1.36-1.38	30	Cirrus	1.36-1.38	30	-	-	-
Band 10	Thermal Infrared (TIRS) 1	10.6-11.19	100	Thermal Infrared (TIRS) 1	10.6-11.19	100	-	-	-
Band 11	Thermal Infrared (TIRS) 2	11.50-12.51	100	Thermal Infrared (TIRS) 2	11.50-12.51	100	-	-	-

Annex 2: Spatial images in larger formats

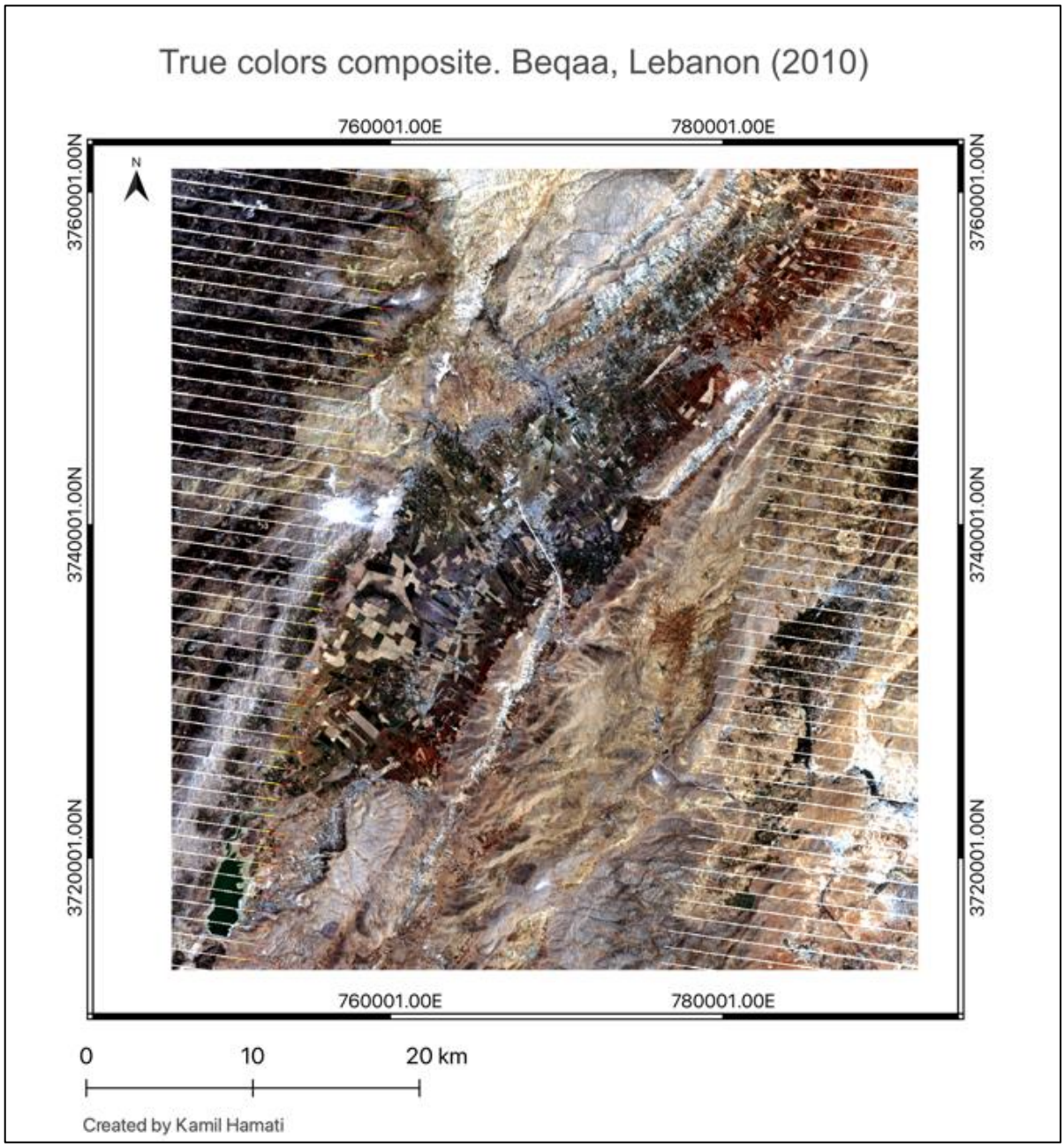

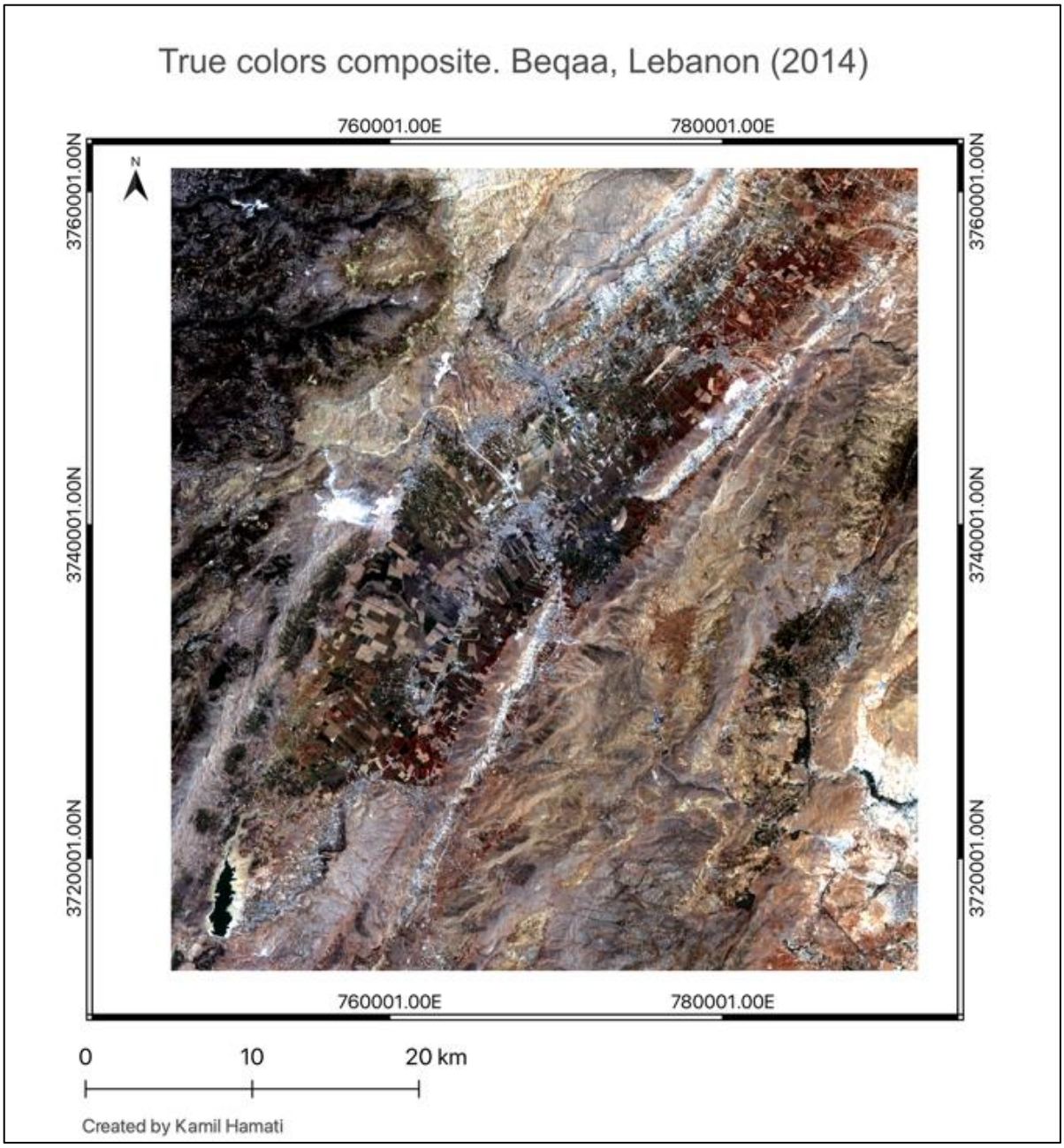
True colors composite. Beqaa, Lebanon (2014)
760001.00E
780001.00E
3760001.00N
3740001.00N
3720001.00N
N
0
10
20 km
Created by Kamil Hamati

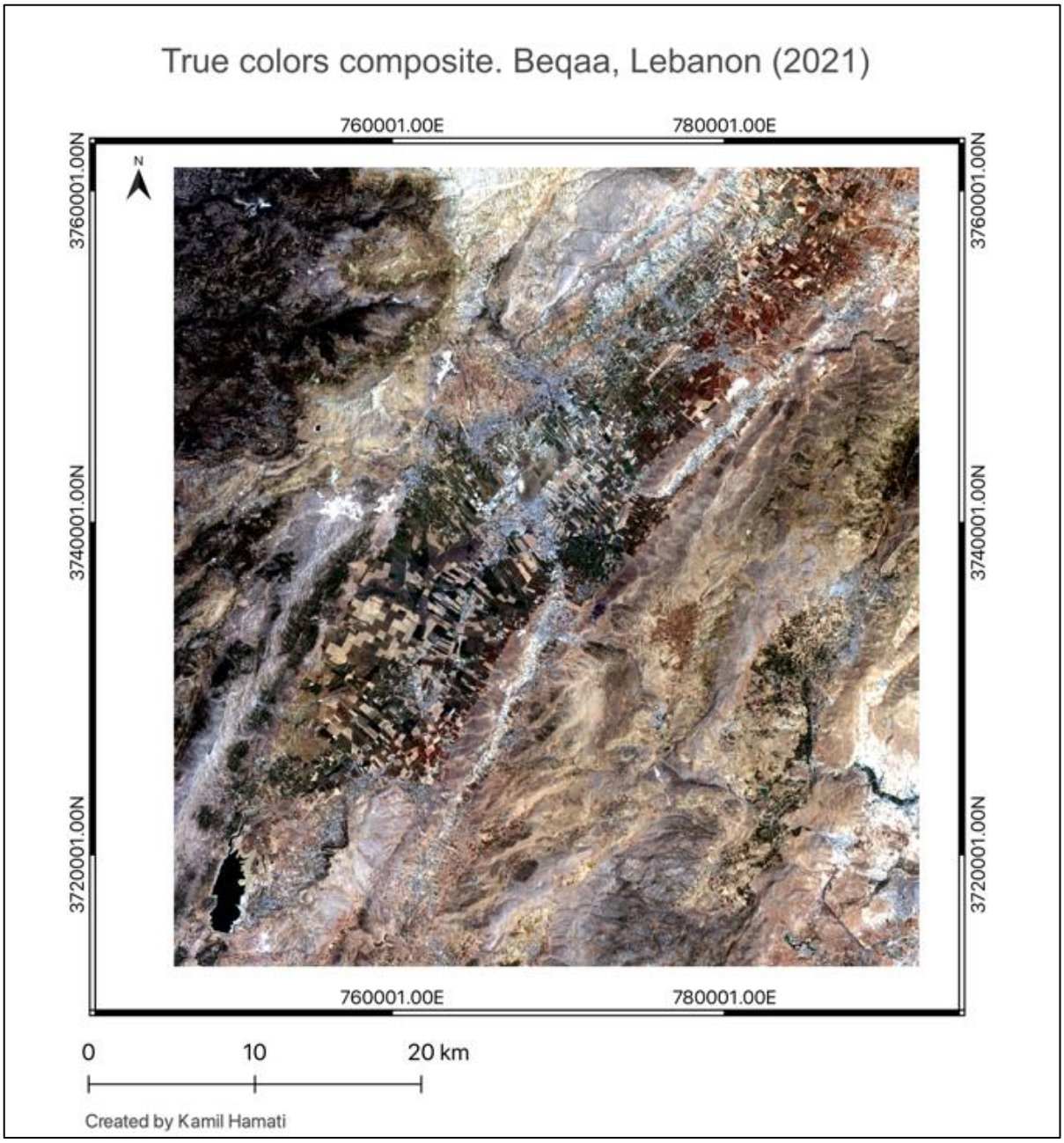
True colors composite. Beqaa, Lebanon (2021)
760001.00E
780001.00E
3760001.00N
3740001.00N
3720001.00N
N
0
10
20 km
Created by Kamil Hamati

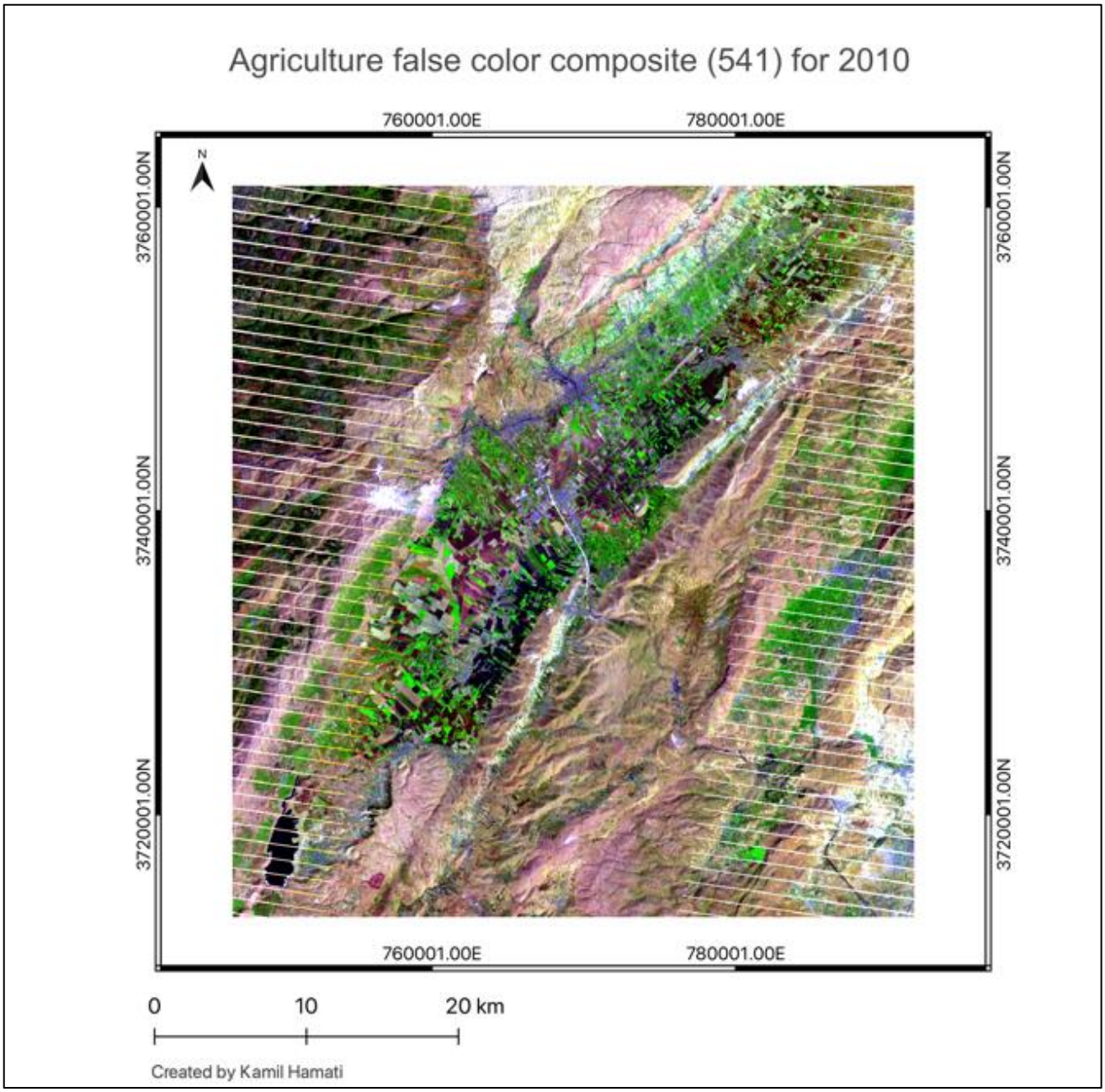
Agriculture false color composite (541) for 2010
760001.00E
780001.00E
3760001.00N
3740001.00N
3720001.00N
N
0
10
20 km
Created by Kamil Hamati

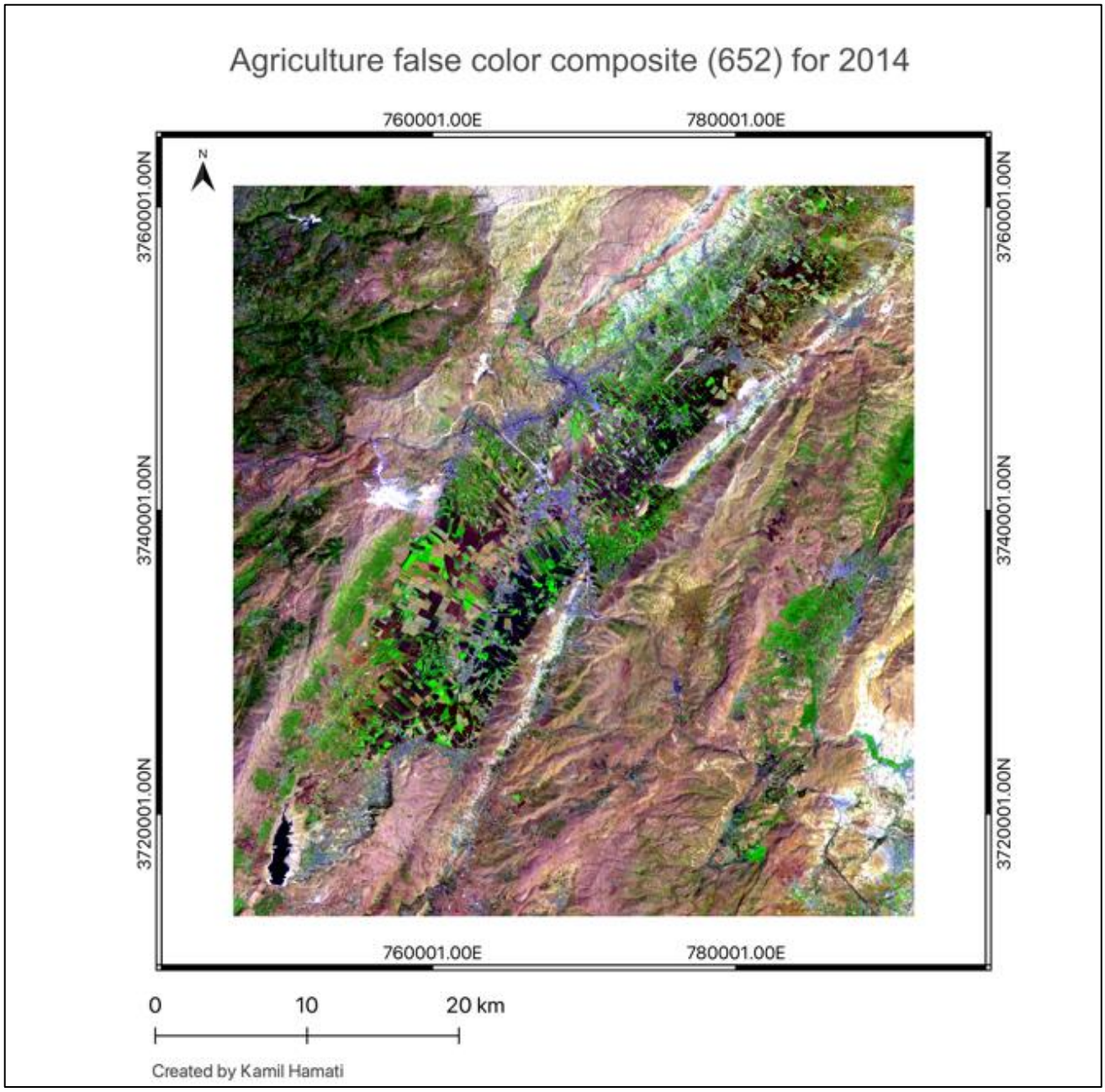
Agriculture false color composite (652) for 2014
760001.00E
780001.00E
N
3760001.00N
3740001.00N
3720001.00N
760001.00E
780001.00E
0
10
20 km
Created by Kamil Hamati

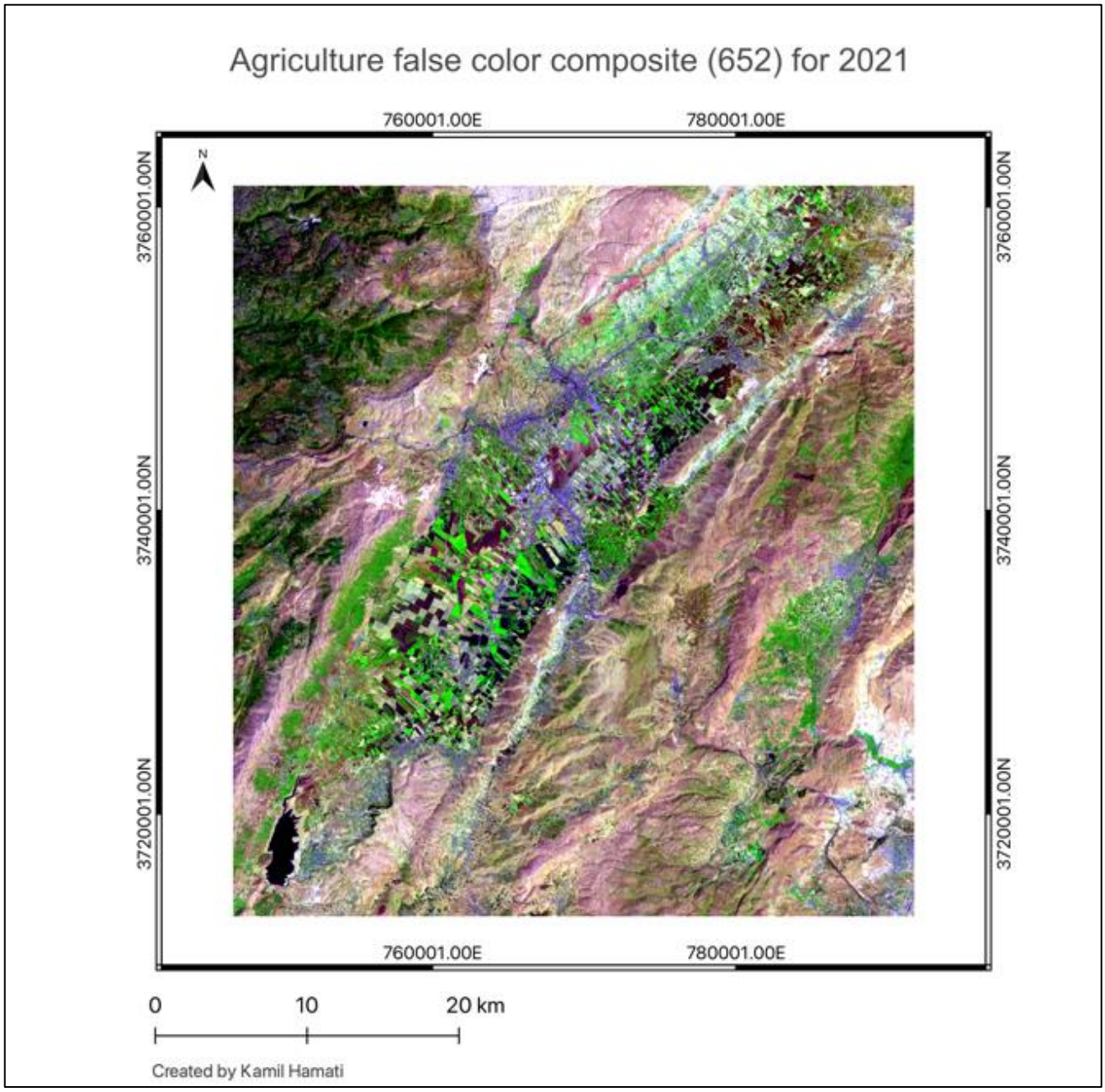
Agriculture false color composite (652) for 2021
760001.00E
780001.00E
N
3760001.00N
3740001.00N
3720001.00N
760001.00E
780001.00E
0
10
20 km
Created by Kamil Hamati

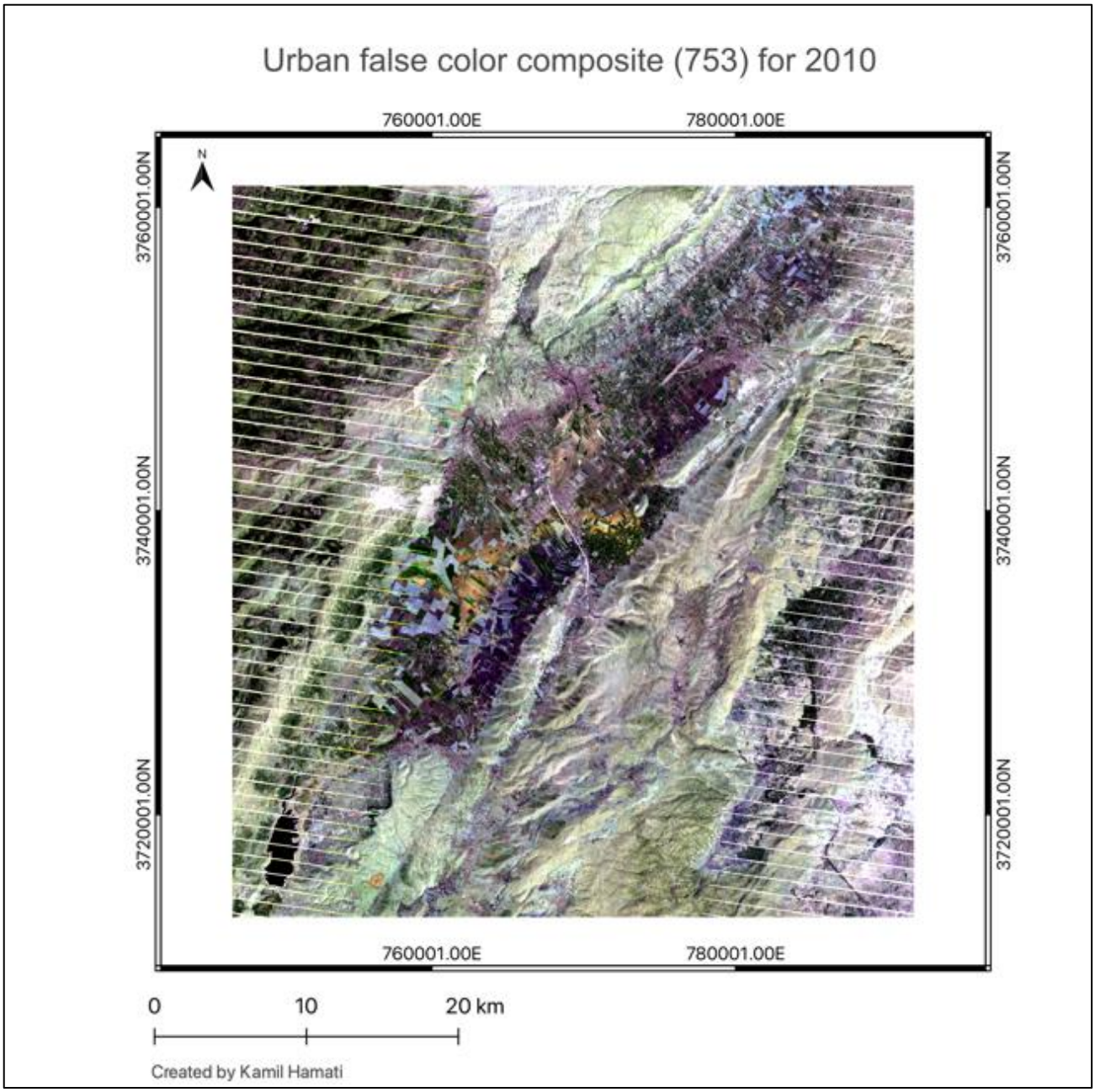
Urban false color composite (753) for 2010
760001.00E
780001.00E
3760001.00N
3740001.00N
3720001.00N
N
0
10
20 km
Created by Kamil Hamati

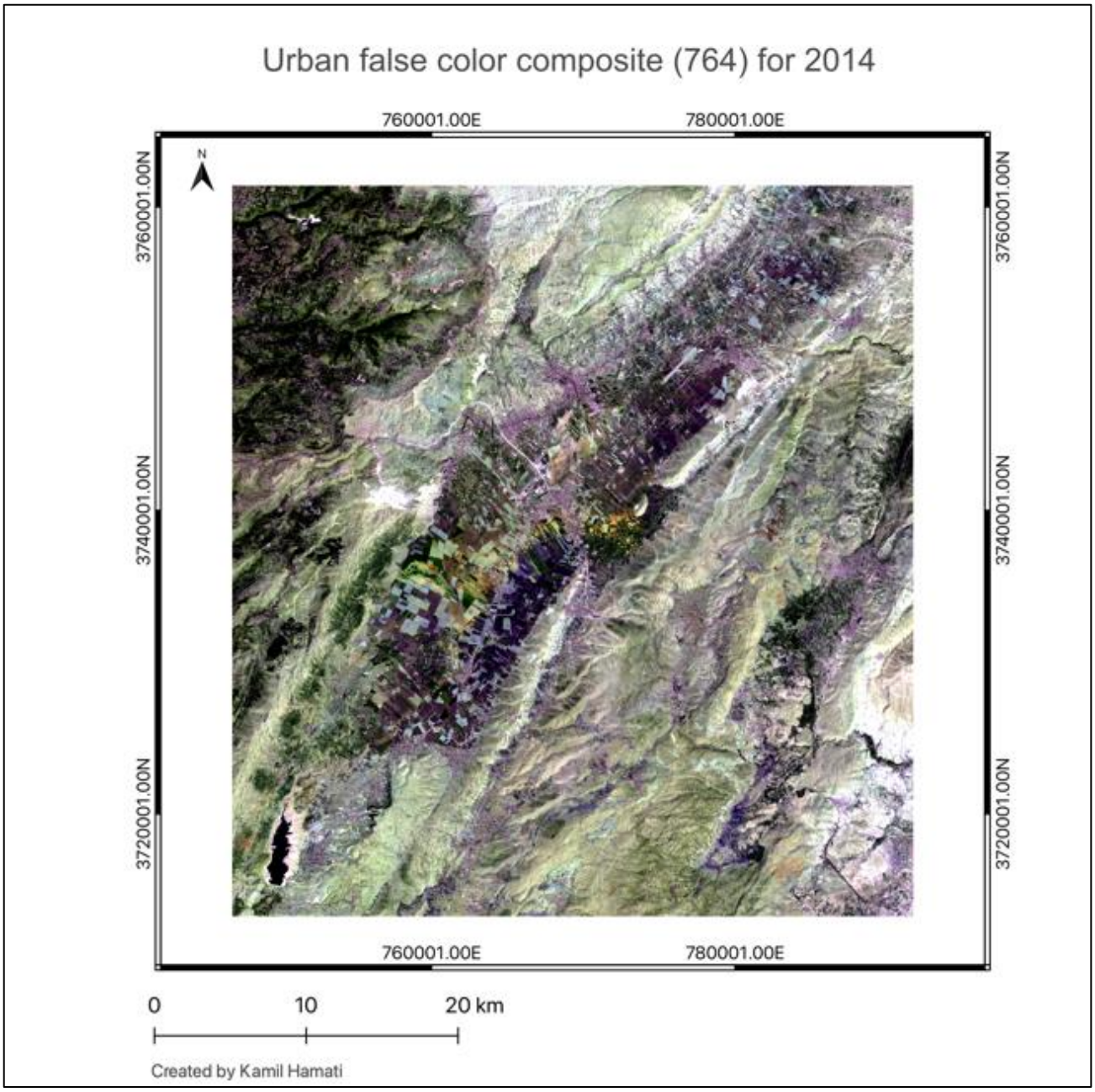
Urban false color composite (764) for 2014
760001.00E
780001.00E
3760001.00N
3740001.00N
3720001.00N
N
0
10
20 km
Created by Kamil Hamati

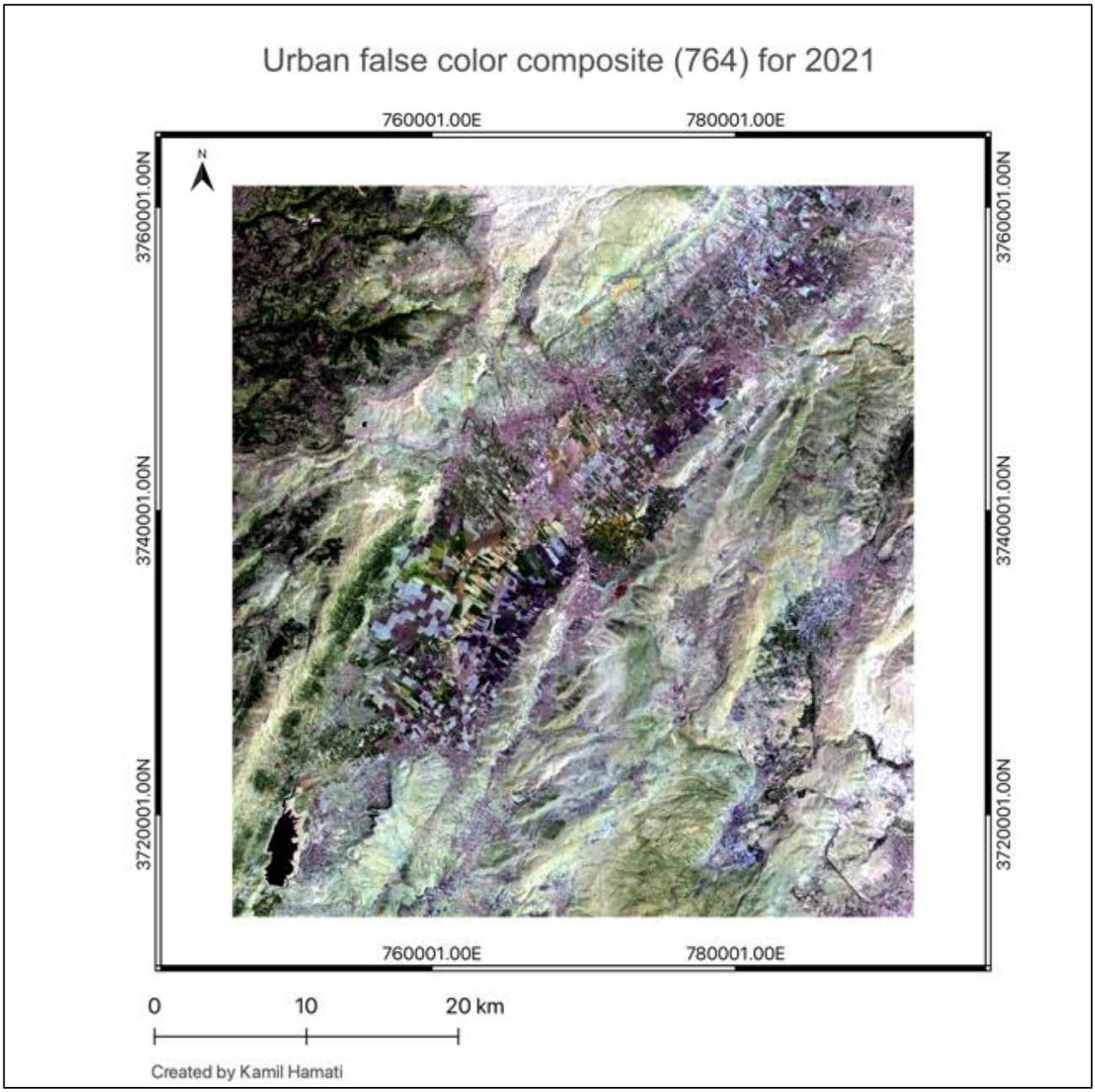
Urban false color composite (764) for 2021
760001.00E
780001.00E
3760001.00N
3740001.00N
3720001.00N
N
0
10
20 km
Created by Kamil Hamati

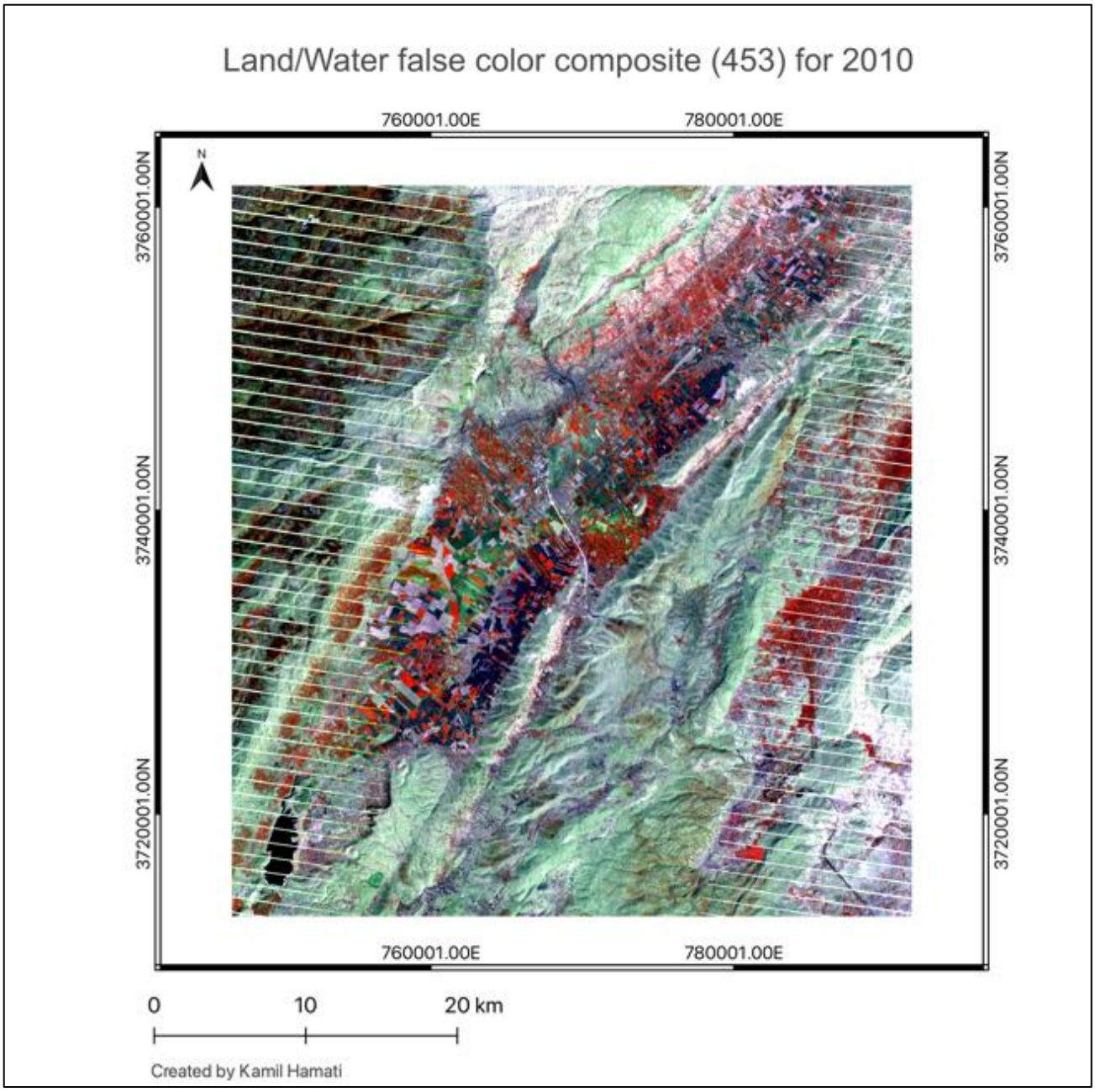
Land/Water false color composite (453) for 2010
760001.00E
780001.00E
3760001.00N
3740001.00N
3720001.00N
N
0
10
20 km
Created by Kamil Hamati

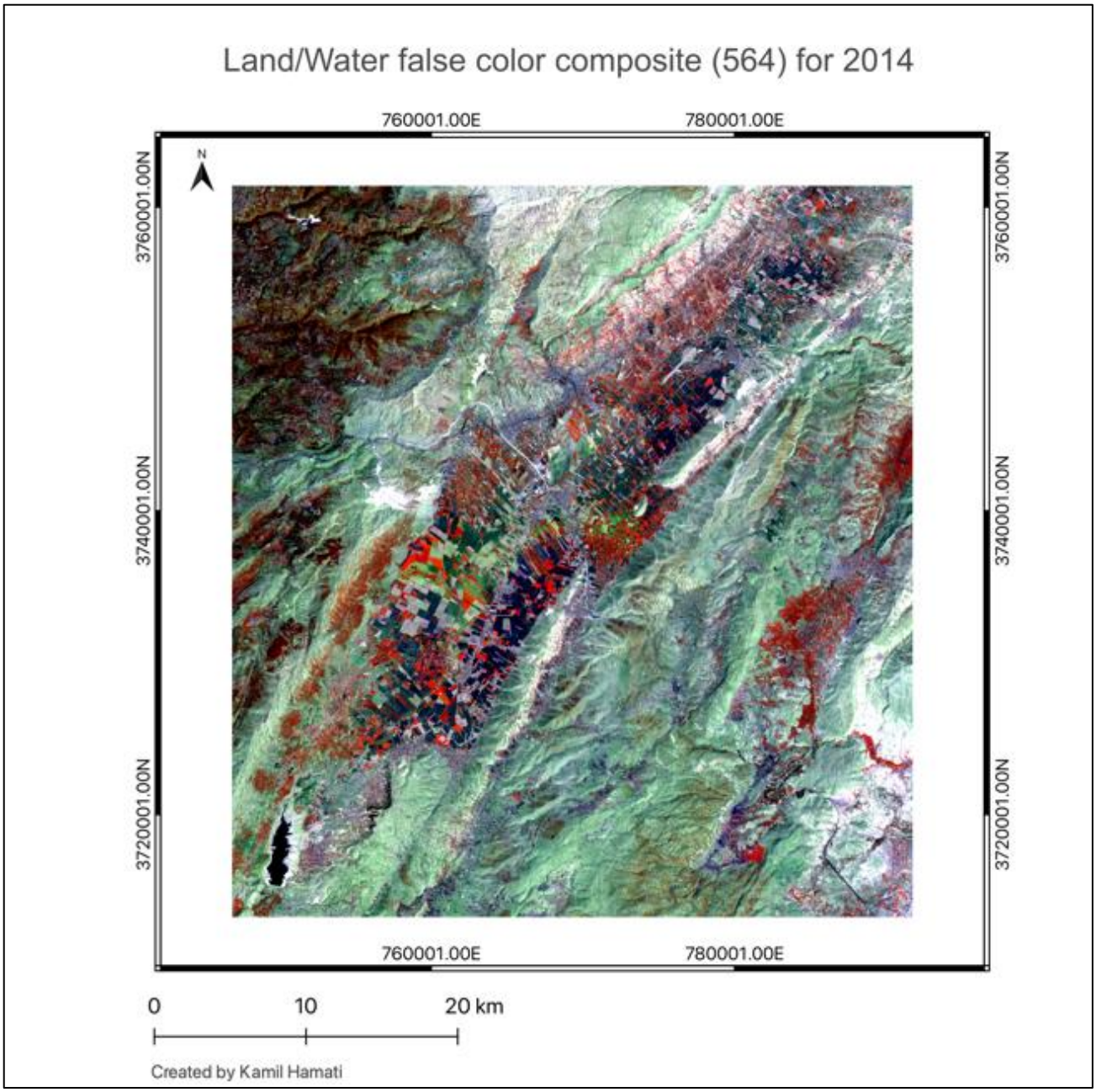
Land/Water false color composite (564) for 2014
760001.00E
780001.00E
N
3760001.00N
3740001.00N
3720001.00N
760001.00E
780001.00E
0
10
20 km
Created by Kamil Hamati

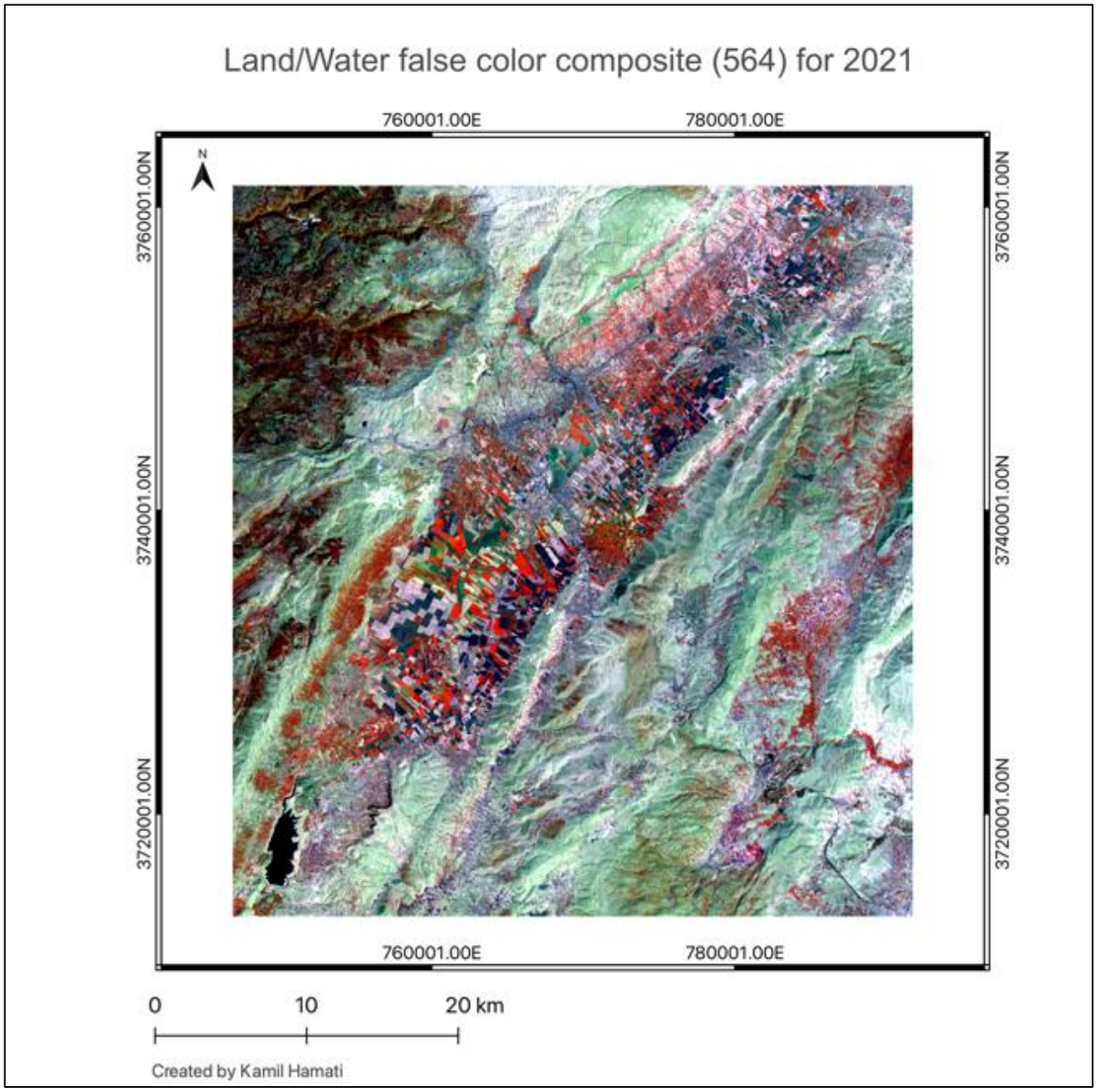
Land/Water false color composite (564) for 2021
760001.00E
780001.00E
N
3760001.00N
3740001.00N
3720001.00N
760001.00E
780001.00E
0
10
20 km
Created by Kamil Hamati

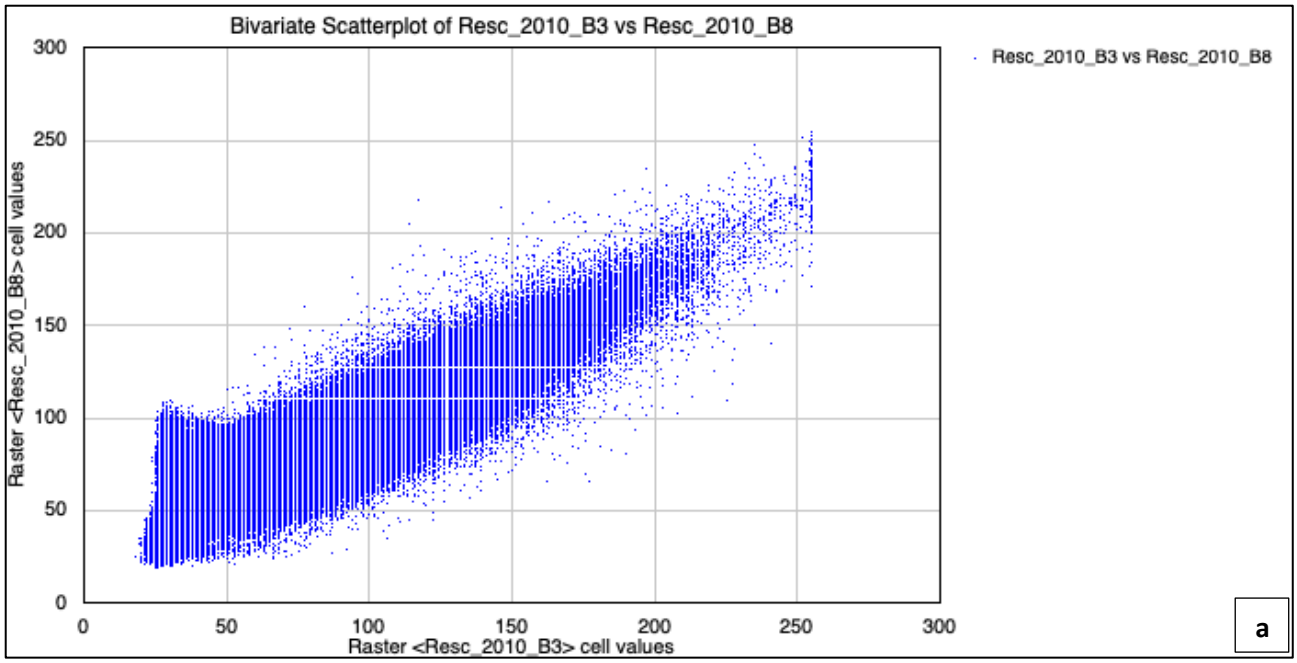
Bivariate Scatterplot of Resc_2010_B3 vs Resc_2010_B8
Resc_2010_B3 vs Resc_2010_B8
Raster <Resc_2010_B8> cell values
Raster <Resc_2010_B3> cell values
0
50
100
150
200
250
300
a

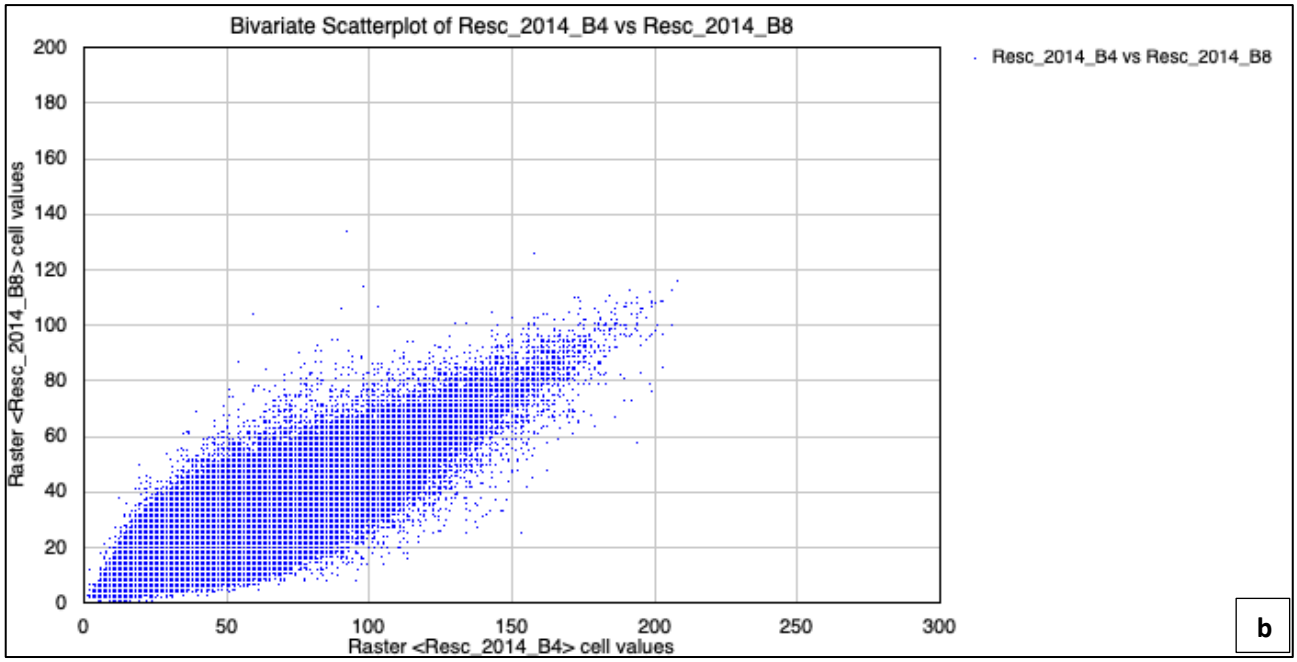
Bivariate Scatterplot of Resc_2014_B4 vs Resc_2014_B8
Resc_2014_B4 vs Resc_2014_B8
Raster <Resc_2014_B8> cell values
Raster <Resc_2014_B4> cell values
0
20
40
60
80
100
120
140
160
180
200
50
150
250
300
b

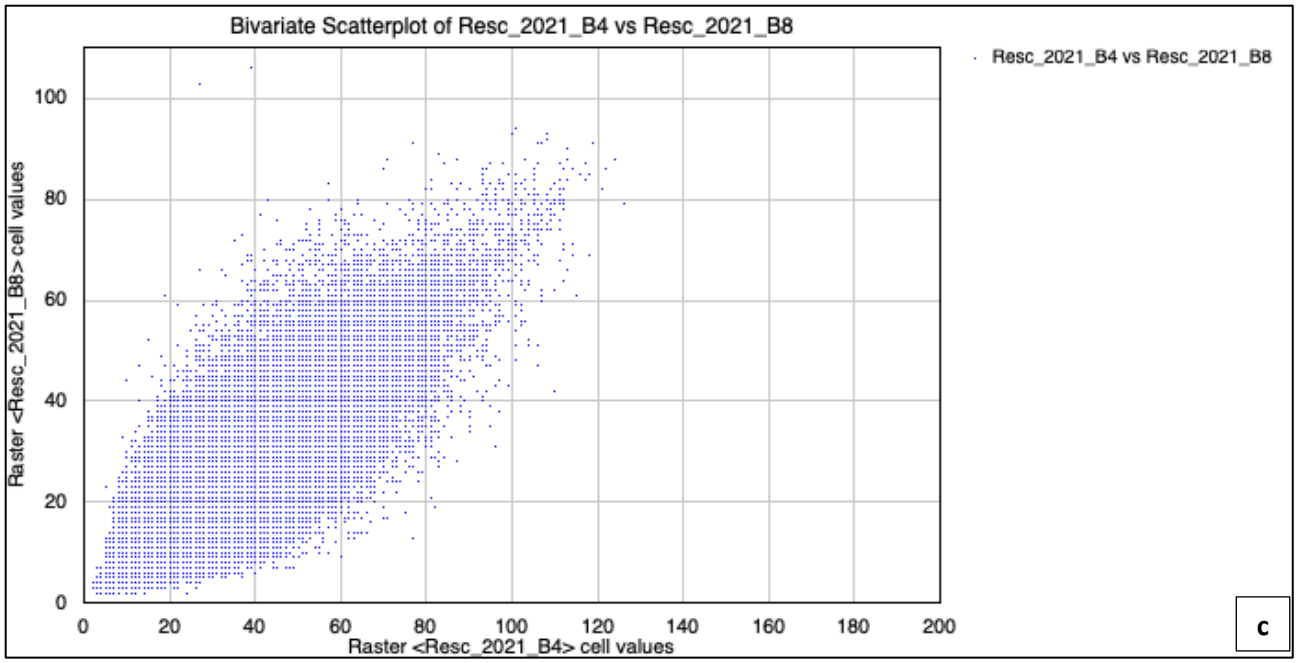
Bivariate Scatterplot of Resc_2021_B4 vs Resc_2021_B8
Resc_2021_B4 vs Resc_2021_B8
Raster <Resc_2021_B8> cell values
Raster <Resc_2021_B4> cell values
0
20
40
60
80
100
120
140
160
180
200
c